UNIVERSITY OF CALIFORNIA,

IRVINE

The PI3K/mTOR/eIF4E Signaling Network in B Cell Differentiation

DISSERTATION

submitted in partial satisfaction of the requirements

for the degree of

DOCTOR OF PHILOSOPHY

in Biological Sciences

by

Honyin Chiu

Dissertation Committee:
Professor David A Fruman, Chair
Professor Craig M Walsh
Assistant Professor Matthew A Inlay

2018

DEDICATION

To:

My parents,

Dr. Chinchuan Andrew Chiu

for always believing in me and inspiring me to follow his footsteps

Ling Ming Amber Liu

for gifting me at a young age with the love of biology and science

and to

Brian Ching-wen Wang

for encouraging me to always pursue my dreams

TABLE OF CONTENTS

	Page
LIST OF FIGURES	iv
LIST OF TABLES	vi
ACKNOWLEDGMENTS	vii
CURRICULUM VITAE	ix
ABSTRACT OF THE DISSERTATION	xi
CHAPTER 1: Introduction	1
CHAPTER 2: The Selective Phosphoinoside-3-Kinase p110δ Inhibitor IPI-3063 Potently Suppresses B Cell Survival, Proliferation, and Differentiation	23
CHAPTER 3: mTORC1 and mTORC2 Have Opposing Roles in Antibody Class Switching	45
CHAPTER 4: The mTORC1/4E-BP/eIF4E Axis Promotes Antibody Class Switching in B Lymphocytes	62
CHAPTER 5: Differential Effects of Eif4e Gene Dosage in Murine Primary B Cells and Leukemia Cells	99
CHAPTER 6: Discussion	113
APPENDIX 1: mTOR Kinase Inhibitors Promote Antibody Class Switching via mTORC2 Inhibition	125

LIST OF FIGURES

		Page
Figure 1.1	Model for activated B cell differentiation	2
Figure 1.2	B cell activation signals through the PI3K/AKT/mTOR pathway	5
Figure 1.3	Schematic diagram of mTORC1 and mTORC2	9
Figure 1.4	mTORC1 promotes eIF4F formation and cap-dependent translation though the phosphorylation of inhibitory 4E-BPs	12
Figure 2.1	Inhibition of p110δ, but not p110γ, reduces p-AKT and p-ERK1/2 in αIgM +IL-4 stimulated mouse B cells	31
Figure 2.2	Inhibition of p110δ, but not p110γ, reduces p-AKT in LPS stimulated mouse B cells	33
Figure 2.3	IPI-3063 potently inhibits mouse B cell survival	34
Figure 2.4	IPI-3063 potently inhibits mouse B cell proliferation	35
Figure 2.5	IPI-3063 potently inhibits mouse B cell proliferation, Part II	36
Figure 2.6	IPI-3063 potently inhibits human B cell proliferation	37
Figure 2.7	IPI-3063 potently promotes mouse B cell antibody switching and inhibits plasmablast differentiation	38
Figure 3.1	TOR-KIs increase in vitro B-cell CSR and decrease plasmablast differentiation	51
Figure 3.2	Rapamycin has a more profound effect on B-cell proliferation and CSR than TOR-KIs	53
Figure 3.3	Inactivation of mTORC1 vs. mTORC2 has opposing effects on CSR	55
Figure 4.1	Low concentrations of rapamycin reduce IgG1 production during SRBC immunization	70
Figure 4.2	mTORC1 control of IgG1 switching is not due to inhibition of division	72
Figure 4.3	Glutamine deprivation reduces switching to IgG1	74
Figure 4.4	Genetic targeting of eIF4E activity reduces antibody class switching	76

Figure 4.5	Pharmacological targeting of eIF4E activity with SBI-756 reduces antibody class switching	78
Figure 4.6	Inhibitors that reduce switching disrupt cap-complex formation	80
Figure 4.7	48 hour addition of Rap or SBI-756 reduces AID protein but not Aicda mRNA	83
Figure S4.1	48 hour addition of Rap but not MLN0128 reduces switching	93
Figure S4.2	IL-4 promotes switching to IgG1, and late addition of Rap reduces IgG1 switching but not cell division in B cells stimulated with a range of LPS and IL-4 concentrations	94
Figure S4.3	S6K1 inhibitor reduces switching to IgG1	95
Figure S4.4	Early addition of Rap reduces germline transcript production	96
Figure S4.5	Rap reduces switching to IgG3 but not IgA under IgA conditions	97
Figure S4.6	48 hour treatment with Rap or SBI-756 does not decrease FOXO nuclear localization	98
Figure 5.1	WT p190 cells outgrow *Eif4e*+/- p190 cells in a competitive growth assay	104
Figure 5.2	*Eif4e*+/- p190 cells have reduced eIF4E protein	105
Figure 5.3	Stimulated *Eif4e*+/- mouse splenic B cells have reduced eIF4E and 4E-BP2	106
Figure 5.4	*Eif4e*+/- activated B cells have no defect in switching to IgG1	107
Figure 5.5	Model of eIF4E and 4E-BP ratios in normal B cells and transformed p190 cells	108

LIST OF TABLES

		Page
Table 2.1	Summary of IC_{50} values for IPI-3063 and IPI-443 using purified enzymes	26
Table 2.2	Summary of IC_{50} values for IPI-3063 and IPI-443 in isoform-specific cell-based assays	31
Table 4.1	Summary of results by antibody isotype	77

ACKNOWLEDGMENTS

The first person I'd like to acknowledge is my graduate thesis advisor David Fruman. He has been supportive even before I joined his lab and his patience and understanding throughout the years has given me the freedom to grow as a scientist and person. I will always be indebted for the time and energy he has spent training and mentoring me. David is a widely respected scientist and human being and the lessons I have learned while working for him have made a lasting impact on my life.

My lab family has always made work an enjoyable environment for me where I can both have fun and learn from them. They all have their own attributes as scientists that I admire and try to emulate. I would like to thank: Lomon So (Solomon), Trang Vo, Scott Lee, Sharmila Mallya, Christine Pai, Lee-or Herzog, Dennis Juarez, Kwon Ik Oh, Moran Gotesman, and Amos Fung. I am grateful for all their advice and friendship.

I was extremely lucky to have worked with talented and dedicated Bio-199 students. I would like to acknowledge Leandra Jackson, Anni Mai, and Phuong Nguyen for their contributions to this work. I was honored to have been their mentor and am proud of their success.

I would like to thank Dr. Craig Walsh for mentoring me during my masters and for serving on my PhD committee. I would also like to thank Dr. Matt Inlay for his time and support serving on my committee as well. I would also like to acknowledge our joint lab meeting members in the Edinger, Razorenova, Kong, and Wang labs for their insightful comments and helpful suggestions. Lastly, I would like to acknowledge Egest Pone for his knowledge and expertise in antibody class switching.

Our lab neighbors have been gracious and kind enough to lend us reagents and access to their equipment, so I would like to thank the Lodoen, Chaput, Pedersen, Walsh, Tenner and Kong labs.

Much of this work would not have been possible without the generosity of our collaborators, so I would also like to thank Dr. Ruggero and Dr. Ze'ev Ronai for their support and advice.

I would also like to acknowledge Bessy Varela, Morgan Oldham, Cecilia Arceo, and Joyce Penh of the administrative staff in the Molecular Biology & Biochemistry department and Rebecca Taylor in the Immunology of Institute for all their support behind the scenes.

Lastly, I am very grateful for the Immunology of Institute community at UC Irvine for hosting seminars, journal clubs, the annual Immunology Fair, and for the NIH Immunology training grant T32 funding I have received for the last two years.

CURRICULUM VITAE

HONYIN CHIU

EDUCATION

- 2010 B.S. in Biochemistry & Molecular Biology, University of California, San Diego
- 2013 M.S. in Biotechnology, University of California, Irvine
- 2018 PhD in Biological Sciences, University of California, Irvine

GRADUATE RESEARCH

- 2013-present Graduate Researcher
  Dr. David A Fruman
  University of California, Irvine
  - Completed project demonstrating the effects of mTOR kinase inhibitors (TOR-KIs) on B cell differentiation
  - Tested the effects of novel PI3Kδ and dual PI3Kδ/γ inhibitors on B cell function and activation
  - Investigated mechanism by which mTORC1 signaling regulates B cell differentiation

EXPERIENCE

- 2010-2011 Assistant Chemist
  TriLink Biotechnologies, San Diego
  Processed and purified manufactured custom oligonucleotides, modified nucleoside triphosphates, long RNA transcripts and CleanAmp PCR products

- 2011 Chemist I
  Bio-Rad Laboratories, Irvine
  Processed intermediate blood components used to formulate in vitro diagnostic products and controls for testing medical devices

- 2012-2013 M.S. Research
  Dr. Craig Walsh
  University of California, Irvine
  Cell and molecular biology research on T cell-caspase independent death known a necroptosis and the degradation of cellular components by macroautophagy

- 2013 Internship
  Allergan
  Biological Sciences Department

Created several HEK293T cell lines overexpressing specific chemokine receptors and performed drug screenings for receptor antagonism using a calcium based Fluorometric Imaging Plate Reader (FLIPR) Assay

PUBLICATIONS

- Limon JJ, So L, Jellbauer S, **Chiu H,** Corado J, Sykes SM, Raffatellu M, Fruman DA. (2014) mTOR kinase inhibitors promote antibody class switching via mTORC2 inhibition. Proc. Natl. Acad. Sci. U S A. 111: E5076-85
- **Chiu, H.,** Mallya, S., Nguyen, P., Mai, A., Jackson, L.V., Winkler, D.G., DiNitto, J.P., Brophy, E.E., McGovern, K., Kutok, J.L. and Fruman, D.A. (2017). The Selective Phosphoinoside-3-Kinase p110δ Inhibitor IPI-3063 Potently Suppresses B Cell Survival, Proliferation, and Differentiation. Frontiers in Immunology 8, p. 747.
- Fruman DA, **Chiu H,** Hopkins BD, Bagrodia S, Cantley LC, Abraham RT. The PI3K pathway in human disease. Cell. 2017 Aug 10;170(4):605–635.
- **Chiu H**, So L, Fruman DA. (2016) Phosphoinositide 3-Kinase. In Sangdun Choi (Ed.), Encyclopedia of Signaling Molecules, 2nd Edition, Springer. pp 1-12, 19 December 2016

AWARDS AND HONORS

- American Association of Immunologists Young Investigator Award 2016, La Jolla Immunology Conference
- NIH T32 UC Irvine Immunology Research Training Grant (Sept 2016-Aug 2018)

ORAL PRESENTATIONS

- **Chiu H,** So L, Fruman DA. (2017) A Novel Role for the 4E-BP/eIF4E Axis in B Cell Antibody Class Switching. Keystone Symposium: "PI3K Pathways in Immunology, Growth Disorders and Cancer"
- **Chiu, H.,** Jackson, L.V., Mai, A., and Ronai, Z.., Ruggero, D., Fruman, D.A. (2018) A Novel Role for the 4E-BP/eIF4E Axis in B Cell Antibody Class Switching. Midwinter's Conference of Immunologists at Asilomar

POSTER PRESENTATIONS

- **Chiu H,** So L, Fruman DA (2016) "A Novel Role for the 4E-BP/eIF4E Axis in B Cell Antibody Class Switching." American Association of Immunologists Annual Meeting, Seattle, WA, USA, May 13-17
- **Chiu H,** So L, Fruman DA (2016) "A Novel Role for the 4E-BP/eIF4E Axis in B Cell Antibody Class Switching." La Jolla Immunology Conference, San Diego, CA, USA, October 11-13

ABSTRACT OF THE DISSERTATION

The PI3K/mTOR/eIF4E Signaling Network in B Cell Differentiation

By

Honyin Chiu

Doctor of Philosophy in Biological Sciences

University of California, Irvine, 2018

Professor David A Fruman, Chair

As humans, we have evolved to build a complex humoral immune response against infection. The process of differentiating B cells into antibody secreting cells is highly regulated and when dysfunctional can lead to various human malignancies. Central to both an effective host response and disease progression is the PI3K/AKT/mTOR network and targeting this pathway has already led to some success in treating certain B-cell malignancies and autoimmune diseases. However, there are still many questions about how this process is regulated by this signaling network. This thesis investigates the immunomodulatory effects of pharmacological and genetic perturbations on B cell function.

Chapter 2 of this thesis characterizes the effects of novel PI3Kδ and PI3Kδ/γ inhibitors on B cell function and differentiation. I show *in vitro* that B cell survival, proliferation, and plasmablast differentiation are reduced at nanomolar concentrations of these inhibitors. PI3Kδ was found to be the dominant isoform involved and the inhibitors also potently increased antibody class switching.

Chapter 3 provides mechanistic investigation of mTORC1 and mTORC2 function in antibody class switching *in vitro.* I tested both rapamycin and mTOR kinase inhibitors (TORKi)

and found that they had opposite effects on antibody class switching. Genetic deletion of Raptor and Rictor for mTORC1 and mTORC2 inhibition in B cells phenocopied the effects of the inhibitors.

In Chapter 4, I further investigate the mechanism of mTORC1 in B cell differentiation and characterized the two downstream substrates S6Ks and 4E-BPs, and their effects on antibody class switching. The main finding of this chapter was that mTORC1 promotes switching in part by inhibiting 4E-BPs, thereby elevating eIF4E activity and cap-dependent translation to increase expression of AID protein.

Chapter 5 characterizes the effects of reduced eIF4E protein on antibody class switching in normal B cells and tumorigenesis in a mouse model of leukemia. These experiments demonstrate that primary B cells can regulate their ratio of 4E-BPs to eIF4E but reduced eIF4E is rate-limiting for tumorigenesis.

The work presented here establishes the contributions of the PI3K/mTOR/eIF4E signaling network to B cell differentiation and provides insight in how the humoral immune response is regulated.

CHAPTER 1

Introduction

This chapter contains a figure taken from our review article published in *Cell,* 170: 605–635 (2017) entitled “The PI3K pathway in human disease” (1) and text from a book chapter published in Encyclopedia of Signaling Molecules, 2nd Edition, Springer. pp 1-12 (2018) entitled “Phosphoinositide 3-Kinase”.

PI3K/mTOR/eIF4E signaling is highly activated in many cancers and various pathway components are attractive targets for cancer therapies. However, this pathway is also important for normal immune function and dysregulated in immune diseases. Therapies targeting the signaling network may affect B cell survival, proliferation and differentiation. The goal of my thesis is to better understand how this central pathway regulates B cell differentiation, particularly antibody class switching, and how perturbation of this pathway impacts primary B cell function. A better understanding of PI3K/mTOR/eIF4E signaling in B cell function has potential to improve therapeutic approaches for B cell immunodeficiencies and antibody-driven autoimmune diseases.

B Cells and Humoral Immunity

The humoral immune response is important for effective pathogen elimination and is mediated by plasma cells that have undergone B cell differentiation. This process is initiated when the B-cell receptor (BCR) binds antigen and also requires costimulatory signals from other immune cells. The B cell then undergoes clonal expansion and differentiates to secrete antigen-specific antibodies of various classes with distinct effector functions (2). Immunoglobulin M

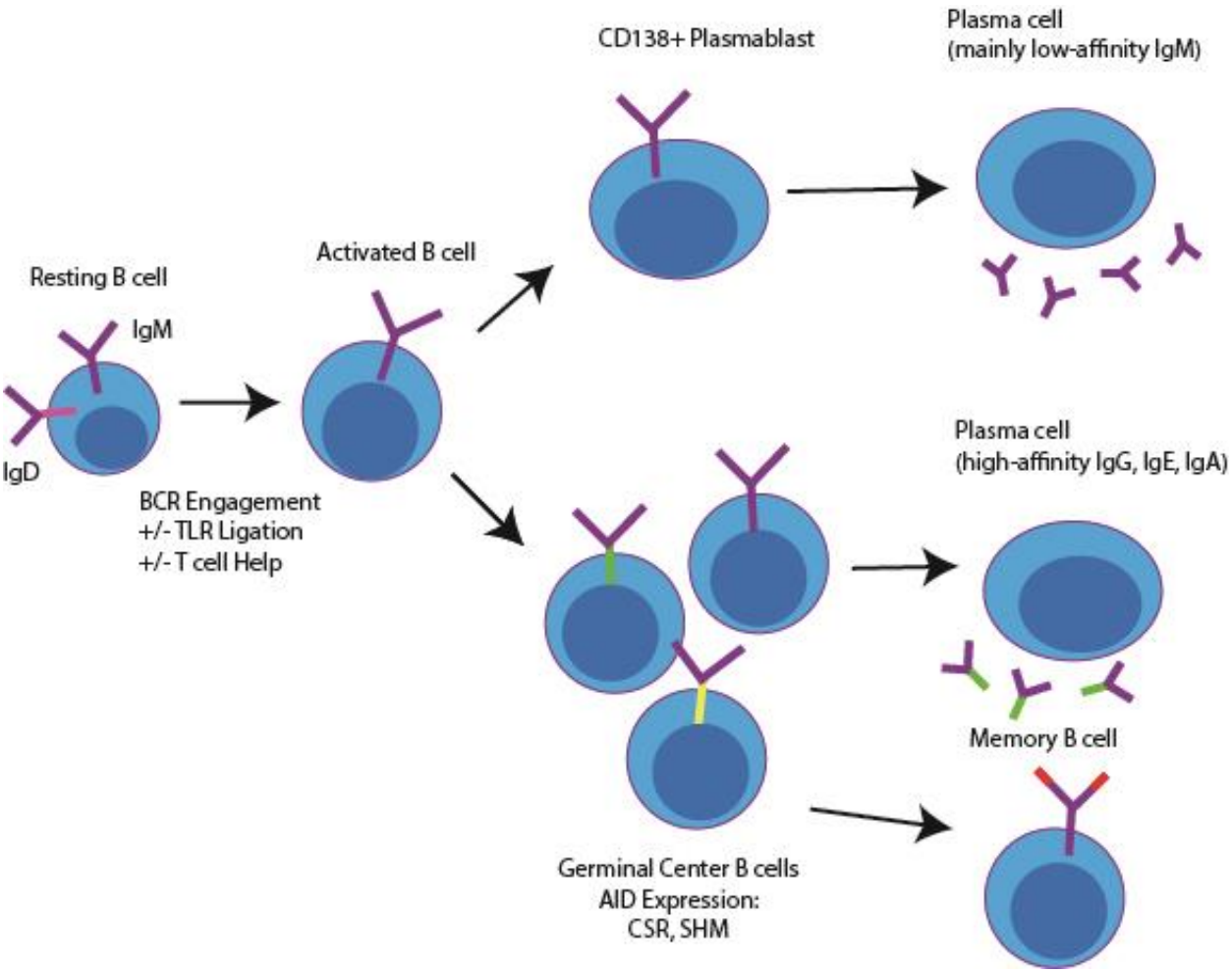

Figure 1.1 Model for activated B cell differentiation. B cells function in humoral immunity by secreting antibodies. When naïve B cells bind to antigen, they can either quickly become plasmablasts or they can become germinal center B cells. During the germinal center reaction the heavy and light chain genes undergo somatic hypermutation, which after selection leads to production of higher affinity antibodies, while the heavy chain genes undergo class switch recombination to produce antibodies with varying effector functions. The activated B cells will also undergo several rounds of proliferation before completing differentiation to plasma cells or memory B cells.

(IgM) and IgD are referred to as the non-class switched antibodies. These are normally expressed as surface transmembrane receptors on mature naïve B cells **(Fig. 1.1)** that have undergone successful rearrangement of immunoglobulin heavy and light chain genes during development. After a naïve B cell encounters antigen, rapid proliferation ensues and a fraction of the daughter B cells quickly differentiate (within 4-7 days) into plasmablast cells and secrete mainly low

affinity IgM antibodies **(Fig. 1.1).** Other activated B cells become germinal center (GC) B cells and through T cell-dependent interactions undergo somatic hypermutation (SHM) to diversify and produce higher affinity antibodies. They can also undergo class switch recombination (CSR) to produce the class-switched antibodies IgG, IgA and IgE (3) **(Fig. 1.1).**

There are several subsets of B cells, each of which has a distinct differentiation program depending on its location and developmental programming. Marginal zone (MZ) B cells, resident in the marginal zone of the spleen, are the first to encounter bloodborne antigen. MZ B cells rapidly differentiate into plasmablasts independent of T-cell help, although there is emerging evidence for other accessory cell signals (4, 5). Similarly, B-1 cells that reside mainly in body cavities are programmed to quickly differentiate into plasmablasts independent of T-cell co-stimulation. While MZ B cells have the potential to form germinal centers, the more common subset is the follicular B cells found in the follicles of the spleen and other secondary lymphoid tissues (lymph node, Peyer's Patch). Follicles are B-cell areas located next to T-cell rich regions and contain follicular dendritic cells (FDCs) that can retain and display intact antigens to the B cells. The follicular structures are organized by stromal CXCL13 chemokine, a ligand for the CXCR5 receptor that is constitutively expressed by follicular B cells. The T-cell regions are organized by stromal secretion of CCL19 and CCL21, which are ligands for the receptor CCR7 expressed on T-cells. Following activation by antigen, B and T cells upregulate CCR7 (6) and CXCR5 (7), respectively, to facilitate their migration towards the follicle borders and initiate T cell:B cell cognate interactions. Additionally, T follicular helper (TfH) cells subsequently lose expression of CCR7 which allows them to localize into follicles and germinal centers (8).

GC formation produces an organized structure with histologically disparate dark and light zones. The dark zone contains proliferating B cells termed centroblasts, and it is the predominant

site for somatic hypermutation. Centroblasts that come out of cell cycle migrate to the light zone (now termed centrocytes) where CSR occurs. The B cells also undergo selection in the light zone by competing for binding to antigen on FDCs and for interaction with the CD4+ TfH cells. Those clones with mutations improving affinity for antigen are able to acquire more antigen from the FDCs and present peptides more effectively to CD4+ TfH cells, thereby receiving a stronger signal promoting survival, proliferation, and differentiation. The resulting B cells that survive selection then either become plasma cells that secrete these antibodies to fight off the infection or become long-lived memory B cells that initiate a faster response during a second infection.

During the GC response, SHM and CSR play a central role in antibody maturation. These two processes require activation-induced cytidine deaminase (AID), a DNA mutator protein that catalyzes the deamination of deoxycytidine (dC) residues into deoxyuridine (dU). This results in a mismatch dU:dG pair which then can be processed as a point-mutation for SHM or as double-strand breaks to initiate CSR (9). In humans, AID deficiency causes hyper-IgM syndrome where patients produce elevated levels of IgM and are deficient in class-switched antibodies (10). On the other hand, aberrant AID activity is associated with autoimmunity and cancer (11). In autoimmune systemic lupus erythematosus, dysregulation of AID leads to increased SHM, CSR, and auto-antibody production (12). In chronic lymphocytic leukemia (CLL), increased AID is associated with drug resistance (13). As a DNA mutator, AID expression is confined to activated B cells and is highly regulated at the transcriptional, post-transcriptional, and post-translational levels (14–17). It is not known whether AID expression is regulated at the level of mRNA translation, which I aimed to explore as part of my thesis work.

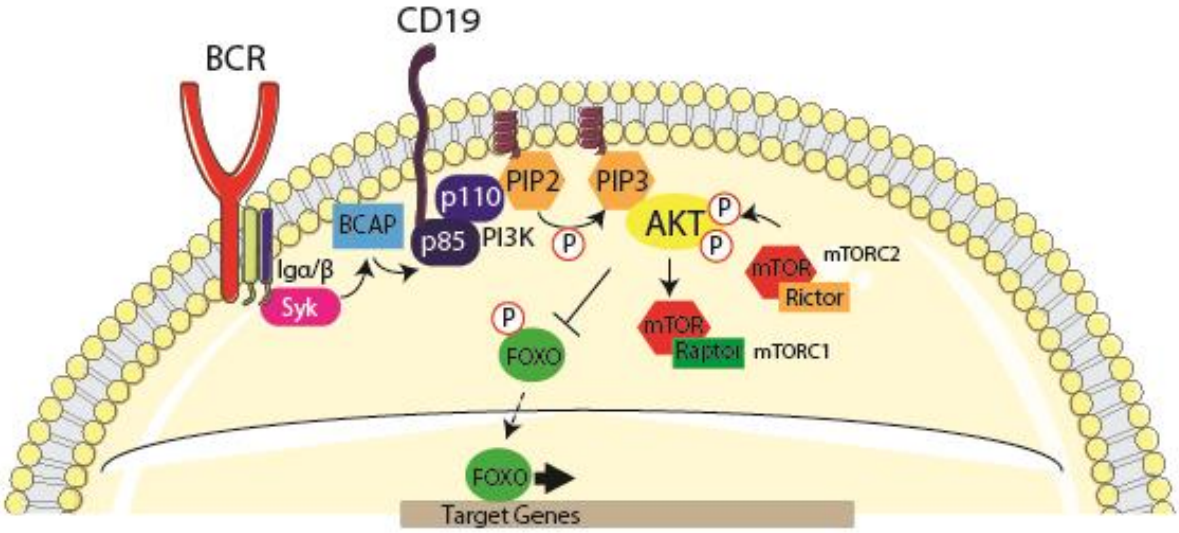

Figure 1.2 B cell activation signals through the PI3K/AKT/mTOR pathway. PIP3 production by class IA PI3K recruits AKT to be phosphorylated at the plasma membrane by PDK1 (not shown) and by mTORC2. Active AKT then phosphorylates FOXO proteins which reduces transcription of FOXO target genes in the nucleus. AKT can also promote mTORC1 activation via intermediates not shown.

PI3K Signaling and B Cell Function

When a B cell is stimulated by antigen, the BCR initiates signaling pathways that promote growth and proliferation. One of the key signaling events is activation of phosphoinositide-3-kinase (PI3K) **(Fig. 1.2)**. PI3K is a lipid kinase composed of a catalytic and regulatory subunit. In mammals, there are four class I catalytic isoforms p110α, β, γ, and δ. p110α, β, and δ can associate with regulatory subunits such as p85α encoded by *PIK3R1*, p85β encoded by *PIK3R2*, or p55γ encoded by *PIK3R3*. p110γ associates with regulatory subunits p101 or p87. p110α and p110β are ubiquitously expressed while p110δ and γ expression is enriched in immune cells.

PI3K activity is important in a variety of central cellular functions including growth, proliferation, differentiation and survival. In B cells, class I PI3K activation is necessary for B cell receptor (BCR) dependent proliferation and sufficient for BCR dependent survival (18–20). When the BCR is stimulated, active PI3K produces 3'-phosphorylated phosphoinositides

including PI-3,4,5-P_3 (PIP3) and PI-3,4-P_2 that then act as second messengers to recruit cytoplasmic proteins to the cellular membrane. One of the downstream targets, AKT (also known as PKB), is recruited to the membrane and phosphorylated to become activated **(Fig. 1.2)** (18). AKT has many downstream substrates, one of which the transcription factor family Forkhead Box Subgroup O (FOXO) plays an important role in B cell development and differentiation (21). Active AKT phosphorylates and inhibits FOXO, thereby down-regulating transcription of its target genes **(Fig. 1.2)**. The PI3K pathway is opposed by the lipid phosphatase PTEN, which dephosphorylates PIP3 and PI-3,4-P_2 to terminate the signal.

PI3Kδ is the dominant isoform in B cells critical for lymphocyte development, survival, activation and differentiation. However, the remaining Class I isoforms have also been found to play some roles in B cell development and activation. Inhibition of either PI3Kα or β using isoform-selective compounds partially reduces signaling and functional responses in activated B cells (22). PI3Kα also has partially overlapping roles with PI3Kδ in B cell development (23). Little is known about the role of PI3Kγ in B cells and the effects of chemical inhibition of PI3Kγ on B cell function has not been reported. One study reported that mice lacking both PI3Kδ and PI3Kγ had greater defects in B cell survival and proliferation compared to PI3Kδ knock-out alone (24). In chapter 2 I address whether dual inhibition of both PI3Kδ/γ can have greater effects on B cell function than inhibition of PI3Kδ alone.

B cell differentiation is directed depending on the level of PI3K/AKT signaling and inactivation of FOXO transcription factors (18). Elevated PI3K signaling through the loss of PTEN strongly suppresses class switch recombination while increasing the frequency of cells differentiating into IgM-secreting plasmablasts (25). This was shown to be a FOXO dependent mechanism as FOXO deficient B cells have severe defects in CSR and expression of

constitutively active FOXO proteins restores CSR in PTEN-deficient cells (25). Conversely, PI3Kδ inhibition increases AID expression and CSR and reduces plasmablast differentiation (25).

While these studies were done in genetic models of mice, naturally occurring human mutations have been found that disrupt PI3K signaling and cause certain immune diseases. A homozygous premature stop codon in exon 6 of *PIK3R1* results in the absence of p85α and leads to a severe defect in B cell development and agammaglobulinemia (26). A gain-of-function mutation in the p110δ protein in which the glutamic acid residue 1021 is replaced by a lysine (E1021K) causes elevated PI3K signaling in patients with Activated PI3Kδ Syndrome (APDS) (27). A similar immunodeficiency termed APDS2 was found to be caused by splice site mutations in PIK3R1 affecting the p85α subunit leading to loss of p85α-mediated inhibition of p110 activity (28). Lymphocytes from these patients have increased levels of PIP3 and phosphorylated AKT protein and are prone to activation-induced cell death (AICD). This leads to primary immunodeficiency characterized by recurrent respiratory infections, airway damage, lymphopenia, increased circulating transitional B cells, altered immunoglobulin levels in serum and impaired vaccine responses. Selective p110δ inhibitors IC87114 and GS-1101 can reduce the mutant PI3K activity *in vitro* which suggests that this may be a therapeutic approach for patients (28).

The mechanism by which PI3K signaling directs B cell differentiation and GC formation is still under investigation. One study reported that unequal PI3K signaling in sibling B lymphocytes bifurcates transcriptional networks that direct the fate of the daughter cells (29). This asymmetric division leads to one daughter cell differentiating into an antibody-secreting plasma cell while the other maintains a germinal center or memory cell fate. PI3K and FOXO1

transcription factor activity have also been shown to direct B cells cycling between the proliferative state of the germinal center (GC) dark zone and the non-proliferative state in the light zones (30, 31). PI3K activity was found to be restricted to the light zone while nuclear FOXO1 was largely absent. A fraction of cells in the light zone fate that did express FOXO1 were destined for dark zone re-entry as FOXO1 is needed to instruct the dark zone gene program. FOXO1 deletion or increased PI3K activity lead to loss of architectural polarity and lack of dark zones while impairing somatic hypermutation and class switching.

The PI3Kδ isoform is mainly expressed in hematopoietic cells and is hyperactivated in B-cell malignancies as a key oncogenic driver. Thus, when targeting the PI3Kδ isoform, one can selectively block signaling in leukocytes with minimal effects on other tissues and organs. In 2014, the PI3Kδ inhibitor idelalisib (also known as CAL-101 and GS-1101) was the first PI3K inhibitor approved by regulatory agencies for treatment of cancer. Idelalisib is currently approved for use in patients with relapsed/refractory chronic lymphocytic leukemia (CLL, in combination with rituximab), relapsed follicular lymphoma, and relapsed small lymphocytic lymphoma (as monotherapy) (32). Leniolisib, a novel PI3Kδ inhibitor, has also shown disease improvement at tolerated doses in APDS patients with hyperactive PI3Kδ (33).

PI3Kγ is also mainly expressed in immune cells and has largely non-overlapping functions with PI3Kδ. In general, PI3Kδ is more important in lymphocyte function whereas PI3Kγ is important for innate immune cell migration and function. Therefore, efforts were made to target both with a dual δ/γ inhibitor, IPI-145, which had efficacy in animal models of arthritis, asthma, and lupus (34). Pre-clinical studies with IPI-145 (also known as duvelisib) also showed efficacy against cancer in several models. IPI-145 was successful in killing primary CLL cells and overcoming resistance against the BTK-inhibitor, ibrutinib (35). IPI-145 also showed

clinical activity in a phase I trial in patients with cutaneous (CTCL) and peripheral T-cell lymphoma (PTCL) as well as in the pre-clinical mouse models (36). As a combination therapy, IPI-145 enhanced responses to PD-L1 blockade in tumor models of head and neck cancers (37).

mTOR Signaling and B Cell Function

The mammalian/mechanistic target of rapamycin (mTOR) is a serine/threonine kinase that is evolutionarily conserved from mammals to yeast. It is a member of the PI3K-related kinase family and integrates growth factor and nutrient signals to promote many cellular processes including mRNA translation, lipid biogenesis, and nucleotide synthesis in most cell types. mTOR is activated downstream of PI3K and plays a complex role in which it is involved both upstream and downstream of AKT. Upstream of AKT, the mTOR kinase forms the mTOR complex 2 (mTORC2) defined by the rapamycin-insensitive companion of TOR (Rictor) subunit and also consisting of the mammalian lethal with Sec13 protein 8 (mLST8), the endogenous inhibitor DEP-domain-containing mTOR-interacting protein (Deptor), mammalian stress-activated protein kinase interacting protein (mSIN1) and protein observed with rictor-1 (Protor) **(Fig. 1.3)**. Downstream of AKT, mTOR forms the mTOR complex 1 (mTORC1) defined by the regulatory-associated protein of mTOR (Raptor) subunit and containing mLST8, proline rich

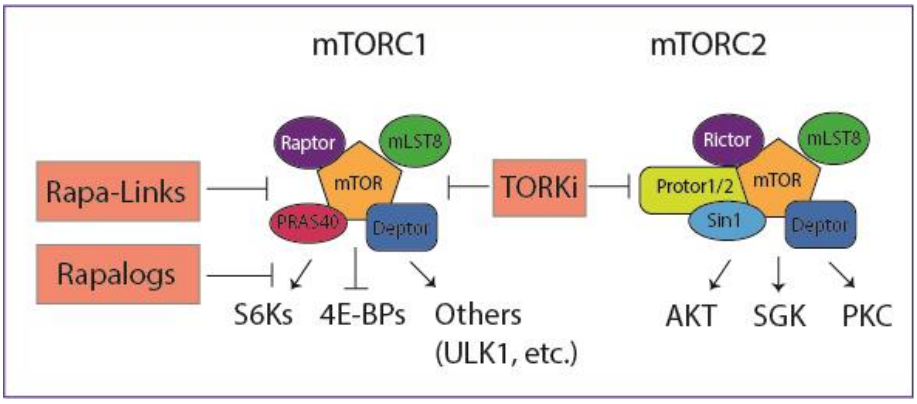

Figure 1.3 Schematic diagram of mTORC1 and mTORC2. The most well-known substrates of the two complexes and different classes of mTOR inhibitors are shown (1).

AKT substrate 40 kDa (PRAS40) and Deptor **(Fig. 1.3)**. mTORC2 phosphorylates serine473 in the hydrophobic domain of AKT which is important for its activation however the functional importance is still debated. mTORC1 is activated by AKT and other signals to promote biosynthetic processes necessary for growth and proliferation **(Fig. 1.2)** (38). Rapamycin allosterically binds to and inhibits mTORC1 formation however does not completely inhibit mTORC1 kinase activity, with differential effects on phosphorylation of distinct mTORC1 substrates (39). Prolonged treatment of rapamycin also leads to mTORC2 inhibition (40).

Rapamycin is a bacterial macrolide isolated in 1975 based on its anti-fungal activity from the soil microbe *Streptomyces hygroscopicus* (41), and later discovered to be a potent immunosuppressant (42). It was found to inhibit proliferation and differentiation in both mammalian T and B lymphocytes (43–45). In T cells, mTOR deficiency was found to block differentiation into T helper 1 (Th1), Th2, or Th17 effector cells and increase differentiation into $Foxp3^+$ regulatory T cells (46) which supports the use of rapamycin as a clinical immunosuppressant for organ transplantation. The mode of rapamycin action in B cells has not been as well characterized as in T cells, but recent efforts have led to novel insights about mTORC1 function in B cells.

Genetic studies with conditional deletion of mTOR or Raptor in splenic B cells showed a decrease in high affinity antibody production in mice; however, these mTORC1-inactivated B cells have a proliferative defect. These studies demonstrated that inhibition of mTORC1 prevented initial B cell activation and further differentiation. It is now appreciated that mTORC1 signaling is important for the later stages of lymphocyte differentiation as well (47–49). Rapamycin at low doses that preserve B cell proliferation can maintain IgM production while suppressing germinal center formation and class switching (48, 50). Supporting this, in Chapter 3

we show that low concentrations of rapamycin *in vitro* suppressed switching with minimal effects on proliferation. Deletion of Raptor post-activation (using inducible Cre or Cγ1-Cre) also reduced germinal center B cells and antigen specific IgG1 while maintaining IgM (51). In the germinal center, mTORC1 signaling is cyclic and controls entry into the light and dark zones (52) and hypoxia diminishes mTORC1 signaling in the dark zone regions (53). Adding further complexity, our laboratory showed that low concentrations of mTOR kinase inhibitors (TOR-KIs) promote rather than inhibit antibody class switching. Mechanistic investigation and deletion of Rictor in B cells showed that this increase in CSR was due to inhibition of mTORC2 (54). These findings contrasted with another group which had found that Rictor deletion using Vav-Cre or Cre-ERT2 systems reduced survival and impaired class switching (55). These deletion systems varied in efficiency which could explain the conflicting results.

While our lab has shown that mTORC2 inhibition reduces AKT activity, thereby increasing FOXO activity to drive CSR, the mechanism by which mTORC1 promotes CSR is not well-defined. Chapter 4 of my thesis aims to address this question by investigating two well-characterized mTORC1 substrates regulating gene expression, the S6Ks and the eIF4E-binding proteins (4E-BPs) (39).

mTORC1 activates S6Ks to promote fundamental cellular processes important for cell growth, while mTORC1 phosphorylation of 4E-BPs releases eIF4E to form the eIF4F complex that promotes translation of certain cap-dependent mRNAs **(Fig. 1.4)** (56). In fibroblasts and other cell types, mTORC1-regulated growth and proliferation are controlled separately; S6Ks promote cell growth while the 4E-BP-eIF4E axis controls proliferation. In lymphocytes, however, activation, growth and proliferation are coupled through the 4E-BP axis while S6Ks are mainly dispensable (57). Additionally, rapamycin reduces 4E-BP1 phosphorylation to a

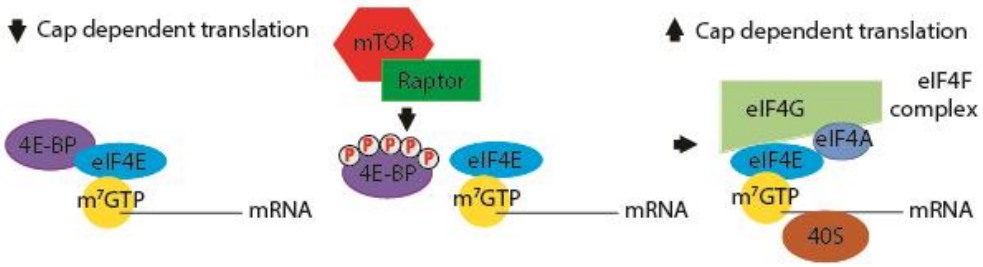

Figure 1.4 mTORC1 promotes eIF4F formation and cap-dependent translation through the phosphorylation of inhibitory 4E-BPs. 4E-BPs inhibit cap-dependent translation by binding to the cap binding factor, eIF4E. Phosphorylation of the 4E-BPs leads to dissociation from eIF4E and allows it to recruit the scaffolding protein eIF4G and eIF4A to form the translation initiation complex known as eIF4F. eIF4G then recruits other factors of the cap-initiation complex (not shown). High levels of eIF4F activity promote translation of a subset of mRNAs with specific 5'UTR features.

variable extent in different cell types whereas lymphocytes highly express the 4E-BP2 isoform whose phosphorylation is effectively inhibited by Rapamycin (57). This might explain the mechanism by which rapamycin is a selectively potent immunosuppressant while unable to block and only delaying cell cycle progression in fibroblasts and many cancer cell lines which have higher amounts of the rapamycin-insensitive 4E-BP1 (39).

Several new generations of mTOR inhibitors have been developed to have more complete inhibition of mTORC1 kinase activity compared to rapamycin and rapalogs. These include the mTOR kinase inhibitors (TORKi, previously termed TOR-KI—see Chapter 3) that fully inhibit mTORC1 and mTORC2 activity (58), and Rapa-links in which TORKi and rapamycin are chemically linked together to specifically target mTORC1 kinase activity. Our lab previously showed that TORKi were more effective than rapamycin at killing mouse and human leukemia cells (59). Rapa-links on the other hand showed better efficacy than rapamycin or TORKi against glioblastoma (60). Both TORKi and Rapa-links caused complete 4E-BP1 de-phosphorylation compared to rapamycin; however, cancer cells can become resistant to all mTOR inhibitors by downregulating 4E-BP expression (61, 62). This has provided one rationale for efforts to directly

target eIF4E and other components of the eIF4F complex. In chapter 4, we make use of a novel eIF4G-binding molecule (SBI-756) in studies of eIF4F function during B cell differentiation.

High eIF4F activity contributes to sustained proliferative signaling, evasion of growth suppression, resistance to programmed cell death, replicative immortality, angiogenesis, invasion and metastasis (63). Increased eIF4E and/or eIF4G expression has been linked to advanced disease and decreased patient survival (64, 65), and mTORC1/eIF4E activity preferentially translates mRNAs involved in metastasis and invasion (66). eIF4F and protein synthesis were also found to be drivers in PI3K/AKT/mTOR driven lymphomagenesis (67) as well as anti-BRAF and anti-MEK resistance in BRAF(V600)-mutant melanoma, colon, and thyroid cancer cell lines (68). This makes cap-dependent translation an attractive target for cancer therapy (64), and efforts are underway to develop small molecule inhibitors of eIF4F for oncology (69, 70). As proof of concept, in a mouse model of Kras-driven lung disease, haploinsufficiency of *Eif4e* (encoding eIF4E) significantly reduced cellular transformation. While *Eif4e* homozygous knock-out is embryonic lethal, these *Eif4e* heterozygous mice had normal development and protein synthesis suggesting that only in cancer does eIF4E activity become a limiting factor (71). In Chapter 5, we further explore this with primary mouse B cell function and tumorigenesis in a mouse leukemia model.

While several studies have investigated the role of mTORC1/eIF4E in cap-dependent translation of cancer cells, only recently has translational regulation been gaining attention in lymphocyte activation and differentiation (72, 73). Several groups have shown that mTOR signaling regulates the translational landscape in cancers through 5'UTR features of mTOR responsive mRNAs (66, 74, 75). While in Chapter 4 we identified a candidate mRNA, the *Aicda*

transcript encoding AID, which other mRNAs are regulated by the mTOR/4E-BP/eIF4E axis during B cell differentiation is a remaining question.

The PI3K/mTOR/eIF4E network is complex in that each component plays different roles in directing B cell differentiation and all these signals are integrated to contribute to the overall outcome of B cell function. Investigation of this pathway in promoting effective host immune response and the effects of pathway inhibitors on B cell antibody responses will have significant implications for human related disease.

References

1. Fruman, D.A., H. Chiu, B.D. Hopkins, S. Bagrodia, L.C. Cantley, and R.T. Abraham. 2017. The PI3K pathway in human disease. Cell. 170: 605–635.

2. Charles A Janeway, J., P. Travers, M. Walport, and M.J. Shlomchik. 2001. The Humoral Immune Response - Immunobiology - NCBI Bookshelf. .

3. Suan, D., C. Sundling, and R. Brink. 2017. Plasma cell and memory B cell differentiation from the germinal center. Curr Opin Immunol. 45: 97–102.

4. Bai, L., S. Deng, R. Reboulet, R. Mathew, L. Teyton, P.B. Savage, and A. Bendelac. 2013. Natural killer T (NKT)-B-cell interactions promote prolonged antibody responses and long-term memory to pneumococcal capsular polysaccharides. Proc Natl Acad Sci U S A. 110: 16097–16102.

5. Gaya, M., P. Barral, M. Burbage, S. Aggarwal, B. Montaner, A. Warren Navia, M. Aid, C. Tsui, P. Maldonado, U. Nair, K. Ghneim, P.G. Fallon, R.-P. Sekaly, D.H. Barouch, A.K. Shalek, A. Bruckbauer, J. Strid, and F.D. Batista. 2018. Initiation of Antiviral B Cell Immunity Relies on Innate Signals from Spatially Positioned NKT Cells. Cell. 172: 517–533.e20.

6. Reif, K., E.H. Ekland, L. Ohl, H. Nakano, M. Lipp, R. Förster, and J.G. Cyster. 2002. Balanced responsiveness to chemoattractants from adjacent zones determines B-cell position. Nature. 416: 94–99.

7. Haynes, N.M., C.D.C. Allen, R. Lesley, K.M. Ansel, N. Killeen, and J.G. Cyster. 2007. Role of CXCR5 and CCR7 in follicular Th cell positioning and appearance of a programmed cell death gene-1high germinal center-associated subpopulation. J Immunol. 179: 5099–5108.

8. Breitfeld, D., L. Ohl, E. Kremmer, J. Ellwart, F. Sallusto, M. Lipp, and R. Förster. 2000. Follicular B helper T cells express CXC chemokine receptor 5, localize to B cell follicles, and support immunoglobulin production. J Exp Med. 192: 1545–1552.

9. Xu, Z., H. Zan, E.J. Pone, T. Mai, and P. Casali. 2012. Immunoglobulin class-switch DNA recombination: induction, targeting and beyond. Nat Rev Immunol. 12: 517–531.

10. Revy, P., T. Muto, Y. Levy, F. Geissmann, A. Plebani, O. Sanal, N. Catalan, M. Forveille, R. Dufourcq-Labelouse, A. Gennery, I. Tezcan, F. Ersoy, H. Kayserili, A.G. Ugazio, N. Brousse, M. Muramatsu, L.D. Notarangelo, K. Kinoshita, T. Honjo, A. Fischer, and A. Durandy. 2000. Activation-induced cytidine deaminase (AID) deficiency causes the autosomal recessive form of the Hyper-IgM syndrome (HIGM2). Cell. 102: 565–575.

11. Okazaki, I., H. Hiai, N. Kakazu, S. Yamada, M. Muramatsu, K. Kinoshita, and T. Honjo. 2003. Constitutive expression of AID leads to tumorigenesis. J Exp Med. 197: 1173–1181.

12. White, C.A., J. Seth Hawkins, E.J. Pone, E.S. Yu, A. Al-Qahtani, T. Mai, H. Zan, and P. Casali. 2011. AID dysregulation in lupus-prone MRL/Fas(lpr/lpr) mice increases class switch DNA recombination and promotes interchromosomal c-Myc/IgH loci translocations: modulation by HoxC4. Autoimmunity. 44: 585–598.

13. Palacios, F., P. Moreno, P. Morande, C. Abreu, A. Correa, V. Porro, A.I. Landoni, R. Gabus, M. Giordano, G. Dighiero, O. Pritsch, and P. Oppezzo. 2010. High expression of AID and active class switch recombination might account for a more aggressive disease in unmutated CLL patients: link with an activated microenvironment in CLL disease. Blood. 115: 4488–4496.

14. Crouch, E.E., Z. Li, M. Takizawa, S. Fichtner-Feigl, P. Gourzi, C. Montaño, L. Feigenbaum, P. Wilson, S. Janz, F.N. Papavasiliou, and R. Casellas. 2007. Regulation of AID expression in the immune response. J Exp Med. 204: 1145–1156.

15. Wang, J., S. Liu, B. Hou, M. Yang, Z. Dong, H. Qi, and W. Liu. 2018. PTEN-Regulated AID Transcription in Germinal Center B Cells Is Essential for the Class-Switch Recombination and IgG Antibody Responses. Front Immunol. 9: 371.

16. Park, S.-R., H. Zan, Z. Pal, J. Zhang, A. Al-Qahtani, E.J. Pone, Z. Xu, T. Mai, and P. Casali. 2009. HoxC4 binds to the promoter of the cytidine deaminase AID gene to induce AID expression, class-switch DNA recombination and somatic hypermutation. Nat Immunol. 10: 540–550.

17. He, M., E.M. Cortizas, R.E. Verdun, and E. Severinson. 2015. Cyclin-dependent kinases regulate Ig class switching by controlling access of AID to the switch region. J Immunol. 194: 4231–4239.

18. Limon, J.J., and D.A. Fruman. 2012. Akt and mTOR in B Cell Activation and Differentiation. Front Immunol. 3: 228.

19. Okkenhaug, K., and B. Vanhaesebroeck. 2003. PI3K in lymphocyte development, differentiation and activation. Nat Rev Immunol. 3: 317–330.

20. Hawkins, P.T., and L.R. Stephens. 2015. PI3K signalling in inflammation. Biochim Biophys Acta. 1851: 882–897.

21. Dengler, H.S., G.V. Baracho, S.A. Omori, S. Bruckner, K.C. Arden, D.H. Castrillon, R.A. DePinho, and R.C. Rickert. 2008. Distinct functions for the transcription factor Foxo1 at various stages of B cell differentiation. Nat Immunol. 9: 1388–1398.

22. So, L., S.S. Yea, J.S. Oak, M. Lu, A. Manmadhan, Q.H. Ke, M.R. Janes, L.V. Kessler, J.M. Kucharski, L.-S. Li, M.B. Martin, P. Ren, K.A. Jessen, Y. Liu, C. Rommel, and D.A. Fruman. 2013. Selective inhibition of phosphoinositide 3-kinase p110α preserves lymphocyte function. J Biol Chem. 288: 5718–5731.

23. Ramadani, F., D.J. Bolland, F. Garcon, J.L. Emery, B. Vanhaesebroeck, A.E. Corcoran, and K. Okkenhaug. 2010. The PI3K isoforms p110alpha and p110delta are essential for pre-B cell receptor signaling and B cell development. Sci Signal. 3: ra60.

24. Beer-Hammer, S., E. Zebedin, M. von Holleben, J. Alferink, B. Reis, P. Dresing, D. Degrandi, S. Scheu, E. Hirsch, V. Sexl, K. Pfeffer, B. Nürnberg, and R.P. Piekorz. 2010. The catalytic PI3K isoforms p110gamma and p110delta contribute to B cell development and maintenance, transformation, and proliferation. J Leukoc Biol. 87: 1083–1095.

25. Omori, S.A., M.H. Cato, A. Anzelon-Mills, K.D. Puri, M. Shapiro-Shelef, K. Calame, and R.C. Rickert. 2006. Regulation of class-switch recombination and plasma cell differentiation by phosphatidylinositol 3-kinase signaling. Immunity. 25: 545–557.

26. Conley, M.E., A.K. Dobbs, A.M. Quintana, A. Bosompem, Y.-D. Wang, E. Coustan-Smith, A.M. Smith, E.E. Perez, and P.J. Murray. 2012. Agammaglobulinemia and absent B lineage cells in a patient lacking the p85α subunit of PI3K. J Exp Med. 209: 463–470.

27. Angulo, I., O. Vadas, F. Garçon, E. Banham-Hall, V. Plagnol, T.R. Leahy, H. Baxendale, T. Coulter, J. Curtis, C. Wu, K. Blake-Palmer, O. Perisic, D. Smyth, M. Maes, C. Fiddler, J. Juss, D. Cilliers, G. Markelj, A. Chandra, G. Farmer, A. Kielkowska, J. Clark, S. Kracker, M. Debré, C. Picard, I. Pellier, N. Jabado, J.A. Morris, G. Barcenas-Morales, A. Fischer, L. Stephens, P. Hawkins, J.C. Barrett, M. Abinun, M. Clatworthy, A. Durandy, R. Doffinger, E.R. Chilvers, A.J. Cant, D. Kumararatne, K. Okkenhaug, R.L. Williams, A. Condliffe, and S. Nejentsev. 2013. Phosphoinositide 3-kinase δ gene mutation predisposes to respiratory infection and airway damage. Science. 342: 866–871.

28. Deau, M.-C., L. Heurtier, P. Frange, F. Suarez, C. Bole-Feysot, P. Nitschke, M. Cavazzana, C. Picard, A. Durandy, A. Fischer, and S. Kracker. 2014. A human immunodeficiency caused by mutations in the PIK3R1 gene. J Clin Invest. 124: 3923–3928.

29. Lin, W.-H.W., W.C. Adams, S.A. Nish, Y.-H. Chen, B. Yen, N.J. Rothman, R. Kratchmarov, T. Okada, U. Klein, and S.L. Reiner. 2015. Asymmetric PI3K signaling driving developmental and regenerative cell fate bifurcation. Cell Rep. 13: 2203–2218.

30. Sander, S., V.T. Chu, T. Yasuda, A. Franklin, R. Graf, D.P. Calado, S. Li, K. Imami, M. Selbach, M. Di Virgilio, L. Bullinger, and K. Rajewsky. 2015. PI3 kinase and FOXO1 transcription factor activity differentially control B cells in the germinal center light and dark zones. Immunity. 43: 1075–1086.

31. Dominguez-Sola, D., J. Kung, A.B. Holmes, V.A. Wells, T. Mo, K. Basso, and R. Dalla-Favera. 2015. The FOXO1 transcription factor instructs the germinal center dark zone program. Immunity. 43: 1064–1074.

32. Yang, Q., P. Modi, T. Newcomb, C. Quéva, and V. Gandhi. 2015. Idelalisib: First-in-Class PI3K Delta Inhibitor for the Treatment of Chronic Lymphocytic Leukemia, Small Lymphocytic Leukemia, and Follicular Lymphoma. Clin Cancer Res. 21: 1537–1542.

33. Rao, V.K., S. Webster, V.A.S.H. Dalm, A. Šedivá, P.M. van Hagen, S. Holland, S.D. Rosenzweig, A.D. Christ, B. Sloth, M. Cabanski, A.D. Joshi, S. de Buck, J. Doucet, D. Guerini, C. Kalis, I. Pylvaenaeinen, N. Soldermann, A. Kashyap, G. Uzel, M.J. Lenardo, D.D. Patel, C.L. Lucas, and C. Burkhart. 2017. Effective "activated PI3Kδ syndrome"-targeted therapy with the PI3Kδ inhibitor leniolisib. Blood. 130: 2307–2316.

34. Winkler, D.G., K.L. Faia, J.P. DiNitto, J.A. Ali, K.F. White, E.E. Brophy, M.M. Pink, J.L. Proctor, J. Lussier, C.M. Martin, J.G. Hoyt, B. Tillotson, E.L. Murphy, A.R. Lim, B.D. Thomas, J.R. Macdougall, P. Ren, Y. Liu, L.-S. Li, K.A. Jessen, C.C. Fritz, J.L. Dunbar, J.R. Porter, C. Rommel, V.J. Palombella, P.S. Changelian, and J.L. Kutok. 2013. PI3K-δ and PI3K-γ inhibition by IPI-145 abrogates immune responses and suppresses activity in autoimmune and inflammatory disease models. Chem Biol. 20: 1364–1374.

35. Dong, S., D. Guinn, J.A. Dubovsky, Y. Zhong, A. Lehman, J. Kutok, J.A. Woyach, J.C. Byrd, and A.J. Johnson. 2014. IPI-145 antagonizes intrinsic and extrinsic survival signals in chronic lymphocytic leukemia cells. Blood. 124: 3583–3586.

36. Horwitz, S.M., R. Koch, P. Porcu, Y. Oki, A. Moskowitz, M. Perez, P. Myskowski, A. Officer, J.D. Jaffe, S.N. Morrow, K. Allen, M. Douglas, H. Stern, J. Sweeney, P. Kelly, V. Kelly, J.C. Aster, D. Weaver, F.M. Foss, and D.M. Weinstock. 2018. Activity of the PI3K-δ,γ inhibitor duvelisib in a phase 1 trial and preclinical models of T-cell lymphoma. Blood. 131: 888–898.

37. Davis, R.J., E.C. Moore, P.E. Clavijo, J. Friedman, H. Cash, Z. Chen, C. Silvin, C. Van Waes, and C. Allen. 2017. Anti-PD-L1 Efficacy Can Be Enhanced by Inhibition of Myeloid-Derived Suppressor Cells with a Selective Inhibitor of PI3Kδ/γ. Cancer Res. 77: 2607–2619.

38. Saxton, R.A., and D.M. Sabatini. 2017. mTOR Signaling in Growth, Metabolism, and Disease. Cell. 168: 960–976.

39. Choo, A.Y., S.-O. Yoon, S.G. Kim, P.P. Roux, and J. Blenis. 2008. Rapamycin differentially inhibits S6Ks and 4E-BP1 to mediate cell-type-specific repression of mRNA translation. Proc Natl Acad Sci U S A. 105: 17414–17419.

40. Sarbassov, D.D., S.M. Ali, S. Sengupta, J.-H. Sheen, P.P. Hsu, A.F. Bagley, A.L. Markhard, and D.M. Sabatini. 2006. Prolonged rapamycin treatment inhibits mTORC2 assembly and Akt/PKB. Mol Cell. 22: 159–168.

41. Vézina, C., A. Kudelski, and S.N. Sehgal. 1975. Rapamycin (AY-22,989), a new antifungal antibiotic. I. Taxonomy of the producing streptomycete and isolation of the active principle. J Antibiot. 28: 721–726.

42. Martel, R.R., J. Klicius, and S. Galet. 1977. Inhibition of the immune response by rapamycin, a new antifungal antibiotic. Can J Physiol Pharmacol. 55: 48–51.

43. Aagaard-Tillery, K.M., and D.F. Jelinek. 1994. Inhibition of human B lymphocyte cell cycle progression and differentiation by rapamycin. Cell Immunol. 156: 493–507.

44. Kay, J.E., L. Kromwel, S.E. Doe, and M. Denyer. 1991. Inhibition of T and B lymphocyte proliferation by rapamycin. Immunology. 72: 544–549.

45. Kim, H.S., J. Raskova, D. Degiannis, and K. Raska. 1994. Effects of cyclosporine and rapamycin on immunoglobulin production by preactivated human B cells. Clin Exp Immunol. 96: 508–512.

46. Delgoffe, G.M., T.P. Kole, Y. Zheng, P.E. Zarek, K.L. Matthews, B. Xiao, P.F. Worley, S.C. Kozma, and J.D. Powell. 2009. The mTOR kinase differentially regulates effector and regulatory T cell lineage commitment. Immunity. 30: 832–844.

47. Araki, K., A.P. Turner, V.O. Shaffer, S. Gangappa, S.A. Keller, M.F. Bachmann, C.P. Larsen, and R. Ahmed. 2009. mTOR regulates memory CD8 T-cell differentiation. Nature. 460: 108–112.

48. Keating, R., T. Hertz, M. Wehenkel, T.L. Harris, B.A. Edwards, J.L. McClaren, S.A. Brown, S. Surman, Z.S. Wilson, P. Bradley, J. Hurwitz, H. Chi, P.C. Doherty, P.G. Thomas, and M.A. McGargill. 2013. The kinase mTOR modulates the antibody response to provide cross-protective immunity to lethal infection with influenza virus. Nat Immunol. 14: 1266–1276.

49. Jones, D.D., B.T. Gaudette, J.R. Wilmore, I. Chernova, A. Bortnick, B.M. Weiss, and D. Allman. 2016. mTOR has distinct functions in generating versus sustaining humoral immunity. J Clin Invest. .

50. Ye, L., J. Lee, L. Xu, A.-U.-R. Mohammed, W. Li, J.S. Hale, W.G. Tan, T. Wu, C.W. Davis, R. Ahmed, and K. Araki. 2017. mTOR Promotes Antiviral Humoral Immunity by Differentially Regulating CD4 Helper T Cell and B Cell Responses. J Virol. 91.

51. Raybuck, A.L., S.H. Cho, J. Li, M.C. Rogers, K. Lee, C.L. Williams, M. Shlomchik, J.W. Thomas, J. Chen, J.V. Williams, and M.R. Boothby. 2018. B Cell–Intrinsic mTORC1 Promotes Germinal Center–Defining Transcription Factor Gene Expression, Somatic Hypermutation, and Memory B Cell Generation in Humoral Immunity. The Journal of Immunology. .

52. Ersching, J., A. Efeyan, L. Mesin, J.T. Jacobsen, G. Pasqual, B.C. Grabiner, D. Dominguez-Sola, D.M. Sabatini, and G.D. Victora. 2017. Germinal Center Selection and Affinity Maturation Require Dynamic Regulation of mTORC1 Kinase. Immunity. 46: 1045–1058.e6.

53. Cho, S.H., A.L. Raybuck, K. Stengel, M. Wei, T.C. Beck, E. Volanakis, J.W. Thomas, S. Hiebert, V.H. Haase, and M.R. Boothby. 2016. Germinal centre hypoxia and regulation of antibody qualities by a hypoxia response system. Nature. 537: 234–238.

54. Limon, J.J., L. So, S. Jellbauer, H. Chiu, J. Corado, S.M. Sykes, M. Raffatellu, and D.A. Fruman. 2014. mTOR kinase inhibitors promote antibody class switching via mTORC2 inhibition. Proc Natl Acad Sci U S A. 111: E5076–85.

55. Lee, K., L. Heffington, J. Jellusova, K.T. Nam, A. Raybuck, S.H. Cho, J.W. Thomas, R.C. Rickert, and M. Boothby. 2013. Requirement for Rictor in homeostasis and function of mature B lymphoid cells. Blood. 122: 2369–2379.

56. Magnuson, B., B. Ekim, and D.C. Fingar. 2012. Regulation and function of ribosomal protein S6 kinase (S6K) within mTOR signalling networks. Biochem J. 441: 1–21.

57. So, L., J. Lee, M. Palafox, S. Mallya, C.G. Woxland, M. Arguello, M.L. Truitt, N. Sonenberg, D. Ruggero, and D.A. Fruman. 2016. The 4E-BP-eIF4E axis promotes rapamycin-sensitive growth and proliferation in lymphocytes. Sci Signal. 9: ra57.

58. Rodrik-Outmezguine, V.S., M. Okaniwa, Z. Yao, C.J. Novotny, C. McWhirter, A. Banaji, H. Won, W. Wong, M. Berger, E. de Stanchina, D.G. Barratt, S. Cosulich, T. Klinowska, N. Rosen, and K.M. Shokat. 2016. Overcoming mTOR resistance mutations with a new-generation mTOR inhibitor. Nature. 534: 272–276.

59. Janes, M.R., J.J. Limon, L. So, J. Chen, R.J. Lim, M.A. Chavez, C. Vu, M.B. Lilly, S. Mallya, S.T. Ong, M. Konopleva, M.B. Martin, P. Ren, Y. Liu, C. Rommel, and D.A. Fruman. 2010. Effective and selective targeting of leukemia cells using a TORC1/2 kinase inhibitor. Nat Med. 16: 205–213.

60. Fan, Q., O. Aksoy, R.A. Wong, S. Ilkhanizadeh, C.J. Novotny, W.C. Gustafson, A.Y.-Q. Truong, G. Cayanan, E.F. Simonds, D. Haas-Kogan, J.J. Phillips, T. Nicolaides, M. Okaniwa, K.M. Shokat, and W.A. Weiss. 2017. A Kinase Inhibitor Targeted to mTORC1 Drives Regression in Glioblastoma. Cancer Cell. 31: 424–435.

61. Mallya, S., B.A. Fitch, J.S. Lee, L. So, M.R. Janes, and D.A. Fruman. 2014. Resistance to mTOR kinase inhibitors in lymphoma cells lacking 4EBP1. PLoS ONE. 9: e88865.

62. Alain, T., M. Morita, B.D. Fonseca, A. Yanagiya, N. Siddiqui, M. Bhat, D. Zammit, V. Marcus, P. Metrakos, L.-A. Voyer, V. Gandin, Y. Liu, I. Topisirovic, and N. Sonenberg. 2012. eIF4E/4E-BP ratio predicts the efficacy of mTOR targeted therapies. Cancer Res. 72: 6468–6476.

63. Malka-Mahieu, H., M. Newman, L. Désaubry, C. Robert, and S. Vagner. 2017. Molecular Pathways: The eIF4F Translation Initiation Complex-New Opportunities for Cancer Treatment. Clin Cancer Res. 23: 21–25.

64. Pelletier, J., J. Graff, D. Ruggero, and N. Sonenberg. 2015. Targeting the eIF4F translation initiation complex: a critical nexus for cancer development. Cancer Res. 75: 250–263.

65. Shull, A.Y., S.K. Noonepalle, F.T. Awan, J. Liu, L. Pei, R.J. Bollag, H. Salman, Z. Ding, and H. Shi. 2015. RPPA-based protein profiling reveals eIF4G overexpression and 4E-BP1 serine 65 phosphorylation as molecular events that correspond with a pro-survival phenotype in chronic lymphocytic leukemia. Oncotarget. 6: 14632–14645.

66. Hsieh, A.C., Y. Liu, M.P. Edlind, N.T. Ingolia, M.R. Janes, A. Sher, E.Y. Shi, C.R. Stumpf, C. Christensen, M.J. Bonham, S. Wang, P. Ren, M. Martin, K. Jessen, M.E. Feldman, J.S. Weissman, K.M. Shokat, C. Rommel, and D. Ruggero. 2012. The translational landscape of mTOR signalling steers cancer initiation and metastasis. Nature. 485: 55–61.

67. Hsieh, A.C., M. Costa, O. Zollo, C. Davis, M.E. Feldman, J.R. Testa, O. Meyuhas, K.M. Shokat, and D. Ruggero. 2010. Genetic dissection of the oncogenic mTOR pathway reveals druggable addiction to translational control via 4EBP-eIF4E. Cancer Cell. 17: 249–261.

68. Boussemart, L., H. Malka-Mahieu, I. Girault, D. Allard, O. Hemmingsson, G. Tomasic, M. Thomas, C. Basmadjian, N. Ribeiro, F. Thuaud, C. Mateus, E. Routier, N. Kamsu-Kom, S. Agoussi, A.M. Eggermont, L. Désaubry, C. Robert, and S. Vagner. 2014. eIF4F is a nexus of resistance to anti-BRAF and anti-MEK cancer therapies. Nature. 513: 105–109.

69. Moerke, N.J., H. Aktas, H. Chen, S. Cantel, M.Y. Reibarkh, A. Fahmy, J.D. Gross, A. Degterev, J. Yuan, M. Chorev, J.A. Halperin, and G. Wagner. 2007. Small-molecule inhibition of the interaction between the translation initiation factors eIF4E and eIF4G. Cell. 128: 257–267.

70. Feng, Y., A.B. Pinkerton, L. Hulea, T. Zhang, M.A. Davies, S. Grotegut, Y. Cheli, H. Yin, E. Lau, H. Kim, S.K. De, E. Barile, M. Pellecchia, M. Bosenberg, J.-L. Li, B. James, C.A. Hassig, K.M. Brown, I. Topisirovic, and Z.A. Ronai. 2015. SBI-0640756 Attenuates the Growth of Clinically Unresponsive Melanomas by Disrupting the eIF4F Translation Initiation Complex. Cancer Res. 75: 5211–5218.

71. Truitt, M.L., C.S. Conn, Z. Shi, X. Pang, T. Tokuyasu, A.M. Coady, Y. Seo, M. Barna, and D. Ruggero. 2015. Differential Requirements for eIF4E Dose in Normal Development and Cancer. Cell. 162: 59–71.

72. Araki, K., M. Morita, A.G. Bederman, B.T. Konieczny, H.T. Kissick, N. Sonenberg, and R. Ahmed. 2017. Translation is actively regulated during the differentiation of CD8+effector T cells. Nat Immunol. 18: 1046–1057.

73. Bjur, E., O. Larsson, E. Yurchenko, L. Zheng, V. Gandin, I. Topisirovic, S. Li, C.R. Wagner, N. Sonenberg, and C.A. Piccirillo. 2013. Distinct translational control in CD4+ T cell subsets. PLoS Genet. 9: e1003494.

74. Gandin, V., L. Masvidal, L. Hulea, S.-P. Gravel, M. Cargnello, S. McLaughlan, Y. Cai, P. Balanathan, M. Morita, A. Rajakumar, L. Furic, M. Pollak, J.A. Porco, J. St-Pierre, J. Pelletier, O. Larsson, and I. Topisirovic. 2016. nanoCAGE reveals 5' UTR features that define specific modes of translation of functionally related MTOR-sensitive mRNAs. Genome Res. 26: 636–648.

75. Thoreen, C.C., L. Chantranupong, H.R. Keys, T. Wang, N.S. Gray, and D.M. Sabatini. 2012. A unifying model for mTORC1-mediated regulation of mRNA translation. Nature. 485: 109–113.

CHAPTER 2

The Selective PI3K p110δ Inhibitor IPI-3063 Potently Suppresses B Cell Survival, Proliferation and Differentiation

This chapter contains text and figures from a manuscript published in *Frontiers of Immunology*, 8, p. 747 (2017) (1).

Abstract

The class I PI3Ks are important enzymes that relay signals from cell surface receptors to downstream mediators driving cellular functions. Elevated PI3K signaling is found in B cell malignancies and lymphocytes of patients with autoimmune disease. The p110δ catalytic isoform of PI3K is a rational target since it is critical for B lymphocyte development, survival, activation, and differentiation. In addition, activating mutations in *PIK3CD* encoding p110δ cause a human immunodeficiency known as activated PI3K delta syndrome (APDS). Currently idelalisib is the only selective p110δ inhibitor that has been FDA approved to treat certain B cell malignancies. p110δ inhibitors can suppress autoantibody production in mouse models but limited clinical trials in human autoimmunity have been performed with PI3K inhibitors to date. Thus, there is a need for additional tools to understand the effect of pharmacological inhibition of PI3K isoforms in lymphocytes. In this study, we tested the effects of a potent and selective p110δ inhibitor, IPI-3063, in assays of B cell function. We found that IPI-3063 potently reduced mouse B cell proliferation, survival, and plasmablast differentiation while increasing antibody class switching to IgG1, almost to the same degree as a pan-PI3K inhibitor. Similarly, IPI-3063 potently inhibited human B cell proliferation *in vitro*. The p110γ isoform has partially overlapping roles with p110δ in B cell development but little is known about its role in B cell function. We found

that the p110γ inhibitor AS-252424 had no significant impact on B cell responses. A novel dual p110δ/γ inhibitor, IPI-443, had comparable effects to p110δ inhibition alone. These findings show that p110δ is the dominant isoform mediating B cell responses and establish that IPI-3063 is a highly potent molecule useful for studying p110δ function in immune cells.

Introduction

Phosphoinoside-3-kinase (PI3K) enzymes are lipid kinases that produce 3'-phosphorylated phosphoinositides, which act as second messengers to relay signals from cell-surface receptors to downstream mediators. The class I PI3Ks produce phosphatidylinositol-3,4,5-triphosphate (PIP_3) that recruits cytoplasmic proteins to the membrane to drive downstream signaling responses. Class IA PI3Ks are heterodimers composed of two subunits, a regulatory subunit (p85) and one of three catalytic subunits (p110α, p110β, p110δ). The class IB PI3K is composed of unique regulatory subunits (p101 or p84) with the catalytic subunit p110γ. Whereas p110α and p110β are ubiquitously expressed, p110δ and p110γ expression is mainly restricted to leukocytes. The importance of PI3K activation in various cancers has led to development of many small molecule PI3K inhibitors targeting individual isoforms or subgroups (2).

Elevated PI3K signaling is commonly detected in malignant B cells and in peripheral lymphocytes from patients with antibody-driven autoimmune diseases like lupus (3). Both genetic and pharmacological studies have implicated p110δ to be critical for B lymphocyte development, survival, activation, and differentiation (4–6). Moreover, activating mutations in *PIK3CD* encoding p110δ cause a human immunodeficiency known as APDS, which is associated with chronically activated lymphocytes that undergo apoptosis or senescence (7,8). Therefore, p110δ has been extensively studied as a potential target for treating B cell

malignancies, B cell-mediated autoimmune diseases and potentially APDS. Impressive responses in clinical trials of idelalisib (previously known as GS-1101 or CAL-101) led to FDA approval of this drug for treatment of certain B cell malignancies (9).

Other p110δ inhibitors have shown activity in animal models of autoimmunity. For example, IC87114 reduced autoantibody production in a rat model of collagen-induced arthritis (10). Another recently developed p110δ inhibitor, AMG319, reduced KLH-specific IgM and IgG production *in vivo* (11) while duvelisib (IPI-145), a dual p110δ/γ inhibitor, showed potent activity in reducing inflammation in collagen-induced arthritis, ovalbumin-induced asthma, and systemic lupus erythematosus rodent models (12). Currently however, there are no approved treatments targeting p110δ in B-cell mediated autoimmune diseases. Additional p110δ inhibitors with high potency and selectivity are needed as research tools for B cell biology and as potential lead compounds for B cell-driven diseases. Characterizing the effects of isoform-selective PI3K inhibitors on normal B cell function will provide insight toward finding effective therapeutic windows that can target B cell malignancies while maintaining effective host defense, and may justify clinical exploration of these inhibitors in treating B cell mediated autoimmune disease.

Previous studies have demonstrated that p110δ is not the only PI3K isoform that contributes to B cell function. We used isoform-selective compounds to show that acute inhibition of either p110α or p110β partially reduce signaling and functional responses in activated B cells (13). Genetic analysis has shown partially overlapping roles of p110δ and p110α in B cell development (14). Little is known about the role of the class IB isoform p110γ in B cells. In T cells, p110γ plays a role in early development and is important for trafficking of activated effector cells (15,16). One study reported that mice lacking both p110δ and p110γ had

greater defects in B cell survival and proliferation compared to p110δ knockout alone (17). The effects of chemical p110γ inhibition on B cell function have not been reported.

In this study we utilized a novel, potent and selective p110δ inhibitor, IPI-3063 (**Table 2.1**) that has good pharmacokinetics in mice (12). Here we tested the effects of IPI-3063 on mouse B cell survival, proliferation and differentiation. We found that IPI-3063 is highly potent, modulating B cell responses at low nanomolar concentrations to an extent similar to a pan-PI3K inhibitor. In contrast, a selective chemical inhibitor of p110γ had no effect in various assays of B cell function. We also tested a novel dual p110δ/γ inhibitor, IPI-443 (**Table 2.1**), to determine whether p110γ inhibition increases the effects beyond blockade of p110δ alone. Dual inhibition of p110δ/γ with IPI-443 had comparable effects to IPI-3063 on B cell function. These results confirm that p110δ is the dominant isoform that mediates B cell responses to diverse stimuli and establish that IPI-3063 is a highly potent molecule to probe p110δ function in immune cells.

Table 2.1 Summary of IC_{50} values for IPI-3063 and IPI-443 using purified enzymes

PI3K isoform	Biochemical IC_{50}, nM (n)	
	IPI-3063	**IPI-443**
p110α	1171 ± 533 (6)	990 ± 695 (6)
p110β	1508 ± 624 (5)	4005 ± 2563 (6)
p110δ	2.5 ± 1.2 (5)	6.3 ± 3.2 (6)
p110γ	2187 ± 1529 (4)	23.4 ± 12.3 (6)

Materials and Methods

PI3K Enzymatic Assay (done by collaborators at Infinity Pharmaceuticals)

Human recombinant PI3K–α (cat. no. 14-602-K), –β (cat. no. 14-603-K), –δ (cat. no. 14-604-K) and –γ (cat. no. 14-558-K) were purchased from Millipore. Phosphatidylinositol 4,5 bis phosphate (diC8-PtdIns(4,5)P2) was purchased from Avanti Polar Lipids, Inc. PI3K–α, β and δ are heterodimers consisting of full length p110α, p110β or p110δ catalytic subunit and the p85α regulatory subunit. PI3K-γ is a monomer of the p110γ catalytic subunit. Sample of kinase (10 nM -α, –β, and –δ, 20 nM -γ) were incubated with inhibitor for 30 minutes at room temperature in reaction buffer (15 mM HEPES pH 7.4, 20 mM NaCl, 1 mM EGTA, 0.02% Tween 20, 10 mM MgCl2, 0.2 mg/ml bovine-γ-globulins) followed by addition of ATP/diC8-PtdIns(4,5)P2 mixture to give final concentrations of 3 mM ATP and 500 μM diC8-PtdIns(4,5)P2. Reactions were incubated at room temperature for 2 hours, with PI3K activity assessed via the Promega ADP-Glo Max assay kit (cat. no. V7002) according to the manufacture's instruction. Plates were read on Envision plate reader in luminescence mode.

pAKT S473 ELISA Assay (Infinity Pharmaceuticals, for data in Table 2)

Phospho-Akt1 (S473) sandwich ELISA antibody kit (Cell Signaling Technology, cat. no. 7143) was utilized to analyze pAKT signal in cells as described previously by Winkler et al.[11] Briefly, SKOV3 and 786.0 cells were seeded into 96 well cell culture-graded plates at a density of two million per 200 μl culture media per well. Raji and Raw264.7 were seeded at the same density in FBS-free media. After overnight incubation at 5% CO2 and 37°C, the cells were treated with inhibitor for 30 minutes. Raji cells were stimulated with 10 μg/mL anti-human IgM (Jackson ImmunoResearch) for 30 minutes and Raw264.7 cells with 25 nM C5a (RnD Systems) for 3 minute in the presence of inhibitor. SKOV3 and 786.0 cells were not stimulated. Media was then

aspirated and 50 μL/well of ice-cold lysis buffer was added. pAKT level was determined according to the manufacture's instruction.

Mice and reagents

C57BL/6 mice were bred at the University of California, Irvine, and used at between 6 and 12 weeks of age. All animals were studied in compliance with protocols approved by the Institutional Animal Care and Use Committees of the University of California, Irvine. The p110δ-selective PI3K inhibitor IPI-3063 and p110δ/γ PI3K inhibitor IPI-443 were synthesized at Infinity Pharmaceuticals. These compounds and the pan-PI3K class I inhibitor GDC-0941 (LC laboratories) were dissolved in DMSO. The p110γ PI3K inhibitor AS-252424 (Chemdea) was dissolved in ethanol. Inhibitors were included throughout the indicated cell treatment periods.

Mouse B cell culture

Mouse splenic B cells were purified by negative selection (eBioscience Magnisort Mouse B cell enrichment kit). B-cell purity was >95% as measured by FACS analysis (FACSCalibur and CellQuest software; BD Biosciences) using anti-B220 antibody (BioLegend). Purified B cells were seeded at a final concentration of 0.5 or 0.25 × 10^6 cells per milliliter. For plasmablast differentiation, B cells were stimulated with 5 μg/mL LPS (Sigma) for 72 h, and for IgG1 CSR, B cells were stimulated 5 μg/mL anti-CD40 (HM40-3) agonistic antibody (eBioscience), or 5 μg/mL LPS (Sigma), together with 5 ng/mL mIL-4 (R&D Systems) for 96 h. All B cells were cultured in RPMI 1640 supplemented with 10% (vol/vol) heat-inactivated FCS, 5 mM Hepes, 2 mM L-glutamine, 100 units/mL penicillin, 100 μg/mL streptomycin, 50 μM 2-mercaptoethanol.

Western Blotting Analysis

Analysis was performed on western blots using ImageJ to measure mean fluorescence intensities (MFI) of each band. Phosph-AKT S473 and phospho-ERK1/2 signal was normalized with actin measurements and fold change was calculated using the stimulated/no drug control.

Flow cytometry, CFSE labeling, and antibodies

Before cell surface staining, cells were incubated with TruStain fcX in FACS buffer (0.5% BSA + 0.02% NaN3 in 1× HBSS) to block Fc receptors for 10 min on ice. Staining with antibodies was subsequently performed, also with FACS buffer and on ice for 20 min. Flow cytometry antibodies and other reagents used were as follows: B220 (RA3-6B2), IgG1 (A85-1), CD138 (281-2), and 7-Aminoactinomycin D. CFSE labeling of B cells to track proliferation was performed by resuspending cells to a concentration of 10 × 10^6 cells per milliliter with a concentration of 2.5μM CFSE. Flow cytometric data were analyzed using FlowJo software (TreeStar).

Immunoglobulin ELISA

For cell culture ELISA to measure total IgM, supernatants from purified B cells stimulated with LPS were collected after 3 d and diluted 1:1000 in 2% (wt/vol) BSA in PBS. Nunc Maxisorp plates (Thermo Fisher) were coated with anti-mouse IgM (RMM-1; BioLegend) at 10 μg/mL in 50 μL of total sample in PBS and allowed to incubate overnight at 4 °C. Diluted supernatant samples were incubated on coated plates for 1 h at 37 °C. HRP-conjugated rabbit anti-mouse IgM secondary antibody (Zymed) was used.

Human B cell culture

Peripheral blood from normal volunteers was obtained through an Institutional Review Board (IRB)-approved protocol. Peripheral blood mononuclear cells (PBMCs) were first purified from blood by density gradient centrifugation using Ficoll-pacque. Human B cells were then purified from PBMCs by negative selection (eBioscience Magnisort Human B cell enrichment kit). B-cell purity was increased from 4% to >70% as measured by FACS analysis (FACSCalibur and CellQuest software; BD Biosciences) using anti-CD19 PE conjugated antibody (eBioscience). Purified B cells were seeded at a final concentration of 0.1 × 10^6 cells per milliliter and cultured with 2 μg/mL human CD40L (eBioscience) + 5 μg/mL anti-human IgM/IgG (eBioscience) + 100 U hIL-2 (R&D Systems) + 100 U hIL-21 (R&D Systems). All B cells were cultured in RPMI 1640 supplemented with 10% (vol/vol) heat-inactivated FCS, 5 mM Hepes, 2 mM L-glutamine, 100 units/mL penicillin, 100 μg/mL streptomycin, 50 μM 2-mercaptoethanol.

Results

Inhibition of p110δ, but not p110γ, reduces p-AKT in activated mouse B cells

IPI-3063 is a p110δ selective compound with an IC_{50} = 0.1 nM in p110δ-specific cell-based assays and cellular IC_{50} values for the other class I PI3K isoforms are at least 1000-fold higher (**Table 2.2**) (12). IPI-443 is a selective p110δ/γ dual inhibitor with a cellular IC_{50} = 0.29 nM for p110δ and IC_{50} = 7.1 nM for p110γ. IPI-443 activity for p110α and p110β is > 600-fold less potent compared to activity for p110δ **(Table 2.2)**. To test the effects of p110γ inhibition we used AS-252424 compound with a biochemical IC_{50} = 30nM for p110γ (18). We assessed the effects of both IPI-3063 and IPI-443 on PI3K activity in mouse primary B cells stimulated with αIgM+IL-4, by evaluating phosphorylation of AKT at the serine 473 residue **(Fig. 2.1A, 2.1C)**

Table 2.2. Summary of IC_{50} values for IPI-3063 and IPI-443 in isoform-specific cell-based assays

PI3K isoform	Cellular IC_{50}, nM (n)	
	IPI-3063	**IPI-443**
p110α	1901 ± 1318 (4)	901.8 ± 62.4 (3)
p110β	102.8 ± 35.7 (4)	185.2 ± 17.2 (3)
p110δ	0.1 ± 0.01 (6)	0.29 ± 0.03 (4)
p110γ	418.8 ± 117.2 (2)	7.1 ± 0.5 (3)

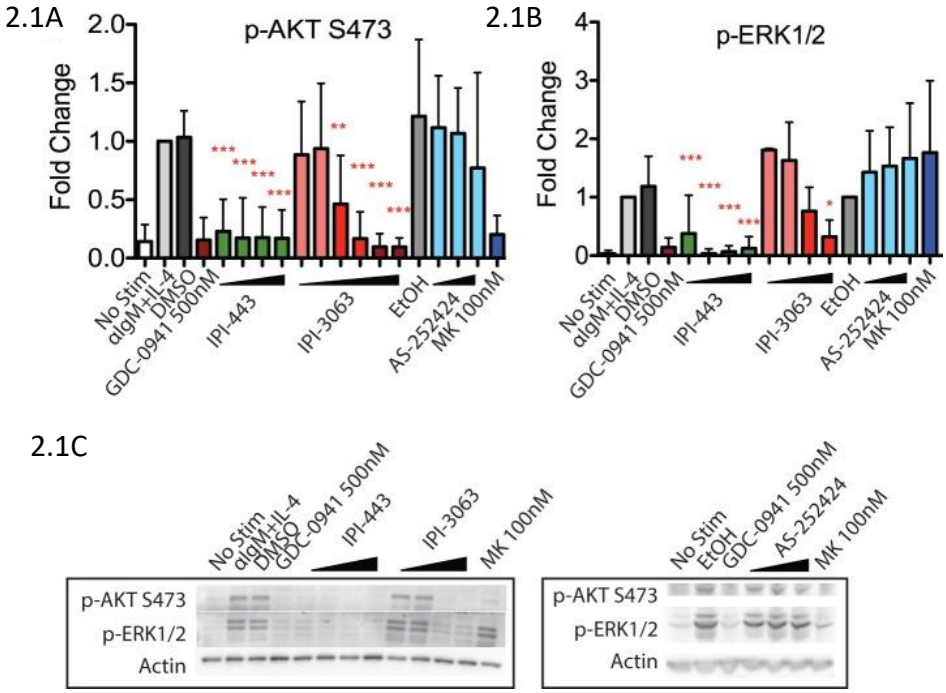

Figure 2.1 Inhibition of p110δ, but not p110γ, reduces p-AKT and p-ERK1/2 in αIgM+IL-4 stimulated mouse B cells. Purified B cells were pre-treated with inhibitors as indicated for 30 minutes then activated with 5 μg/mL αIgM+ 10ng/ml IL-4 for 1 hour before harvest for western blot. (2.1A, 2.1B) Concentrations used were 1nM, 10nM, 100nM, 1μM for IPI-443 and 0.01nM, 0.1nM, 1nM, 10nM, 30nM, 100nM for IPI-3063. AS252424 concentrations were 100nM, 300nM, and 1μM, and GDC-0941 was at 500nM. (2.1B, 2.1C) Concentrations of IPI-3063 used to measure p-ERK1/2 were 0.01nM, 0.1nM, 1nM, and 10nM. For the graphs in panels A and B, data were normalized to the stimulated, DMSO 0.1% condition. (*P < 0.05, **P<0.001, ***P<0.0001 one-way ANOVA with Newman–Keuls multiple comparison test).

as well as the phosphorylation of ERK1/2 on Thr202/Tyr204 residues **(Fig. 2.1B, 2.1C)**. Cells were treated with a pan-PI3K inhibitor GDC-0941 or with various concentrations of IPI-3063 or IPI-443, or DMSO (0.1%) as the diluent control. Separate cultures were treated with the p110γ inhibitor AS-252424 or its diluent control (0.1% EtOH). MK-2206, an AKT inhibitor which also reduces AKT S473 phosphorylation, was also used as a control to show ERK1/2 phosphorylation is independent of AKT activity. The p110δ inhibitor, IPI-3063, was very potent in reducing p-AKT (significant effect at 1nM) while the p110γ inhibitor, AS-252424, had no significant effect on p-AKT signaling. IPI-3063 also reduced p-ERK1/2 with a significant effect at 10nM, whereas AS-252424 had no significant effect. The dual p110δ/γ inhibitor, IPI-443, was also very potent in decreasing phosphorylation of AKT, with significant effects observed using concentrations as low as 1 nM, which are in the range where p110δ is targeted selectively. These data indicate that both inhibitors are very potent in reducing PI3K signaling output while p110γ inhibition did not have a significant effect. B cells stimulated with LPS showed similar results with p-AKT **(Fig. 2.2A-2.2C)**; however LPS did not induce ERK1/2 phosphorylation (data not shown). AS-252424 caused dose-dependent inhibition of AKT phosphorylation in bone marrow-derived myeloid cells stimulated with macrophage colony stimulating factor, confirming that this compound inhibits PI3Kγ activity in cells (data not shown).

IPI-3063 potently inhibits B cell survival and proliferation

To assess survival, purified mouse B cells were incubated for 48 hours in either B-cell activating factor (BAFF) or interleukin-4 (IL-4) with various concentrations of IPI-3063 and IPI-443. The results showed that both IPI-3063 and IPI-443 reduced BAFF-dependent survival in a

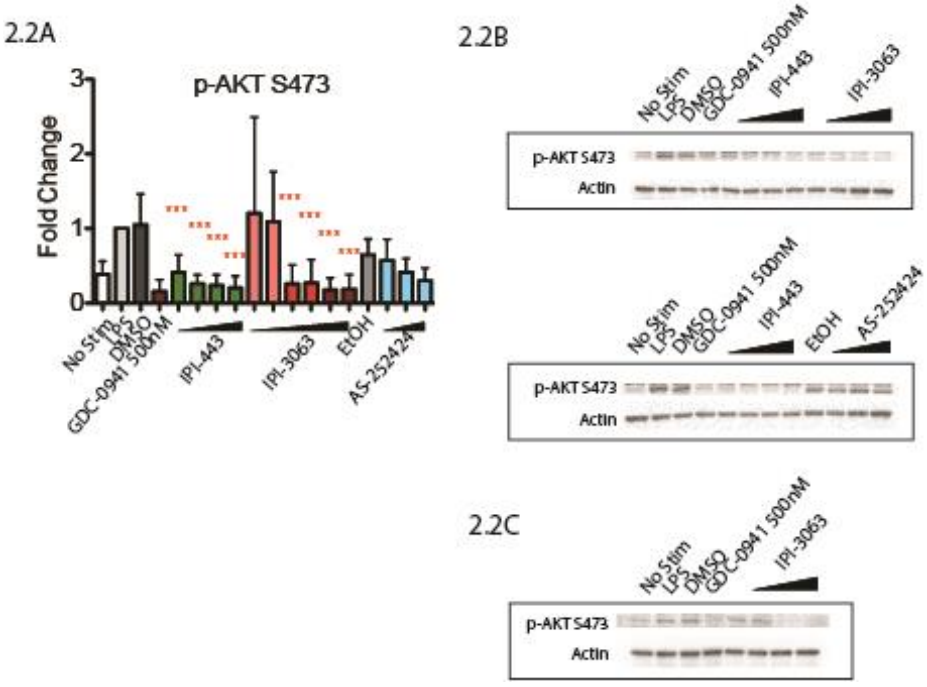

Figure 2.2 Inhibition of p110δ, but not p110γ, reduces p-AKT in LPS stimulated mouse B cells. Purified B cells were pre-treated with inhibitors as indicated for 30 minutes then activated with 5 μg/mL LPS for 1 hour before harvest for western blot. (2.2A, 2.2B) Concentrations used were 1nM, 10nM, 100nM, 1μM for IPI-443 and 1nM, 10nM, 30nM, 100nM for IPI-3063. AS252424 concentrations were 100nM, 300nM, and 1μM, and GDC-0941 was at 500nM. (2.2C) Concentrations of IPI-3063 were 0.01nM, 0.1nM, 1nM and 10nM. For the graph in panel 2.2A, data were normalized to the stimulated, DMSO 0.1% condition. (*P < 0.05, **P<0.001, ***P<0.0001 one-way ANOVA with Newman–Keuls multiple comparison test).

dose-dependent manner, approaching the effect of GDC-0941 **(Fig. 2.3).** The selective PI3K inhibitor IPI-3063 was very potent, achieving a significant decrease in B cell survival when present at 10nM. IPI-443 significantly decreased survival when added at 1nM. The p110γ inhibitor AS-252424 had no significant effect on survival. Cells incubated with IL-4 showed similar trends.

Next, we evaluated the effects of PI3K inhibitors on B cell proliferation. We stimulated CFSE-stained cells with αIgM + IL-4 or with LPs for 72 hr, or with αCD40 + IL-4 or LPS + IL-4 for 96 hours. Cells were treated with vehicle or GDC-0941, IPI-3063, IPI-443, or AS-252424

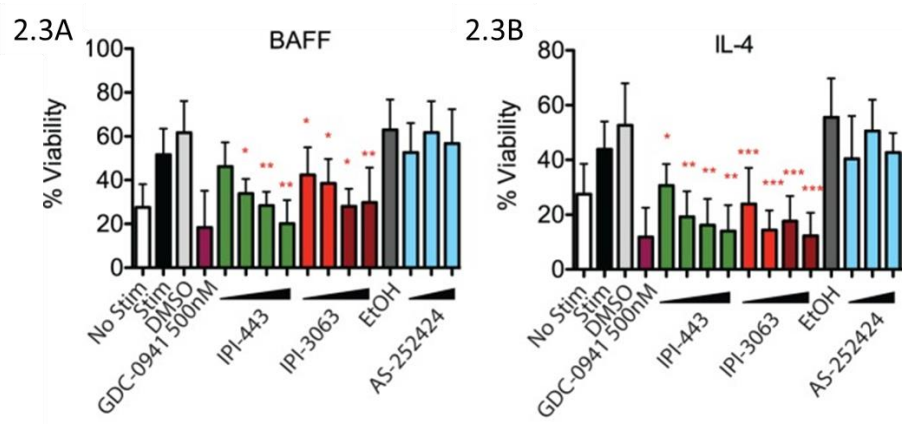

Figure 2.3 IPI-3063 potently inhibits mouse B cell survival. Total splenocytes were pre-treated with inhibitors as indicated then cultured with 5ng/mL IL-4 (2.3A) or 60ng/mL of BAFF (2.3B) for 48 hours. Concentrations used were 1nM, 10nM, 100nM, 1μM for IPI-443 and 1nM, 10nM, 30nM, 100nM for IPI-3063. AS252424 concentrations were 100nM, 300nM, and 1μM, and GDC-0941 was at 500nM. %Viability was calculated by measuring % of $B220^{+}7AAD^{-}$ cells. Samples were collected by time. (*P < 0.05, **P<0.001, ***P<0.0001 one-way ANOVA with Newman–Keuls multiple comparison test).

at various concentrations. Histograms of CFSE fluorescence in the cells show that IPI-3063 blocked proliferation in α-IgM + IL-4 stimulated B cells at the lowest concentration tested (1nM) **(Fig. 2.4A)**. IPI-443 caused a dose-dependent decrease in proliferation, whereas AS-252424 had no effect**.** We measured the total number of divided cells over multiple experiments and found that IPI-3063 significantly reduced cell accumulation at all concentrations tested **(Fig. 2.4B).** IPI-443 had a dose-dependent effect starting at 1nM, with similar effects in LPS stimulated B cells **(Fig. 2.4B, 2.4C)**. In B cells stimulated with LPS + IL-4, the inhibitors had similar trends but with greater variability **(Fig. 2.4D)**. The inhibitors did not affect B cell proliferation following stimulation with α-CD40 + IL-4 **(Fig. 2.4E)**, consistent with previous data showing PI3K-independent proliferation under these conditions (4). We also measured percent of divided cells in these conditions **(Fig. 2.5A-2.5D).** α-IgM+IL-4 was the only stimulus where p110δ inhibition significantly reduced the percentage of cells dividing. This analysis also showed that combined

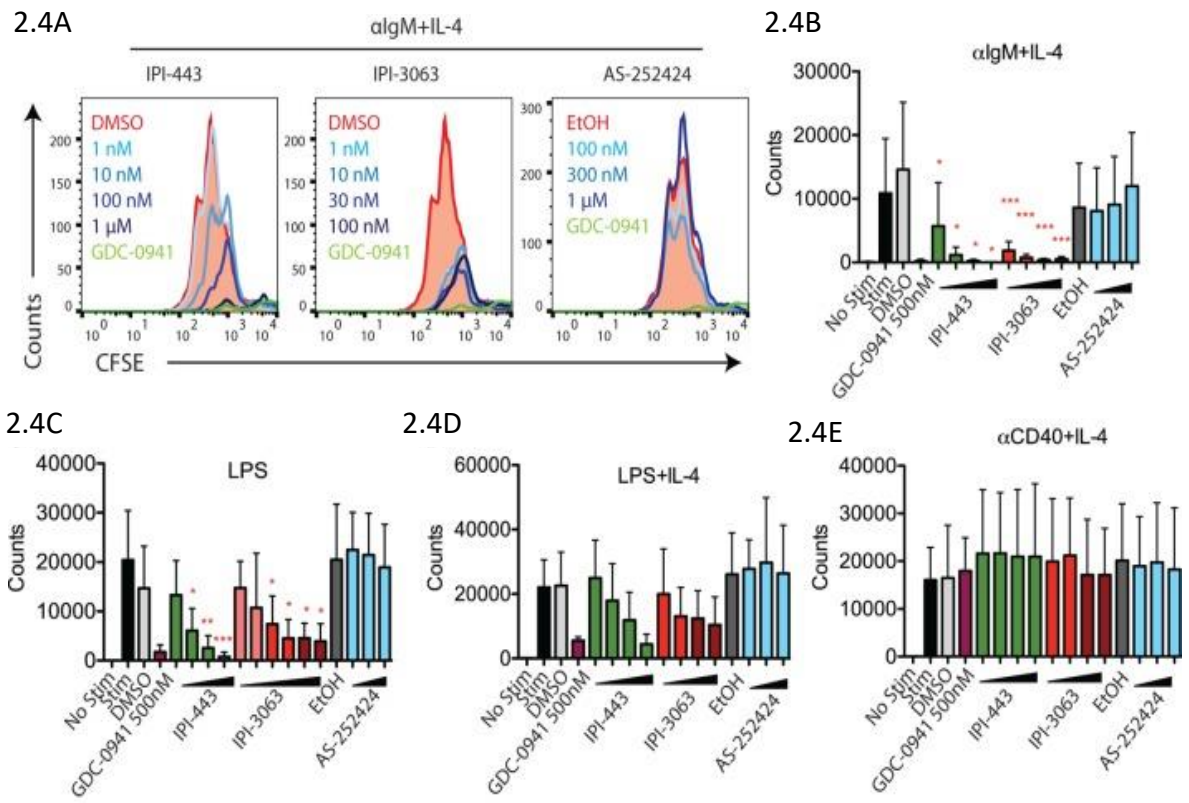

Figure 2.4 IPI-3063 potently inhibits mouse B cell proliferation. Total splenocytes (2.4A, 2.4B) or purified B cells (2.4C-2.4E) were pre-treated with inhibitors for 30 minutes then stimulated with (2.4A, 2.4B) αIgM+IL-4 for 72 hours, (2.4C-2.4E) LPS+IL-4 for 96 hours, LPS for 72 hours or αCD40+IL-4 for 96 hours. Concentrations used were 1nM, 10nM, 100nM, 1μM for IPI-443 and 1nM, 10nM, 30nM, 100nM for IPI-3063. AS252424 concentrations were 100nM, 300nM, and 1μM, and GDC-0941 was at 500nM. The experiments in panel C include low concentrations of IPI-3063 (0.01 and 0.1nM) Total numbers were determined by the number of $B220^{+}7AAD^{-}CFSE^{lo}$ cells. Samples were collected by time. (*P < 0.05, **P<0.001, ***P<0.0001 one-way ANOVA with Newman–Keuls multiple comparison test).

inhibition of p110δ/γ by IPI-443 at 1μM reduced the percentage of divided cells more than inhibition of p110δ only. Overall these experiments establish that the selective p110δ inhibitor IPI-3063 is a very potent inhibitor of B cell survival and proliferation *in vitro*. In addition, selective p110γ inhibition alone had no effect on B cell survival or proliferation.

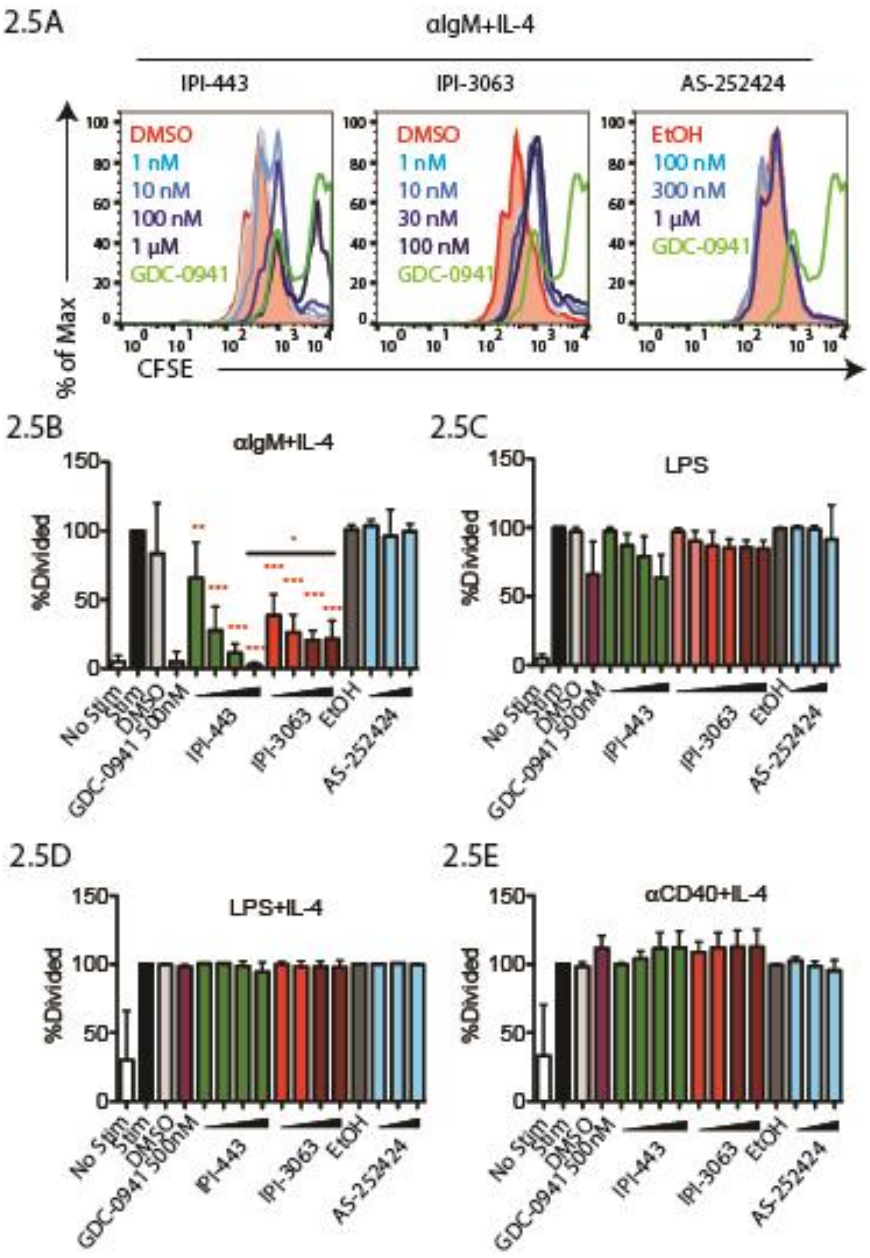

Figure 2.5 IPI-3063 potently inhibits mouse B cell proliferation, Part II. Total splenocytes (2.5A, 2.5B) or purified B cells (2.5C-2.5E) were pre-treated with inhibitors for 30 minutes then stimulated with (2.4A, 2.4B) αIgM+IL-4 for 72 hours, (2.5C-2.5E) LPS+IL-4 for 96 hours, LPS for 72 hours or αCD40+IL-4 for 96 hours. Concentrations used were 1nM, 10nM, 100nM, 1μM for IPI-443 and 1nM, 10nM, 30nM, 100nM for IPI-3063. AS252424 concentrations were 100nM, 300nM, and 1μM, and GDC-0941 was at 500nM. The experiments in panel C include low concentrations of IPI-3063 (0.01 and 0.1nM). Panel 2.5A shows proliferation of cells by CFSE histograms. Right peak in GDC and IPI-443 1μM treated cells represents dead cells. Percent divided were determined by the percent of $B220^{+}7AAD^{-}CFSE^{lo}$ cells and normalized to no drug treated. Samples were collected by time. (*P < 0.05, **P<0.001, ***P<0.0001 one-way ANOVA with Newman–Keuls multiple comparison test).

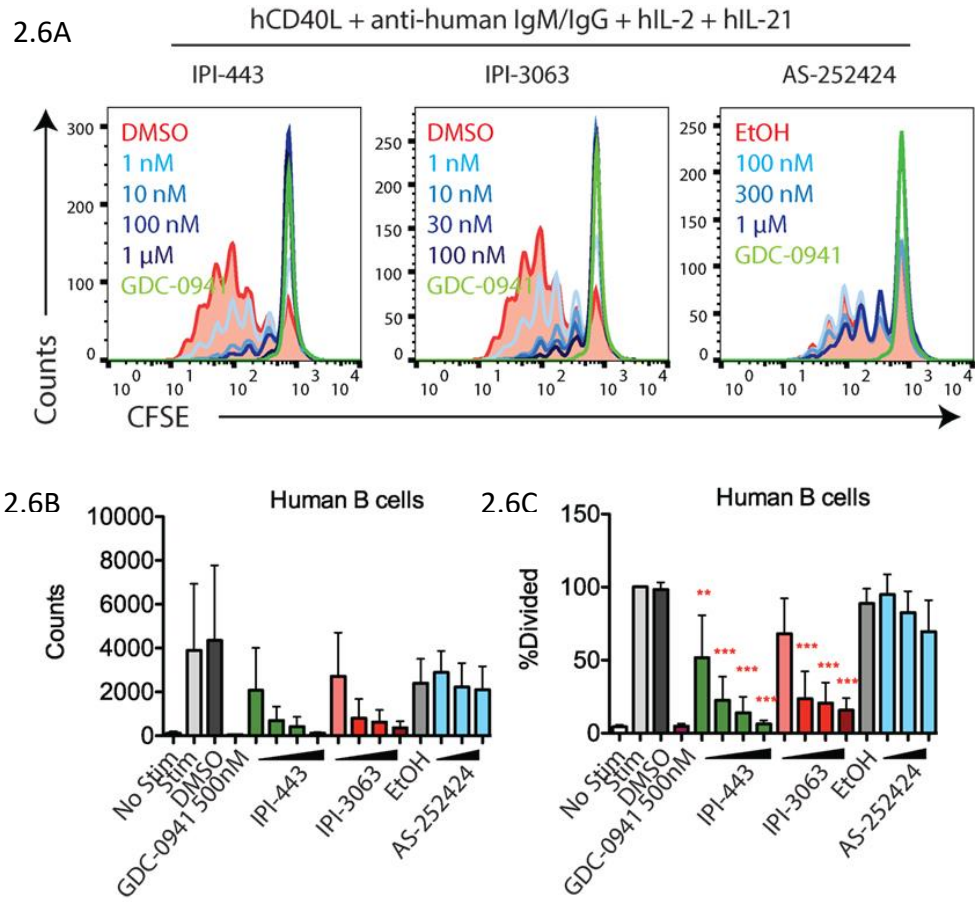

Figure 2.6 IPI-3063 potently inhibits human B cell proliferation. (2.6A-2.6C) Purified human B cells were pre-treated with inhibitors for 30 minutes then stimulated with human CD40L + anti-human IgM/IgG + human IL-2 + human IL-21 for 120 hours. Concentrations used were 1nM, 10nM, 100nM, and 1µM for IPI-443 and 0.1nM, 1nM, 10nM, and 100nM for IPI-3063. AS252424 concentrations were 100nM, 300nM, and 1µM, and GDC-0941 was at 500nM. Total numbers and percent divided were determined by the number of $CD19^{+}7AAD^{-}CFSE^{lo}$ cells. Samples were collected by time. (*P < 0.05, **P<0.001, ***P<0.0001 one-way ANOVA with Newman–Keuls multiple comparison test).

We also tested the effects of these inhibitors on human B cell proliferation stimulated with human CD40L + anti-human IgM/IgG + hIL-2 + hIL-21. We stimulated CFSE-stained human B cells for 120 hrs in the presence of GDC-0941, IPI-3063, IPI-443, or AS-252424 at various concentrations. Histograms of CFSE fluorescence in the cells show that IPI-3063 blocked proliferation at 1nM **(Fig. 2.6A)**. IPI-443 caused a dose-dependent decrease in proliferation, whereas AS-252424 had no effect**.** We measured the total number of divided cells

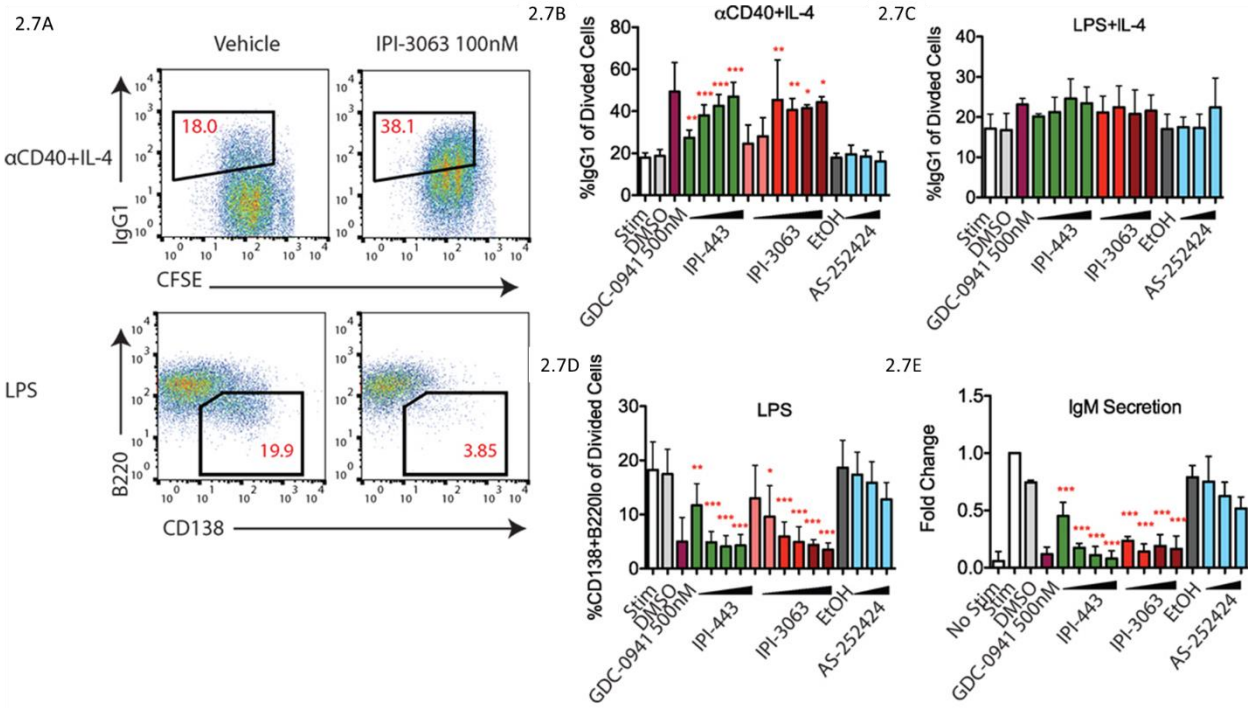

Figure 2.7 IPI-3063 potently promotes mouse B cell antibody switching and inhibits plasmablast differentiation. Purified B cells were with pre-treated with inhibitors then stimulated with αCD40+IL-4 (2.7B) or LPS+IL-4 (2.7C) for 96 hours to induce switching to IgG1 or LPS (2.7D) for 72 hours to induce plasmablast differentiation. Class switching to IgG1 was measured by the $7AAD^{-}CFSE^{lo}B220^{+}IgG1^{+}$ cells (2.7A, upper panels). Plasmablast percentages were calculated by % $7AAD^{-}CFSE^{lo}CD138^{+}B220^{lo}$ population (2.7A, lower). Supernatant was harvested (2.7E) for IgM ELISA. Concentrations used were 1nM, 10nM, 100nM, 1μM for IPI-443 and 1nM, 10nM, 30nM, 100nM for IPI-3063. Low concentrations of IPI-3063 were 0.01nM, and 0.1nM (2.7D). AS252424 concentrations were 100nM, 300nM, and 1μM, and GDC-0941 was at 500nM. Samples were collected by time. (*P < 0.05, **P<0.001, ***P<0.0001 one-way ANOVA with Newman–Keuls multiple comparison test).

and the percent divided over multiple experiments and found that IPI-3063 significantly reduced proliferation starting at 1nM **(Fig. 2.6B, 2.6C).** IPI-443 also had a dose-dependent effect starting at 1nM **(Fig. 2.6B, 2.6C)**. These experiments extend our findings by showing that, similar to mouse B cells, human B cells treated with the selective p110δ inhibitor IPI-3063 have markedly reduced ability to proliferate *in vitro.* In addition, selective p110γ inhibition also did not impair human B cell proliferation.

IPI-3063 potently promotes mouse B cell antibody switching and inhibits plasmablast differentiation

Studies with p110δ inhibitors have shown that low PI3K signaling in B cells promotes antibody class switch recombination (CSR) and decreases differentiation into plasmablasts that secrete low-affinity IgM (19,20). Activation of mouse primary B cells with αCD40 + IL-4 or LPS + IL-4 both induce IgG1 class switching while treatment with LPS alone induces the plasmablast differentiation fate **(Fig. 2.7A).** In B cells stimulated with αCD40 + IL-4, IPI-3063 increased the percentage of $B220^{+}$ cells switching to IgG1 starting at 1nM and approached the effect of GDC-0941 **(Fig. 2.7B).** IPI-443 followed a similar trend, significantly increasing IgG1 switching at concentrations of 1nM or higher, while p110γ inhibitor AS-252424 had no effect. **(Fig. 2.7B).** In cells activated with LPS+IL-4, none of the inhibitors significantly increased %IgG1+.

We also evaluated plasmablast differentiation and IgM secretion in LPS-stimulated cells **(Fig. 2.7D).** IPI-3063 potently decreased plasmablast differentiation starting at 1nM, as measured by the percentage of the $CD138^{+}B220^{lo}$ population. IPI-443 also caused a dose dependent decrease starting at 1nM. In cells treated with IPI-3063 or IPI-443, the highest concentrations inhibited plasmablast differentiation to the same degree as GDC-0941. Measuring IgM secretion by ELISA showed similar trends **(Fig. 2.7E).** In the plasmablast and IgM secretion assays, the p110γ inhibitor AS-252424 caused no significant effect.

Overall, these results show that IPI-3063 is very potent at increasing B cell antibody class switching to IgG1 in B cells stimulated with αCD40 + IL-4, while potently reducing plasmablast differentiation in cells stimulated with LPS. Combined inhibition of p110δ/γ by IPI-443 had a

similar effect that was not significantly greater than inhibition of p110δ only, and importantly, p110γ specific inhibition did not show any significant effect.

Discussion

In this study we have used novel inhibitors of p110δ, p110δ/γ and p110γ to study how acute inhibition of these isoforms impacts B cell function. Consistent with previous studies (6,19,21), our results show that p110δ inhibition decreased several mouse B cell functions including survival, αIgM+IL-4-induced proliferation, and plasmablast differentiation while increasing class switching to IgG1. We also show that these inhibitors are potent at reducing human B cell proliferation *in vitro.* Importantly, additional p110γ inhibition had little to no effect, indicating that the class IB isoform p110γ has a minor role in the function of mature B cells. Both IPI-3063 and IPI-443 were highly potent at inhibiting these B cell functions, with activity in the nanomolar ranges that achieved similar results to the pan-class I inhibitor GDC-0941.

In contrast with a previous study using genetic deletion of the mouse genes encoding both p110δ and p110γ (17), dual inhibition with IPI-443 (achieved at concentrations in the 10 – 1000nM range) did not reduce proliferation and survival more than p110δ inhibition alone in B cells. However, Beer-Hammer et al. also showed that B cell development was impaired at the pre-pro B cell stage when both p110δ/γ are deleted (17). The differences they observed in the double deleted cells compared to single p110δ deletion may be due to developmental defects. In addition, the previous study measured LPS-driven B cell proliferation in the context of total splenocytes, where myeloid cell cytokine production in response to LPS might be a confounding factor. While we did not see any additional effects with p110γ inhibition or additional effects

with dual p110δ/γ inhibition in our assays, these experiments only tested purified B cells *in vitro* and did not test the role of p110γ *in vivo*. Although B cell function is mainly p110δ dependent, p110γ does play an important role in neutrophil, macrophage, and eosinophil recruitment (22) as well as in T cell proliferation and cytokine production (23) and T cell migration (16,24,25). Thus, pharmacological inhibition of p110γ *in vivo* could indirectly affect B cell function.

Small molecule inhibitors that are selective for single PI3K isoforms or pairs of isoforms have been highly useful in delineating the shared and distinct functions of PI3K enzymes in diverse cell types (3,26). Our results show that the selective p110δ inhibitor IPI-3063 and the p110δ/γ dual inhibitor IPI-443 are highly potent, having effects on B cells at the nanomolar range *in vitro*. These data demonstrate that these inhibitors will be useful tools in studying the function of p110δ/γ or p110δ alone. Additional studies will be required to determine whether these or similar compounds will be suitable in treating patients with diseases driven by B cells or other immune cell types in which p110δ and p110γ have key roles.

Acknowledgements

This study was supported by a sponsored research agreement from Infinity Pharmaceuticals to UC Irvine. Access to normal human blood specimens was supported by the National Center for Research Resources and the National Center for Advancing Translational Sciences, National Institutes of Health, through Grant UL1 TR001414.

We would also like to thank Drs. Judith Varner and Megan Kaneda (UCSD) for technical assistance.

References

1. Chiu H, Mallya S, Nguyen P, Mai A, Jackson LV, Winkler DG, DiNitto JP, Brophy EE, McGovern K, Kutok JL, et al. The Selective Phosphoinoside-3-Kinase p110δ Inhibitor IPI-3063 Potently Suppresses B Cell Survival, Proliferation, and Differentiation. *Front Immunol* (2017) **8**:747. doi:10.3389/fimmu.2017.00747

2. Fruman DA, Rommel C. PI3K and cancer: lessons, challenges and opportunities. *Nat Rev Drug Discov* (2014) **13**:140–156. doi:10.1038/nrd4204

3. Puri KD, Gold MR. Selective inhibitors of phosphoinositide 3-kinase delta: modulators of B-cell function with potential for treating autoimmune inflammatory diseases and B-cell malignancies. *Front Immunol* (2012) **3**:256. doi:10.3389/fimmu.2012.00256

4. Fruman DA, Snapper SB, Yballe CM, Davidson L, Yu JY, Alt FW, Cantley LC. Impaired B cell development and proliferation in absence of phosphoinositide 3-kinase p85alpha. *Science* (1999) **283**:393–397.

5. Okkenhaug K, Bilancio A, Farjot G, Priddle H, Sancho S, Peskett E, Pearce W, Meek SE, Salpekar A, Waterfield MD, et al. Impaired B and T cell antigen receptor signaling in p110delta PI 3-kinase mutant mice. *Science* (2002) **297**:1031–1034. doi:10.1126/science.1073560

6. Bilancio A, Okkenhaug K, Camps M, Emery JL, Ruckle T, Rommel C, Vanhaesebroeck B. Key role of the p110delta isoform of PI3K in B-cell antigen and IL-4 receptor signaling: comparative analysis of genetic and pharmacologic interference with p110delta function in B cells. *Blood* (2006) **107**:642–650. doi:10.1182/blood-2005-07-3041

7. Angulo I, Vadas O, Garçon F, Banham-Hall E, Plagnol V, Leahy TR, Baxendale H, Coulter T, Curtis J, Wu C, et al. Phosphoinositide 3-kinase δ gene mutation predisposes to respiratory infection and airway damage. *Science* (2013) **342**:866–871. doi:10.1126/science.1243292

8. Lucas CL, Kuehn HS, Zhao F, Niemela JE, Deenick EK, Palendira U, Avery DT, Moens L, Cannons JL, Biancalana M, et al. Dominant-activating germline mutations in the gene encoding the PI(3)K catalytic subunit p110δ result in T cell senescence and human immunodeficiency. *Nat Immunol* (2014) **15**:88–97. doi:10.1038/ni.2771

9. Fruman DA, Rommel C. PI3Kδ inhibitors in cancer: rationale and serendipity merge in the clinic. *Cancer Discov* (2011) **1**:562–572. doi:10.1158/2159-8290.CD-11-0249

10. Durand CA, Hartvigsen K, Fogelstrand L, Kim S, Iritani S, Vanhaesebroeck B, Witztum JL, Puri KD, Gold MR. Phosphoinositide 3-kinase p110 delta regulates natural antibody production, marginal zone and B-1 B cell function, and autoantibody responses. *J Immunol* (2009) **183**:5673–5684. doi:10.4049/jimmunol.0900432

11. Cushing TD, Hao X, Shin Y, Andrews K, Brown M, Cardozo M, Chen Y, Duquette J, Fisher B, Gonzalez-Lopez de Turiso F, et al. Discovery and in Vivo Evaluation of (S)-N-

(1-(7-Fluoro-2-(pyridin-2-yl)quinolin-3-yl)ethyl)-9H-purin-6-amine (AMG319) and Related PI3Kδ Inhibitors for Inflammation and Autoimmune Disease. *J Med Chem* (2014) doi:10.1021/jm501624r

12. Winkler DG, Faia KL, Dinitto JP, Ali JA, White KF, Brophy EE, Pink MM, Proctor JL, Lussier J, Martin CM, et al. PI3K-δ and PI3K-γ Inhibition by IPI-145 Abrogates Immune Responses and Suppresses Activity in Autoimmune and Inflammatory Disease Models. *Chem Biol* (2013) doi:10.1016/j.chembiol.2013.09.017

13. So L, Yea SS, Oak JS, Lu M, Manmadhan A, Ke QH, Janes MR, Kessler LV, Kucharski JM, Li LS, et al. Selective inhibition of phosphoinositide 3-kinase p110α preserves lymphocyte function. *J Biol Chem* (2013) **288**:5718–5731. doi:10.1074/jbc.M112.379446

14. Ramadani F, Bolland DJ, Garcon F, Emery JL, Vanhaesebroeck B, Corcoran AE, Okkenhaug K. The PI3K isoforms p110alpha and p110delta are essential for pre-B cell receptor signaling and B cell development. *Sci Signal* (2010) **3**:ra60. doi:10.1126/scisignal.2001104

15. Ladygina N, Gottipati S, Ngo K, Castro G, Ma JY, Banie H, Rao TS, Fung-Leung WP. PI3Kγ kinase activity is required for optimal T-cell activation and differentiation. *Eur J Immunol* (2013) doi:10.1002/eji.201343812

16. Martin AL, Schwartz MD, Jameson SC, Shimizu Y. Selective regulation of CD8 effector T cell migration by the p110 gamma isoform of phosphatidylinositol 3-kinase. *J Immunol* (2008) **180**:2081–2088. doi:10.4049/jimmunol.180.4.2081

17. Beer-Hammer S, Zebedin E, von Holleben M, Alferink J, Reis B, Dresing P, Degrandi D, Scheu S, Hirsch E, Sexl V, et al. The catalytic PI3K isoforms p110gamma and p110delta contribute to B cell development and maintenance, transformation, and proliferation. *J Leukoc Biol* (2010) **87**:1083–1095. doi:10.1189/jlb.0809585

18. Pomel V, Klicic J, Covini D, Church DD, Shaw JP, Roulin K, Burgat-Charvillon F, Valognes D, Camps M, Chabert C, et al. Furan-2-ylmethylene thiazolidinediones as novel, potent, and selective inhibitors of phosphoinositide 3-kinase gamma. *J Med Chem* (2006) **49**:3857–3871. doi:10.1021/jm0601598

19. Omori SA, Cato MH, Anzelon-Mills A, Puri KD, Shapiro-Shelef M, Calame K, Rickert RC. Regulation of class-switch recombination and plasma cell differentiation by phosphatidylinositol 3-kinase signaling. *Immunity* (2006) **25**:545–557. doi:10.1016/j.immuni.2006.08.015

20. Limon JJ, So L, Jellbauer S, Chiu H, Corado J, Sykes SM, Raffatellu M, Fruman DA. mTOR kinase inhibitors promote antibody class switching via mTORC2 inhibition. *Proc Natl Acad Sci U S A* (2014) **111**:E5076–E5085. doi:10.1073/pnas.1407104111

21. Limon JJ, Fruman DA. Akt and mTOR in B Cell Activation and Differentiation. *Front Immunol* (2012) **3**:228. doi:10.3389/fimmu.2012.00228

22. Costa C, Martin-Conte EL, Hirsch E. Phosphoinositide 3-kinase p110γ in immunity. *IUBMB Life* (2011) **63**:707–713. doi:10.1002/iub.516

23. Sasaki T, Irie-Sasaki J, Jones RG, Oliveira-dos-Santos AJ, Stanford WL, Bolon B, Wakeham A, Itie A, Bouchard D, Kozieradzki I, et al. Function of PI3Kgamma in thymocyte development, T cell activation, and neutrophil migration. *Science* (2000) **287**:1040–1046.

24. Reif K, Okkenhaug K, Sasaki T, Penninger JM, Vanhaesebroeck B, Cyster JG. Cutting edge: differential roles for phosphoinositide 3-kinases, p110gamma and p110delta, in lymphocyte chemotaxis and homing. *J Immunol* (2004) **173**:2236–2240.

25. Thomas MS, Mitchell JS, DeNucci CC, Martin AL, Shimizu Y. The p110gamma isoform of phosphatidylinositol 3-kinase regulates migration of effector CD4 T lymphocytes into peripheral inflammatory sites. *J Leukoc Biol* (2008) **84**:814–823. doi:10.1189/jlb.0807561

26. Hawkins PT, Stephens LR. PI3K signalling in inflammation. *Biochim Biophys Acta* (2015) **1851**:882–897. doi:10.1016/j.bbalip.2014.12.006

CHAPTER 3

mTOR Kinase Inhibitors Promote Antibody Class Switching via mTORC2 Inhibition

This chapter describes studies I contributed towards a manuscript published in *Proceedings of the National Academies of Science* November 25, 2014. 111 (47) E5076-E5085, entitled "mTOR kinase inhibitors promote antibody class switching via mTORC2 inhibition." This paper reported opposing effects of mTORC1 and mTORC2 inhibition on antibody class switching.

Introduction

B-cell activation by antigen leads to clonal expansion, followed by differentiation into plasma cells secreting antigen-specific antibodies. Early in an immune response, some B cells differentiate rapidly into plasmablasts that secrete antibodies that are mostly of the IgM isotype and of low affinity. Other B cells adopt a germinal center (GC) fate and undergo class switch recombination (CSR) and somatic hypermutation. Ultimately, GC B cells that survive selection become plasma cells secreting high-affinity antibodies of various isotypes or become long-lived memory B cells.

Extracellular inputs including B-cell receptor engagement, Toll-like receptor ligation, and cytokines, all activate the signaling enzyme phosphoinositide 3-kinase (PI3K) and its downstream target AKT (also known as protein kinase B) in B cells (1). PI3K/AKT signaling and other inputs activate the mammalian target of rapamycin (mTOR), a multifunctional kinase that promotes cell growth, division, and metabolic reprogramming (1, 2). The mTOR kinase is present in two cellular complexes, mTOR-complex 1 (mTORC1) defined by the raptor subunit and mTOR-complex 2 (mTORC2) defined by rictor (3). The classical mTOR inhibitor

rapamycin forms a complex with FKBP12 that partially inhibits mTORC1 and can disrupt mTORC2 assembly upon prolonged cellular exposure. mTORC1 acts downstream of AKT and other signals to promote biosynthetic processes essential for cell growth and division. mTORC2 acts upstream of AKT by phosphorylating Ser-473 in the AKT hydrophobic motif. mTORC2 and AKT function are required for subsequent phosphorylation of forkhead box, subgroup O (FoxO) transcription factors (4, 5). When phosphorylated, FoxO factors exit the nucleus and transcription of FoxO target genes is reduced.

Recent studies illustrate the complexity of mTOR function in B cells. Conditional deletion of the mTOR gene in mouse B cells strongly impairs proliferation and GC differentiation (6). Inactivation of mTORC2 in B cells, via rictor deletion, reduces mature B-cell survival and impairs antibody responses and GC formation (7). At concentrations above 1 nM, rapamycin markedly impairs proliferation of both mouse and human B cells and suppresses antibody responses (8, 9). However, at lower concentrations that preserve B-cell proliferation, rapamycin still suppresses class switching but unexpectedly promotes IgM responses that provide heterosubtypic protection from influenza (6, 10). These studies suggest that overall mTOR signaling, as well as the relative activity of mTORC1 and mTORC2, controls the ability of B cells to divide and to differentiate.

ATP-competitive mTOR kinase inhibitors (TOR-KIs) block activity of both mTORC1 and mTORC2, and were developed to overcome limitations of rapamycin as anticancer agents (11, 12). We reported that TOR-KIs do not block proliferation of normal mature B cells at concentrations that cause cell cycle arrest in pre-B leukemia cells (9). However, the impact of TOR-KIs on immune function is still poorly characterized. In this study, we tested whether TOR-KIs can skew the differentiation of activated B cells. We found that partial mTORC1/mTORC2

inhibition or mTORC2 deletion increases CSR, whereas selective inhibition of mTORC1 suppresses CSR.

Methods and Materials

Mice and Reagents.

C57Bl/6 mice were bred at the University of California, Irvine, and used at between 6 and 12 wk of age. Raptorfl/fl mice on a C57BL6 background were obtained from the Jackson Laboratories (stock no. 013138) and have been described previously (29). Rictorfl/fl mice on a C57BL6 background were a generous gift from Mark Magnuson (Vanderbilt University, Nashville, TN) and have been described previously (30). CD21-Cre mice were obtained from the Jackson Laboratories (stock no. 006368). All animals were studied in compliance with protocols approved by the Institutional Animal Care and Use Committees of the University of California, Irvine, and Harvard Medical School. The active site mTORC1/2 inhibitors PP242, AZD8055, WYE-354, and Ku-0063794 were purchased from Chemdea, and INK128 was obtained from Intellikine. The p110δ-selective PI3K inhibitor IC87114 and pan-PI3K class I inhibitor GDC-0941 were obtained from Intellikine. The inhibitor of AKT1 and AKT2, Akt inhibitor VIII, was purchased from Chemdea. The mTOR allosteric inhibitor, rapamycin, was purchased from LC Labs.

Primary Cell Culture.

Mouse splenic B cells were purified by negative selection using anti-CD43 biotinylated antibody, followed by incubation with antibiotin magnetic microbeads and separation on MACS columns (Miltenyi Biotec). B-cell purity was >98% as measured by FACS analysis

(FACSCalibur and CellQuest software; BD Biosciences) using anti-B220 antibody (BioLegend). Purified B cells were seeded at a final concentration of 0.2 × 10^6 cells per milliliter. For ASC differentiation, B cells were stimulated with 5 μg/mL LPS (Sigma) for 72 h, and for IgG1 CSR, B cells were stimulated with 3 units of CD40L (a gift from Paolo Casali, University of California, Irvine), 1 μg/mL anti-CD40 (HM40-3) agonistic antibody (BioLegend), or 5 μg/mL LPS (Sigma), together with 2.5 ng/mL mIL-4 (R&D Systems) for 96 h. All B cells were cultured in RPMI 1640 supplemented with 10% (vol/vol) heat-inactivated FCS, 5 mM Hepes, 2 mM L-glutamine, 100 units/mL penicillin, 100 μg/mL streptomycin, 50 μM 2-mercaptoethanol, 1× MEM nonessential amino acids (Mediatech), and 1× sodium pyruvate (Mediatech). To assess mTORC1 activity after stimulation, cells were fixed and permeabilized using BD Cytofix/Cytoperm buffer (BD Biosciences) for 15 min at room temperature. Cells were subsequently washed with 0.5% Tween-20 in PBS and stained with a p-S6 (S240/244) antibody conjugated to Alexa Fluor 647 (Cell Signaling Technologies).

In Vitro B-Cell Inhibitor Treatment.

Where the use of pharmacological inhibitors was indicated, a 1× concentration of inhibitor was added to corresponding wells containing purified B cells and allowed to incubate for 15 min at 37 °C in a tissue culture incubator. Following the incubation time, another 1× concentration of inhibitor was added to each corresponding well, followed by a 2× concentration of stimuli. Well contents were mixed by pipetting following both inhibitor additions. Pharmacological inhibitors were used at the following concentrations: PP242 (10 nM, 100 nM, and 400 nM), AZD8055 (1 nM and 10 nM), INK128 (1 nM, 5 nM, 10 nM, and 50 nM), Ku-0063794 (100 nM and 300 nM), rapamycin (0.02 nM, 0.04 nM, 0.08 nM, 0.1 nM, 0.2 nM, 0.4 nM, 0.8 nM, 1 nM, 5 nM, 10 nM,

and 20 nM), Akti (500 nM and 1 μM), GDC-0941 (100 nM and 250 nM), and IC87114 (500 nM and 1 μM).

Flow Cytometry, CFSE Labeling, and Antibodies.

Before cell surface staining, cells were incubated with TruStain fcX in FACS buffer (0.5% BSA + 0.02% NaN3 in 1× HBSS) to block Fc receptors for 10 min on ice. Immunophenotyping of mice was performed on splenocytes after RBC lysis. Staining with antibodies was subsequently performed, also with FACS buffer and on ice for 20 min. Flow cytometry antibodies and other reagents used were as follows: B220 (RA3-6B2), IgG1 (RMG1-1) (all from BioLegend); CD138 (281-2) (from BD Biosciences). CFSE labeling of B cells to track proliferation was performed as described elsewhere (32). Flow cytometric data were analyzed using FlowJo software (TreeStar).

Results

The appendix to this thesis contains a reprint of the article "mTOR kinase inhibitors promote antibody class switching via mTORC2 inhibition". Figures 1, 3, 4, and 7 of that article, as well as Supplementary Figures 1-8, evaluate the effects of low concentrations of TOR-KIs in models of antibody class switching. Those experiments were done by others in our laboratory and will not be described in this thesis. The main conclusions of the paper are:

- TOR-KIs at concentrations that cause transient mTORC1/2 inhibition increases antibody class switching in activated B cells.
- The effects of AKT inhibition or partial mTORC1/2 inhibition to increase antibody class switching requires FoxO transcription factors
- TOR-KIs and AKT inhibitors increased expression of *Aicda* mRNA

A key element of this study was to compare the effects of mTORC1/2 inhibition through genetic or pharmacologic manipulations on antibody class switching. This chapter describes those results. I performed many of the experiments described in this chapter; the Figure legends indicate which experiments were done by others in the laboratory, Jose Limon and Lomon So.

TOR-KIs increases B cell isotype switching in vitro

To define the B cell-intrinsic effects of TOR-KIs further, we assessed the differentiation of purified splenic B cells. We used four different TOR-KIs with distinct chemical structures (INK128, PP242, Ku-0063794, and AZD8055) to minimize the potential for off-target effects. Each compound increased the percentage of IgG1-switched B220+ B cells induced by anti-CD40 plus IL-4, a condition that mimics signals during a T cell-dependent (TD) response and favors isotype switching to IgG1 **(Fig. 3.1A and 3.1B).** Direct inhibition of AKT isoforms AKT1 and AKT2 also increased the frequency of switching to IgG1 **(Fig. 3.1A and 3.1B).** Similar results were observed when B cells activated by LPS plus IL-4 were treated with INK128, PP242, Ku-0063794, or AZD8055 **(Fig. 3.1C).** Consistent with increased switching to the IgG1 isotype, post-recombination Iμ-Cγ1 transcripts were increased in B cells treated with TOR-KIs **(Fig S2, Appendix 1).** In addition, TOR-KI–treated B cells displayed an elevation in *Aicda* transcripts encoding activation-induced cytidine deaminase **(Fig. 3.1G),** the mutator protein required for initiation of CSR (13).

We next assessed the effect of TOR-KIs on differentiation into plasmablasts and antibody-secreting cells (ASCs) following stimulation with LPS. Plasmablast differentiation, as measured by cells with a B220lowCD138+ phenotype, was decreased in a concentration-dependent manner by TOR-KIs, whereas AKT inhibition had no significant effect **(Fig. 3.1D**

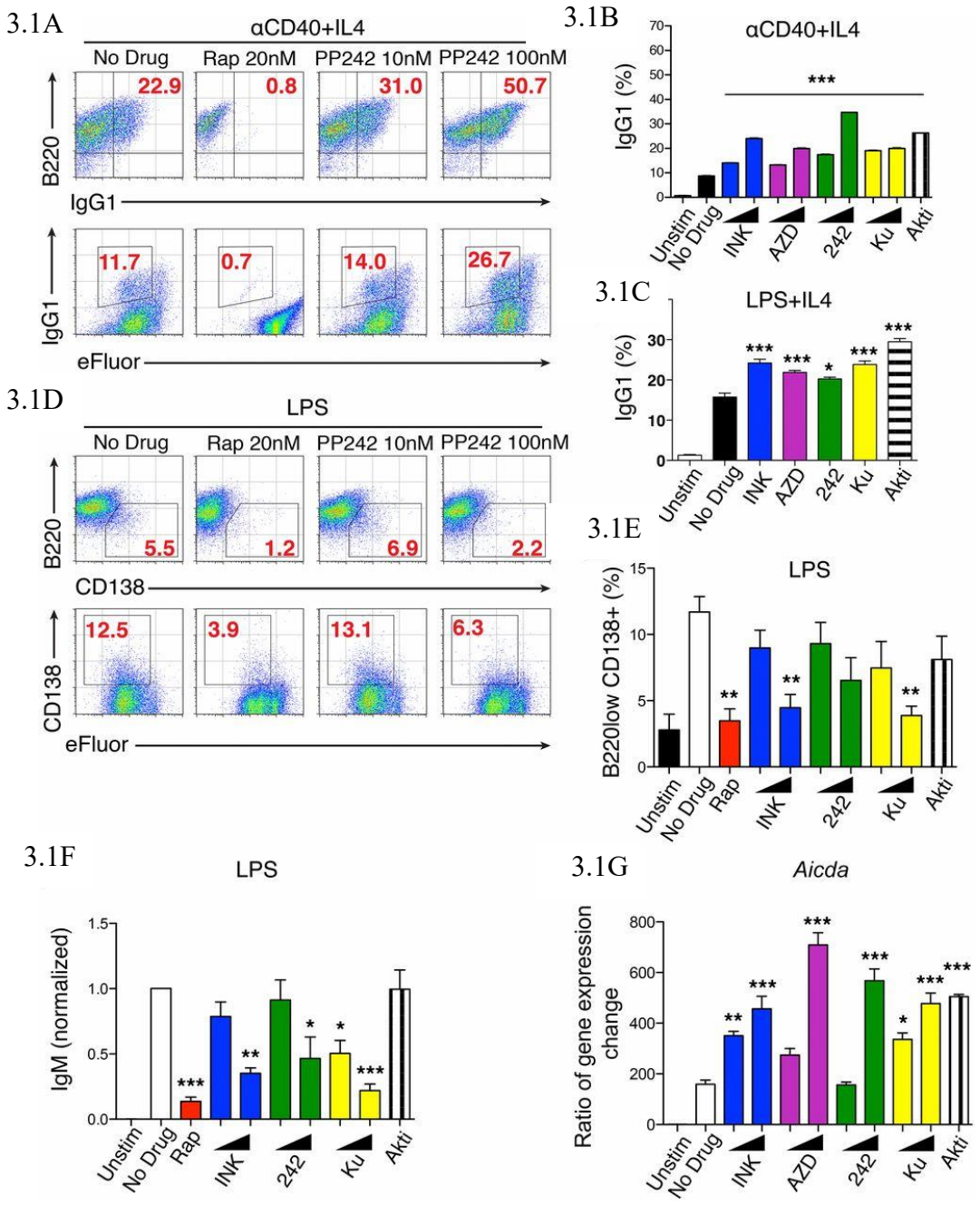

Figure 3.1 TOR-KIs increase in vitro B-cell CSR and decrease plasmablast differentiation. (3.1A-3.1B) Purified B cells were cultured with media only or stimulated with αCD40 + IL-4 in the absence or presence of the inhibitors indicated. (3.1A) Dot plots show IgG1$^+$ B cells (*Top*) and the cell division history of eFluor670-labeled B cells (*Bottom*; eFluor670 is a cell division tracking dye with a different emission spectrum than CFSE), as determined by FACS after 4 d. Other TOR-KIs in this study had similar effects on cell division at the concentrations used for differentiation experiments. (3.1B, Jose Limon) Percentage of live B cells that have divided at least once (based on eFluor670 division history) expressing surface IgG1 was determined by

FACS after 4 d. (3.1C, Jose Limon) Switching to IgG1 was assessed as in *B*, except cells were stimulated with LPS + IL-4. (3.1D) Representative FACS plots of plasmablast differentiation in purified B cells stimulated with LPS or LPS and indicated inhibitors for 3 d. (*Bottom*) B cells were labeled with eFluor670 to track division history. (3.1E, Jose Limon) Graph of the percentage of live B cells with a plasmablast phenotype determined by FACS after 3 d of stimulation as indicated in *D*. (3.1F, Jose Limon) Purified B cells were stimulated with LPS in the absence or presence of the inhibitors indicated. The amount of IgM in cell supernatants was quantitated by ELISA after 4 d, and data were normalized to the stimulated, no-drug treatment condition. (3.1G, Jose Limon) *Aicda* mRNA transcripts were quantitated by qPCR in B cells stimulated with αCD40 + IL-4. For Fig. 3.1A and Fig. 3.1E, data are representative of three or more independent experiments. For *3.1B*, *3.1C*, *3.1E*, *3.1F*, and *3.1G*, graphs depict the mean and SEM of $n \geq 3$ samples per condition. (*$P < 0.05$; **$P < 0.01$; ***$P < 0.001$ by one-way ANOVA with Tukey's multiple comparison test, measured vs. the no-drug sample). Akti, Akt inhibitor VIII; AZD, AZD8055; INK, INK128; Ku, Ku-0063794; 242, PP242.

and 3.1E). TOR-KIs also reduced IgM production, as measured by ELISA from cell culture supernatants of LPS-stimulated B cells **(Fig. 3.1F).** Thus, our results demonstrate that TOR-KIs can directly alter B-cell differentiation fate, causing increased CSR and a reciprocal decrease in plasmablast and ASC differentiation. In contrast to the effects of TOR-KIs, rapamycin reduced both CSR and ASC differentiation **(Fig. 3.1A-3.1G).** The suppression of both differentiation pathways is consistent with early studies of rapamycin action in B cells (8).

Rapamycin Reduces CSR by a Mechanism Partly Independent of Proliferation

To gain further insight into the mechanism of mTOR inhibitor action, we measured B-cell proliferation and IgG1 class switching over an extended dose–response of rapamycin or INK128 **(Fig. 3.2).** The partial mTORC1 inhibitor rapamycin reduced CSR at concentrations as low as 0.02 nM, with complete inhibition achieved by 0.4 nM. INK128 enhanced CSR at 10 nM, but higher concentrations caused increasing inhibition. Notably, rapamycin ablated CSR even at a concentration (0.4 nM) that partially preserved proliferation, whereas some B cells treated with a high concentration of INK128 (100 nM) still switched to IgG1 even without proliferation.

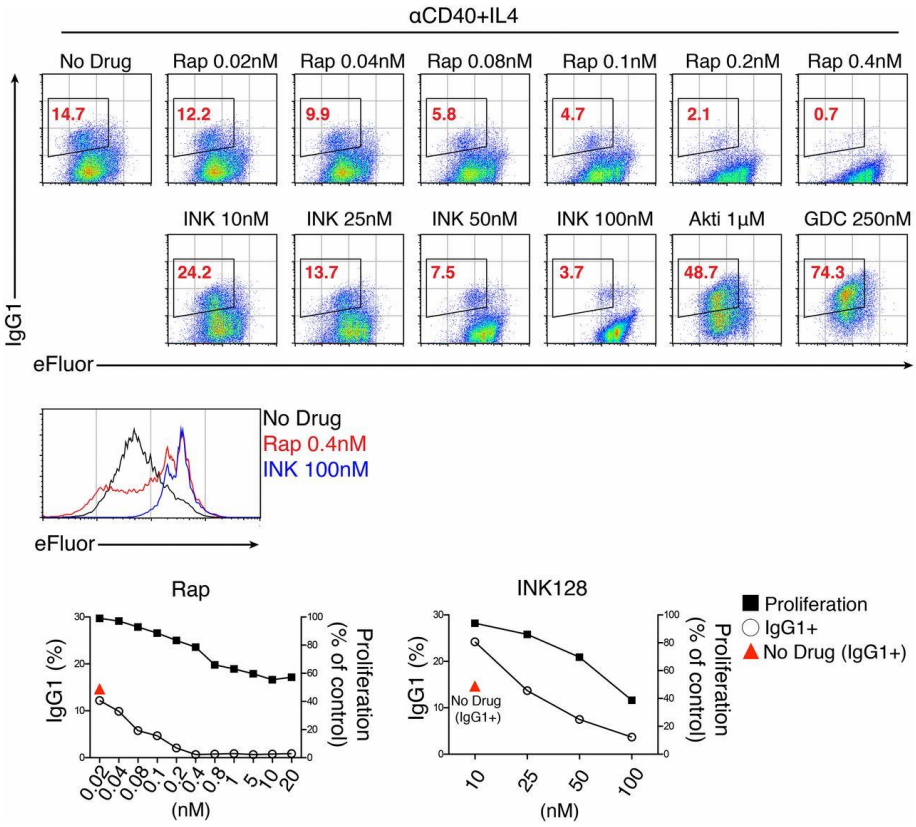

Figure 3.2 Rapamycin has a more profound effect on B-cell proliferation and CSR than TOR-KIs. Purified B cells were labeled with eFluor670 to measure cell division and were stimulated with αCD40 + IL-4 in the presence or absence of indicated inhibitors. Representative FACS plots are shown for the different treatment conditions (*Upper*), and a FACS proliferation histogram is shown for high-dose rapamycin and INK128 (*Middle*). (*Lower*) Effects of inhibitor concentration on cellular proliferation and CSR are represented on line graphs. Data are representative of two independent experiments.

Thus, the roles of mTORC1 and mTORC2 in cell division are partly independent of their roles in differentiation.

Inactivation of mTORC1 and mTORC2 has opposing effects on CSR in vitro

As a genetic approach to assess the roles of mTORC1 and mTORC2, we isolated B cells from mice possessing conditional (floxed) alleles of rictor or raptor. Deletion of rictor using CD19Cre (rictor-flox/CD19Cre; termed rictorΔB) did not significantly alter B-cell subset

frequencies **(Fig. S7A, Appendix I)**. In resting mature B cells, rictor expression was not completely reduced, suggesting incomplete and/or ongoing deletion **(Fig. 3.3A).** Consistent with reduced mTORC2 function, AKT phosphorylation at S473 was lower in B cells from rictorΔB mice **(Fig. 3.3B).** Importantly, this effect was specific to mTORC2, because S6 phosphorylation, a sensitive readout of mTORC1, was unaffected in rictorΔB B cells **(Fig. 3.3C).** To address the role of mTORC1, we analyzed B cells from raptorΔB mice in which the raptor-flox allele is deleted at the transitional B-cell stage using CD21Cre. As with rictorΔB, B-cell development was largely normal in raptorΔB **(Fig. S7B, Appendix 1)**. Raptor expression was also not completely reduced in resting mature B cells **(Fig. 3.3D),** and this partial deletion corresponded to a reduced but not complete reduction in S6 phosphorylation in raptorΔB B cells **(Fig. 3.3D).** Next, we tested functional responses in B cells with partial loss of rictor or raptor. In response to anti-CD40 plus IL-4, rictor-deficient B cells proliferated to a similar degree as WT, whereas raptor-deficient cells proliferated less **(Fig. 3.3C).** To compare the capacity of cells to undergo class switching, we gated on divided cells and calculated the percentage of IgG1+ cells. The results showed consistently less switching in divided raptorΔB B cells compared with division and differentiation **(Fig. 3.2).** These findings are consistent with the effects of rapamycin on B-cell switching division and differentiation **(Fig. 3.2)** In contrast, rictorΔB B cells showed significantly more switching to IgG1 than control **(Fig. 3.3B).** Importantly, adding low-dose TOR-KI (1–5 nM INK128) to rictorΔB B cells did not further increase CSR **(Fig. 3.3C).**

We also measured plasmablast generation in B cells stimulated with LPS alone. The raptorΔB B cells showed reduced ASC generation, whereas the rictorΔB B cells were similar to control **(Fig. 3.3C and 3.3F)**. Together, these genetic interventions support the conclusion that mTORC1 inhibition suppresses both CSR and plasmablast generation, whereas mTORC2

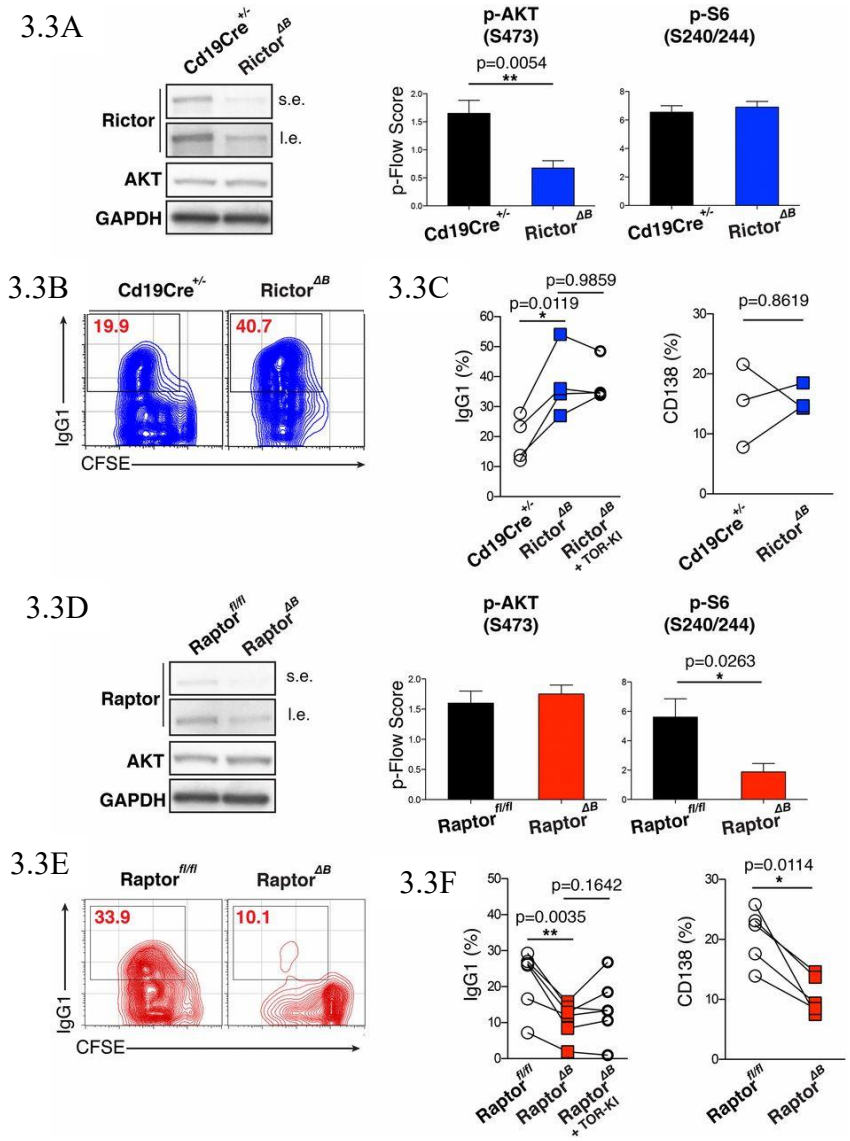

Figure 3.3 Inactivation of mTORC1 vs. mTORC2 has opposing effects on CSR. (3.3A) Purified resting B cells from either control (CD19Cre$^{+/-}$) or rictor-flox/CD19Cre (rictor$^{\Delta B}$) were subjected to Western blotting to check rictor protein levels (*Left*). RBC-lysed total splenocytes from the indicated genotypes were activated with αCD40 + IL-4 for 24 h, and intracellular phosphoflow (p-Flow) analysis was performed to measure mTORC1 (pS6-S240/244) and mTORC2 (pAKT-S473) activity. The fold change in median fluorescence intensity was calculated and subjected to $\log_2$ conversion to obtain p-Flow score values as previously described (9). Data are reported as mean ± SD [n = 3 (pAKT) or n = 2 (pS6)]. An unpaired Student t test was used for statistical analysis of the pAKT data. I.e., long exposure; s.e., short exposure. (3.3B) Purified B cells were labeled with CFSE and activated with αCD40 + IL-4 for 4 d. The percentage of live B cells that had divided at least once (based on CFSE division history) expressing surface IgG1 was determined by FACS after 4 d. (3.3C, *Left*, Lomon So) Percentage of B cells expressing surface IgG1 after 4 d of activation with αCD40 + IL-4 is plotted for several experiments. In the +TOR-KI condition, INK128 was added at a concentration of 1–5

nM. (3.3C, *Right*, Lomon So) Percentage of B cells expressing surface CD138 after 4 d of activation with LPS is plotted. (3.3D, *Left*) Western blotting was performed the same way as in *A* but with resting B cells from control (raptor$^{fl/fl}$) or raptor-flox/CD21Cre (raptor$^{\Delta B}$). (3.3D, *Right*) Intracellular p-Flow analysis to measure mTORC1 and mTORC2 activity after 24 h of αCD40 + IL-4 activation. Data are reported as mean ± SD (n = 3) for both pAKT and pS6. An unpaired Student t test was used for statistical analysis. (3.3E, Lomon So) Representative FACS plots as in Fig. 3.3B. (3.3F, Lomon So) Same analysis as in 3.3*C*. A paired Student t test was used for statistical analysis of both *Fig. 3.3C* and *3.3F*.

inhibition increases CSR with little effect on plasmablast generation.

Discussion

TOR-KIs are a powerful new class of compounds that inhibit both rapamycin-sensitive and rapamycin-resistant mTOR functions. These agents not only have great promise for clinical management of cancer but also represent new chemical tools for probing the function of mTOR kinase activity in various cell types. Here, we have used a panel of chemically distinct TOR-KIs to demonstrate that mTOR kinase inhibition increases the fraction of activated B cells undergoing antibody class switching. These results were seen at TOR-KI concentrations that cause transient mTORC1/2 inhibition and only partially reduced signaling after 24 h in B cells. The effect of AKT inhibition or partial mTORC1/2 inhibition to increase CSR requires FoxO transcription factors **(Appendix 1).** In addition, the expression of Aicda in activated B cells is known to be FoxO1-dependent (22), and Aicda mRNA was increased in cells treated with TOR-KIs or AKT inhibitor. These data support the model that mTORC2 inhibition by TOR-KIs reduces AKT activity, increasing FoxO activity to drive the enhanced class-switching response in TOR-KI–treated B cells **(Fig. 8, Appendix 1).** This model is consistent with previous studies showing that PI3K activity suppresses CSR through AKT-dependent inactivation of FoxO1, whereas PI3K inhibition or FoxO activation promotes CSR (22, 25).

The enhanced production of class-switched antibodies by mTORC1/mTORC2 inhibition is surprising, considering the well-known immunosuppressive activity of rapamycin and the impaired survival and differentiation of mouse B cells lacking mTOR (6). Our in vitro studies establish the importance of using intermediate doses of competitive mTOR inhibitors that transiently inhibit both mTORC1 and mTORC2. At higher concentrations, TOR-KIs sustain mTOR inhibition and block B-cell proliferation to a similar degree as rapamycin, probably through strong mTORC1 inhibition **(Fig. 8, Appendix 1).** Supporting the model that TOR-KIs increase CSR via mTORC2 inhibition, genetic loss of mTORC2 (via partial rictor deletion) causes increased CSR that is not elevated further by TOR-KI treatment. Our findings contrast with a recent report that deletion of rictor in B cells reduces survival and proliferation, and impairs class switching (7). It appears that these systems achieve differential efficiency of rictor deletion. Boothby and coworkers (7) obtained efficient deletion using Vav-Cre, where rictor is deleted in all hematopoietic cells, or using an inducible Cre (fused to the estrogen receptor hormone binding domain) by which chronic in vivo tamoxifen treatment directs rictor deletion in all cell types. We used CD19Cre, which mediated partial deletion of rictor in B cells and partial but not complete loss of mTORC2 signaling. Partial rictor deletion allowed B cells to survive and proliferate, and led to enhanced class switching. The results we obtained with rapamycin titrations are consistent with recent evidence that mTORC1 inhibition can suppress CSR independent of proliferation (10) **(Fig. 8, Appendix 1).** An interesting finding is that when both complexes are partially inhibited by intermediate concentrations of TOR-KIs, the effect of mTORC2 inhibition is dominant for CSR (enhancement), whereas mTORC1 inhibition is dominant for ASC generation (inhibition).

While these studies demonstrated that the mTORC2 effects are mediated through AKT/FoxO, the roles of the downstream effectors of mTORC1 are not characterized which I investigated further in Chapter 4 of this thesis.

References

1. Limon JJ, Fruman DA (2012) Akt and mTOR in B Cell Activation and Differentiation. Front Immunol 3:228.

2. Powell JD, Pollizzi KN, Heikamp EB, Horton MR (2012) Regulation of immune responses by mTOR. Annu Rev Immunol 30:39–68.

3. Laplante M, Sabatini DM (2012) mTOR signaling in growth control and disease. Cell 149(2):274–293.

4. Guertin DA, et al. (2006) Ablation in mice of the mTORC components raptor, rictor, or mLST8 reveals that mTORC2 is required for signaling to Akt-FOXO and PKCalpha, but not S6K1. Dev Cell 11(6):859–871.

5. Jacinto E, et al. (2006) SIN1/MIP1 maintains rictor-mTOR complex integrity and regulates Akt phosphorylation and substrate specificity. Cell 127(1):125–137.

6. Zhang S, et al. (2013) B cell-specific deficiencies in mTOR limit humoral immune responses. J Immunol 191(4):1692–1703.

7. Lee K, et al. (2013) Requirement for Rictor in homeostasis and function of mature B lymphoid cells. Blood 122(14):2369–2379.

8. Aagaard-Tillery KM, Jelinek DF (1994) Inhibition of human B lymphocyte cell cycle progression and differentiation by rapamycin. Cell Immunol 156(2):493–507.

9. Janes MR, et al. (2010) Effective and selective targeting of leukemia cells using a TORC1/2 kinase inhibitor. Nat Med 16(2):205–213.

10. Keating R, et al. (2013) The kinase mTOR modulates the antibody response to provide cross-protective immunity to lethal infection with influenza virus. Nat Immunol 14(12):1266–1276.

11. Janes MR, Fruman DA (2010) Targeting TOR dependence in cancer. Oncotarget 1(1): 69–76.

12. Wander SA, Hennessy BT, Slingerland JM (2011) Next-generation mTOR inhibitors in clinical oncology: How pathway complexity informs therapeutic strategy. J Clin Invest 121(4):1231–1241.

13. Xu Z, Zan H, Pone EJ, Mai T, Casali P (2012) Immunoglobulin class-switch DNA recombination: Induction, targeting and beyond. Nat Rev Immunol 12(7):517–531.

14. Zhang TT, Makondo KJ, Marshall AJ (2012) p110δ phosphoinositide 3-kinase represses IgE switch by potentiating BCL6 expression. J Immunol 188(8):3700–3708.

15. Zhang TT, et al. (2008) Genetic or pharmaceutical blockade of p110delta phosphoinositide-3-kinase enhances IgE production. J Allergy Clin Immunol 122:811–819 e812.

16. Chresta CM, et al. (2010) AZD8055 is a potent, selective, and orally bioavailable ATP-competitive mammalian target of rapamycin kinase inhibitor with in vitro and in vivo antitumor activity. Cancer Res 70(1):288–298.

17. Willems L, et al. (2012) The dual mTORC1 and mTORC2 inhibitor AZD8055 has antitumor activity in acute myeloid leukemia. Leukemia 26(6):1195–1202.

18. Rolf J, et al. (2010) Phosphoinositide 3-kinase activity in T cells regulates the magnitude of the germinal center reaction. J Immunol 185(7):4042–4052.

19. Cunningham AF, et al. (2007) Salmonella induces a switched antibody response without germinal centers that impedes the extracellular spread of infection. J Immunol 178(10):6200–6207.

20. Matsiota-Bernard P, Mahana W, Avrameas S, Nauciel C (1993) Specific and natural antibody production during Salmonella typhimurium infection in genetically susceptible and resistant mice. Immunology 79(3):375–380.

21. Haynes L, Eaton SM, Burns EM, Randall TD, Swain SL (2003) CD4 T cell memory derived from young naive cells functions well into old age, but memory generated from aged naive cells functions poorly. Proc Natl Acad Sci USA 100(25):15053–15058.

22. Dengler HS, et al. (2008) Distinct functions for the transcription factor Foxo1 at various stages of B cell differentiation. Nat Immunol 9(12):1388–1398.

23. Sykes SM, et al. (2011) AKT/FOXO signaling enforces reversible differentiation blockade in myeloid leukemias. Cell 146(5):697–708.

24. Tothova Z, et al. (2007) FoxOs are critical mediators of hematopoietic stem cell resistance to physiologic oxidative stress. Cell 128(2):325–339.

25. Omori SA, et al. (2006) Regulation of class-switch recombination and plasma cell differentiation by phosphatidylinositol 3-kinase signaling. Immunity 25(4):545–557.

26. Jiang Q, et al. (2011) mTOR kinase inhibitor AZD8055 enhances the immunotherapeutic activity of an agonist CD40 antibody in cancer treatment. Cancer Res 71(12):4074–4084.

27. Amiel E, et al. (2012) Inhibition of mechanistic target of rapamycin promotes dendritic cell activation and enhances therapeutic autologous vaccination in mice. J Immunol 189(5):2151–2158.

28. Janes MR, Fruman DA (2009) Immune regulation by rapamycin: moving beyond T cells. Sci Signal 2(67):pe25.

29. Sengupta S, Peterson TR, Laplante M, Oh S, Sabatini DM (2010) mTORC1 controls fasting-induced ketogenesis and its modulation by ageing. Nature 468(7327):1100–1104.

30. Shiota C, Woo JT, Lindner J, Shelton KD, Magnuson MA (2006) Multiallelic disruption of the rictor gene in mice reveals that mTOR complex 2 is essential for fetal growth and viability. Dev Cell 11(4):583–589.

31. Houghton PJ, et al. (2012) Initial testing (stage 1) of the mTOR kinase inhibitor AZD8055 by the pediatric preclinical testing program. Pediatr Blood Cancer 58(2):191–199.

32. Donahue AC, Fruman DA (2003) Proliferation and survival of activated B cells requires sustained antigen receptor engagement and phosphoinositide 3-kinase activation. J Immunol 170(12):5851–5860.

33. Rüssmann H, et al. (1998) Delivery of epitopes by the Salmonella type III secretion system for vaccine development. Science 281(5376):565–568.

34. Kaniga K, Uralil J, Bliska JB, Galán JE (1996) A secreted protein tyrosine phosphatase with modular effector domains in the bacterial pathogen Salmonella typhimurium. Mol Microbiol 21(3):633–641.

35. Hoiseth SK, Stocker BA (1981) Aromatic-dependent Salmonella typhimurium are nonvirulent and effective as live vaccines. Nature 291(5812):238–239.

36. Donahue AC, Fruman DA (2007) Distinct signaling mechanisms activate the target of rapamycin in response to different B-cell stimuli. Eur J Immunol 37(10):2923–2936.

CHAPTER 4

The mTORC1/4E-BP/eIF4E Axis Promotes Antibody Class Switching in B Lymphocytes

Abstract

During an adaptive immune response, activated mature B cells give rise to antibody secreting plasma cells to fight infection. B cells undergo antibody class switching to produce different classes of antibodies with varying effector functions. The mammalian/mechanistic target of rapamycin (mTOR) signaling pathway is activated during this process and disrupting mTOR complex-1 (mTORC1) in B cells impairs class switching by a poorly understood mechanism. In particular, it is unclear which mTORC1 downstream substrates control this process. Here we used an *in vitro* murine model in which the mTORC1 inhibitor rapamycin, when added after a B cell has committed to divide, suppresses class switching while preserving proliferation. Investigation of mTORC1 substrates revealed a role for eukaryotic translation initiation factor 4E (eIF4E) and eIF4E-binding proteins (4E-BPs) in class switching. Mechanistically, we show that genetic or pharmacological disruption of eIF4E binding to eIF4G reduced cap-dependent translation, which specifically affected the expression of activation-induced cytidine deaminase (AID) protein but not *Aicda* mRNA. This translational impairment decreased antibody class switching independently of proliferation. These results uncover a previously undescribed role for mTORC1 and the 4E-BP/eIF4E axis in AID protein expression and antibody class switching in B cells, suggesting that cap-dependent translation regulates key steps in B cell differentiation.

Introduction

During a response to infection, B cells become activated to produce different isotypes of antibodies with varying effector functions (1). Early in the immune response, some activated B cells differentiate into plasmablast cells that mainly secrete low affinity immunoglobulin M (IgM) antibodies. Others become germinal center B cells and through T-cell-dependent interactions undergo class switch recombination (CSR) to produce other classes of antibodies including IgG, IgA and IgE. During the germinal center reaction, they can also undergo somatic hypermutation (SHM) to diversify and produce higher affinity antibodies. The resulting B cells that survive selection will then either become plasma cells that secrete these antibodies to fight off the infection or become long-lived memory B cells that initiate a faster response during a second infection.

Class switching is initiated when the B cell receptor (BCR) recognizes antigen and B cells are further stimulated through CD40 and cytokine receptors. All of these signals activate the mammalian (also known as mechanistic) target of rapamycin (mTOR). This ubiquitously expressed serine/threonine kinase integrates receptor and nutrient signals to promote many cellular processes including mRNA translation, lipid biogenesis, and nucleotide synthesis. The mTOR kinase forms two complexes, mTOR complex 1 (mTORC1) defined by the Raptor subunit and mTORC2 defined by the Rictor subunit. A major function of mTORC2 is to phosphorylate AKT, a kinase that promotes survival and metabolic reprogramming. mTORC1 is activated downstream of PI3K and AKT and phosphorylates many substrates to promote biosynthetic pathways that support cell growth. Key mTORC1 substrates include S6 kinases and a family of mRNA translation inhibitors known as eIF4E-binding proteins (4E-BPs). Phosphorylation of 4E-BPs by mTORC1 leads to the formation of the eIF4F translational

initiation protein complex composed of the cap-binding protein eIF4E, eIF4A helicase and eIF4G scaffold that promote cap-dependent mRNA translation.

The immunosuppressive drug rapamycin (Rap), which allosterically binds and inhibits mTORC1 formation, has long been known to be a potent inhibitor of B cell antibody production (2). Due to the profound anti-proliferative effect of Rap on both B and T cells, it has been difficult to uncouple the roles of mTORC1 in B cell proliferation and differentiation. However, several studies have now presented conclusive evidence that mTORC1 activity is dynamically regulated in germinal center (GC) B cells (3, 4), and that mTORC1 has a B cell-intrinsic role to promote antibody class switching from IgM to IgG and other isotypes (5–8). While these findings highlight the important role of mTORC1 in B cell differentiation, the mechanism by which mTORC1 promotes class switching has not been addressed. Specifically, a key question is which mTORC1 downstream effectors control B cell commitment to isotype switching. Mechanistic investigation of eIF4E activity using both genetic and pharmacological tools show that inhibiting eIF4E decreases antibody class switching and AID protein. Our findings suggest that cap-dependent translation plays a role in class switched antibody production and is a novel mechanism of regulating AID and B cell differentiation.

Methods and Materials

Mice and reagents

C57Bl/6J (B6) mice were bred at the University of California, Irvine, and used at between 6 and 12 weeks of age. All animals were studied in compliance with protocols approved by the Institutional Animal Care and Use Committees of the University of California, Irvine. Mice carrying an AID-GFP reporter on a B6 background were obtained from the Jackson Laboratory

(stock number 018421). Mice harboring a transgenic allele encoding a constitutively active form of 4E-BP (4E-BP1^{M}) under a tetracycline-responsive element were provided by our collaborator Davide Ruggero (UCSF) and described previously (9, 10). These mice were crossed to a strain harboring an optimized form of rtTA (rtTA-M2) inserted downstream of the Rosa26 promoter, which was purchased from the Jackson Laboratory (stock number 006965). MLN0128 and MK-2206 were purchased from Active Biochem. Rapamycin was purchased from Cell Signaling Technology. S6K1 inhibitor LY294002 was purchased from Tocris Bio. SBI-756 was provided by our collaborator Ze'ev Ronai (Sanford Burnham Prebys Institute) and synthesized as described (11). Inhibitors were included throughout the indicated cell treatment periods.

Mouse B cell culture

Splenic B cells were purified by negative selection (eBioscience Magnisort Mouse B cell enrichment kit). B cell purity measured by FACS analysis (FACSCalibur and CellQuest software; BD Biosciences) using anti-B220 antibody (Biolegend) yielded >95% B220+. Purified B cells were seeded at a final concentration of 1.5 x 10^6 cells per milliliter. For class switching experiments, B cells were stimulated 5 μg/mL anti-CD40 (HM40-3) agonistic antibody (eBioscience), or 5 μg/mL LPS (Sigma), together with 5 ng/mL mIL-4 (R&D Systems) for 96 h to induce switching to IgG1. 5 μg/mL LPS (Sigma) induced switching to IgG3. 5 μg/mL LPS (Sigma) with 5 ng/mL mIL-4 (R&D), 5 ng/mL mIL-5 (Tonbo Bioscience), 5 nM retinoic acid (Sigma Aldrich) and 5 ng/mL TGF-β (Thermo Fisher Scientific) induced switching to IgA. All cells were cultured with RPMI 1640 supplemented with 10% (vol/vol) heat-inactivated FCS, 5 mM Hepes, 2 mM L-glutamine, 100 units/mL penicillin, 100 μg/mL streptomycin, 50 μM 2-mercaptoethanol.

Western Blotting Analysis

Phospho-AKT S473 (Cell Signaling), phospho-S6 S244/240 (Cell Signaling), phospho-4E-BP-1 T37/46 (Cell Signaling), and AID (eBioscience) protein on western blots were analyzed using ImageJ to quantitate signal of each band. Signal was normalized with actin measurements and fold change was calculated using the stimulated/no drug control.

Immunizations

Mice were immunized i.p. with 100 μL of a final count of 5 x 10^8 washed SRBCs (Innovative Research) and sacrificed 8 days after immunization. Mice were immunized with 100 μL of NP(18)-LPS (Biosearch Technologies) mixed at a 1:1 ratio with Imject alum (Pierce) at a final concentration of 0.05 mg/mL and sacrificed on day 10. Mice were injected i.p. with 100 μL PBS vehicle, 100 μL at 1 mg/kg, 0.3 mg/kg or 0.075 mg/kg Rapamycin. Blood was collected for serum and spleen was harvested for measuring germinal center and T follicular helper cells.

SRBC-antibody flow cytometry assay

Serum SRBC-antibody production was measured as described in (12).

Immunoglobulin ELISA

For ELISA to measure NP-IgM, Nunc Maxisorp plates (Thermo Fisher) were coated with anti-NP at 10 μg/mL in 50 μL of total sample in PBS and allowed to incubate overnight at 4 °C. Serum was harvested from mice and diluted 1:100 in 2% (wt/vol) BSA in PBS and incubated on

coated plates for 1 h at 37 °C. HRP-conjugated rabbit anti-mouse IgM secondary antibody (Zymed) was used.

Flow cytometry, CFSE labeling, and antibodies

Cells were incubated with TruStain fcX in FACS buffer (0.5% BSA + 0.02% NaN3 in 1× HBSS) for 10 min on ice. Staining with antibodies was performed with FACS buffer and on ice for 20 min. Flow cytometry antibodies and other reagents used: B220 (eBioscience, RA3-6B2), IgG1 (BD, A85-1), IgG3 (BD, R40-82), IgA (BD, Cl0-3), IgD (Biolegend, 11-26c.2a), and 7-Aminoactinomycin D (Invitrogen). CFSE or eFluor 670 labeling of B cells was performed by resuspending cells to a concentration of 10×10^6 cells per mL with a concentration of 2.5 μM. Flow cytometric data were analyzed using FlowJo software (TreeStar).

Proximity Ligation assay

eIF4E-eIF4G interactions were detected in situ using the DuoLink detection kit (Sigma Aldrich) according to manufacturer instructions. Mouse anti-eIF4E (BD Biosciences) and Rabbit anti-eIF4G (Cell Signaling) primary monoclonal antibodies were used. Confocal images were acquired on a Leica SP8 fluorescence microscope using the UV laser for DAPI and an excitation laser of 561. PLA and DAPI signal areas were measured by ImageJ. Fold change relative to vehicle was quantified with PLA signal divided by DAPI signal.

Luciferase assay

Cap-dependent translation was measured using the luciferase reporter construct pRSTF-CVB3 containing the 5’ non-coding region of the Coxsackie B3 virus cloned between the firefly and

renilla luciferase (13). The construct was electroporated in serum-free media and cells recovered in complete RPMI media for 2 hours followed by inhibitor treatment for 8 hours. Following treatment, cells were lysed and renilla and firefly luciferase expression were measured using the Dual luciferase assay kit (Promega) using a luminometer. Renilla luciferase expression was normalized to Firefly luciferase expression and results were expressed relative to vehicle treated.

RNA Extraction, RT, and Quantitative RT-PCR

RNA was extracted using TRIzol reagent (Invitrogen), followed by purification with Quick-RNA MiniPrep according to the manufacturer's protocol (Zymo Research). For *Aicda,* purified B cells were stimulated with αCD40+IL-4, LPS+IL-4, or LPS for 72 hours. For germline transcripts Iγ-Cγ, Iγ3-Cγ3, and Iα-Cα, B cells were stimulated for either 48 hours before harvesting, or with 48hr Rap treatment, an additional 24 hours for a total of 72 hours. cDNA synthesis was carried out on 300 ng to 1 μg of total RNA using iScript Reverse Transcription Supermix (BioRad) for RT-quantitative PCR (qPCR). Gene expression of *Aicda* or germline transcripts was performed using iTaq Universal SYBR Green Supermix (BioRad), appropriate primers, and StepOnePlus Real-Time PCR System by Applied Biosystems. Mouse L32 was used as the housekeeping gene. Ratio of gene expression change was determined by the delta-(delta-Ct) method.

The following primers were used for qPCR:

Aicda forward primer 5′-TGCTACGTGGTGAAGAGGAG-3′ and reverse primer 5′-TCCCAGTCTGAGATGTAGCG-3′, mL32 forward primer 5′-AAGCGAAACTGGCGGAAAC-3′ and reverse primer 5′-TAACCGATGTTGGGCATCAG-3′, Iγ-Cγ forward primer 5'-TCGAGAAGCCTGAGGAATGTG 3'and reverse primer 5'-GGATCCAGAGTTCCAGGTCACT-3', Iγ3-Cγ3 forward primer 5'-

GAGGTGGCCAGAGGAGCAAGAT-3’ and reverse primer 5’-AGCCAGGGACCAAGGGATAGAC-3’, and Iα-Cα forward primer 5’-CAAGAAGGAGAAGGTGATTCAG-3’ and reverse primer 5’-GAGCTGGTGGGAGTGTCAGTG-3’

FOXO nuclear localization assay

Mouse splenic B cells were stimulated with LPS+IL-4 for 48 hours and treated with inhibitors for 4 hours before harvesting. Cells were then fixed in 4% PFA and stained with anti-B220 PE and rabbit anti-FOXO (Cell Signaling) primary and anti-rabbit secondary. Cells were then stained with Hoescht before collection. Samples were analyzed using Amnis ImageStream Mark II Imaging Flow Cytometer (Millipore). FOXO nuclear localization was analyzed using the IDEAS software onboard Nuclear Localization Wizard algorithm. Ratio of Nuclear to Cytoplasmic was determined and expressed as fold change to vehicle.

Results

mTORC1 regulates antibody class switching independently from proliferation

Antibody class switching occurs after activated B cells commit to proliferation (14–17). Since rapamycin inhibits B cell proliferation, further studies were required to establish a separable role for mTORC1 in switching. Experiments in which mice were treated with low doses of Rap after viral infection provided evidence that partial mTORC1 inhibition selectively affects class switching while preserving or enhancing IgM responses that also require B cell clonal expansion (6, 8). In accord, we found that low dose Rap suppressed IgG1 production and GC B cell percentage without reducing IgM responses in mice immunized with the T-dependent

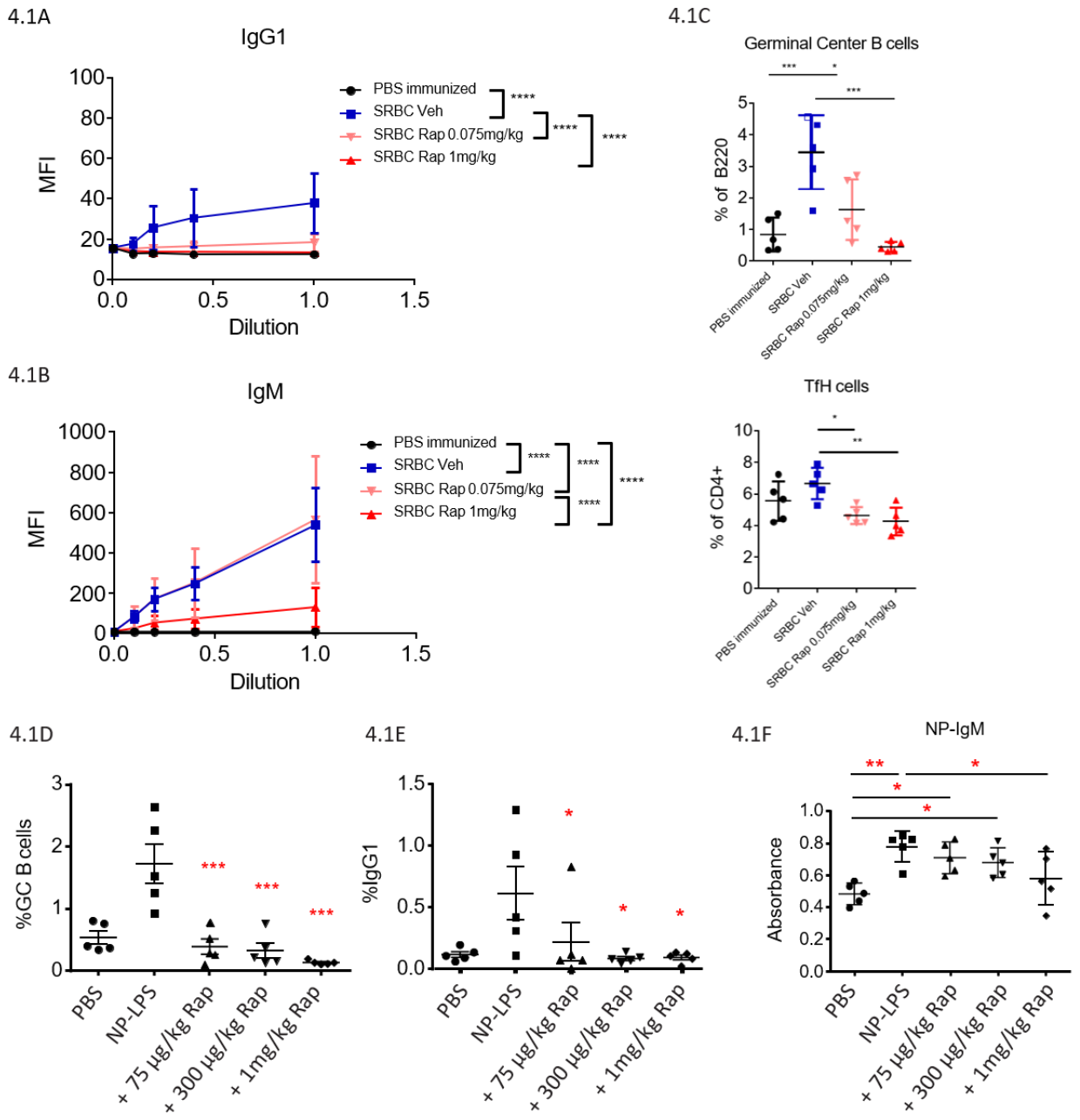

Figure 4.1 Low concentrations of rapamycin reduce IgG1 production during SRBC immunization. Mice were immunized with a T-dependent antigen, sheep red blood cells (SRBC) and treated for 7 days i.p. with vehicle control PBS, a low Rap dose of 75 µg/kg that has been shown to preserve lymphocyte activation, or an immunosuppressive dose of 1mg/kg. Serum was obtained from mice on day 8 and SRBC-specific IgG1 (4.1A) and IgM (4.1B) production were measured by flow cytometry as described in (12). Significance was calculated using two-way ANOVA with Sidak multiple comparison test. (4.1C) Percentage of spleen cells with germinal center (B220+GL7+Fas+) and T follicular helper cell (CXCR5+PD-1+CD4+) phenotype were analyzed by flow cytometry. (4.1D-4.1F) Mice were immunized with 5 µg NP-LPS and treated for 10 days with PBS, 75 µg/kg, 300 µg/kg or 1mg/kg Rapamycin by IP injection daily. (4.1D) Percentage of spleen cells with germinal center (B220+GL7+Fas+)

phenotype and (4.1E) %IgG1+B220+ cells were analyzed by flow cytometry. (4.1F) NP-specific serum IgM was measured by ELISA. Significance was calculated using one-way ANOVA with Newman Keuls multiple comparison test. (*P<0.05; **P<0.01; ***P<0.001; ****P<0.0001)

antigen sheep red blood cells (SRBC) **(Fig. 4.1A-4.1C)** or the T-independent antigen NP-LPS **(Fig. 4.1D-4.1F).** Another study found that deletion of raptor in B cells post-activation (using Cγ1-Cre) suppresses switching to IgG1 while preserving IgM responses *in vivo* (7). Together these findings support the conclusion that mTORC1 promotes class switching in a manner independent from proliferation. This is an important distinction because it may be possible to develop inhibitors of mTORC1 downstream effectors to selectively modulate B cell differentiation without the broad immunosuppressive effects of rapamycin.

We sought to apply *in vitro* methods to study the B cell-intrinsic effects of different genetic and pharmacological perturbations on antibody class switching. Stimulation of purified B cells *in vitro* with αCD40+IL-4 or LPS+IL-4 mimics T cell-dependent or T cell-independent signals (18, 19), respectively, to induce switching to IgG1. By labeling B cells with the cell division tracker CFSE prior to activation, it is possible to control for differences in proliferation by gating on divided cells (CFSE-lo). In B cells stimulated with αCD40+IL-4, Rap caused a dose-dependent decrease in switching to IgG1 among divided cells (**Fig. 4.2A**). We used the cyclin-dependent kinase inhibitor palbociclib to suppress proliferation (**Fig 4.2A**) without affecting mTORC1 signaling **(Fig. 4.2B)**. Notably, palbociclib did not reduce the % IgG1+ among the residual dividing cells (**Fig. 4.2A**). These data confirm that the ability of rapamycin to suppress switching is not due simply to slower proliferation.

To identify conditions where complete mTORC1 inhibition does not block proliferation, we tested different time points at which we added 20 nM Rap or 50 nM MLN0128 (a dual mTORC1/mTORC2 inhibitor, referred to as INK128 in previous chapters). We stimulated

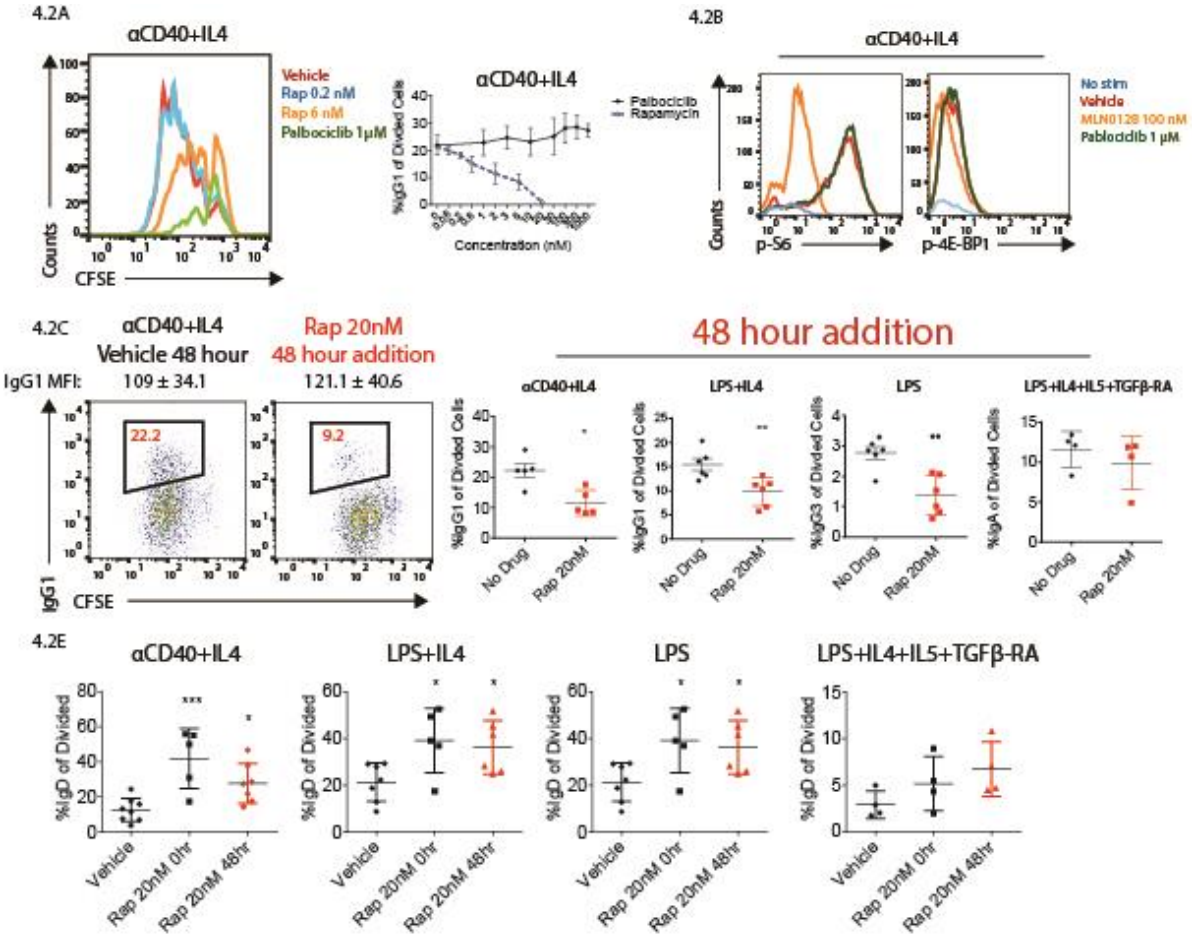

Figure 4.2 mTORC1 control of IgG1 switching is not due to inhibition of division. (4.2A) Purified mouse splenic B cells were stimulated with αCD40+IL-4 and treated with rapamycin or the CDK4/6 inhibitor Palbociclib at the indicated concentrations. The percent of live B cells that have divided at least once (based on CFSE dilution; CFSE-low) expressing IgG1 was determined by flow cytometry at 96h. (4.2B) Intracellular staining of p-S6 and p-4E-BP-1 was measured by flow cytometry. (4.2C-4.2D) Cells were stimulated with αCD40+IL-4, LPS+IL-4, LPS alone, or LPS+IL-4+IL-5+TGF-β+RA. (4.2C) Percent of live B cells that have divided at least once expressing IgG1, IgG3, IgA and (4.2D) IgD was determined by flow cytometry at 96h. Data are representative of three or more experiments and shown as mean ±SD. Significance was calculated using a paired two-tailed student's *t* test. (*P<0.05; **P<0.01; ***P<0.001)

splenic B cells with αCD40+IL-4 or LPS+IL-4 and added the inhibitors at the same time as activation (0hr addition), or 24 hours after activation (24hr addition), or 48 hours after activation (48hr addition) **(Fig. 4.2B, S4.1A)**. 0hr addition completely blocked division as expected, while 24hr addition partly reduced division and 48hr addition had no effect **(Fig. S4.1A)**. Western blot confirmed that 48hr addition Rap reduced p-S6 and partially inhibited 4E-BP2 phosphorylation

while the mTOR kinase inhibitor MLN0128 completely reduced S6, 4E-BP1, 4E-BP2, and AKT phosphorylation (**Fig. S4.1B**). Nevertheless, the B cells were still able to divide and seemed to have committed to cell cycle progression as seen by cyclin D2 expression; 0hr rapamycin addition decreased cyclin D2 measured 4 hours after activation, whereas Rap added at 48 hours did not affect ongoing cyclin D2 expression **(Fig. S4.1C)**. 48hr addition of Rap significantly decreased %IgG1+ in divided cells compared to 0.1% DMSO control **(Fig. 4.2C, Fig. S4.1D)**; similar effects were observed over a range of LPS and IL-4 concentrations **(Fig. S4.2).** 48hr addition of MLN0128 did not affect %IgG1+ (**Fig. S4.1D**), probably due to opposing effects of mTORC1 and mTORC2 inhibition on CSR (5).

We also tested other stimuli that promote switching to IgG3 (LPS alone) or IgA (LPS+IL-4+IL-5+TGF-β+Retinoic Acid; henceforth referred to as IgA stimuli). 48hr Rap addition reduced %IgG3+ in B cells activated with LPS but did not significantly decrease switching to IgA **(Fig. 4.2C).** Overall, this suggests that the role of mTORC1 in switching is confined to a subset of isotypes but not selective to only IgG1.

To exclude the possibility that the lower percentage of IgG+ cells was due to reduced translation of Ig mRNAs, we measured the surface expression of IgG1 (determined by mean fluorescence intensity, MFI) in cells that did switch following Rap treatment. Notably, the MFI was not lower than the vehicle treated cells (121.1 ± 40.6 vs. 109 ± 34.1) (**Fig. 4.2C**). We also assessed the percentage of non-switched B cells (IgD+) and found that 0hr and 48hr addition of Rap increased %IgD+ cells following αCD40+IL-4, LPS+IL-4, or LPS but not IgA stimulation **(Fig. 4.2D).** This suggests that Rap reduces switching overall rather than rerouting the switch to other antibody isotypes.

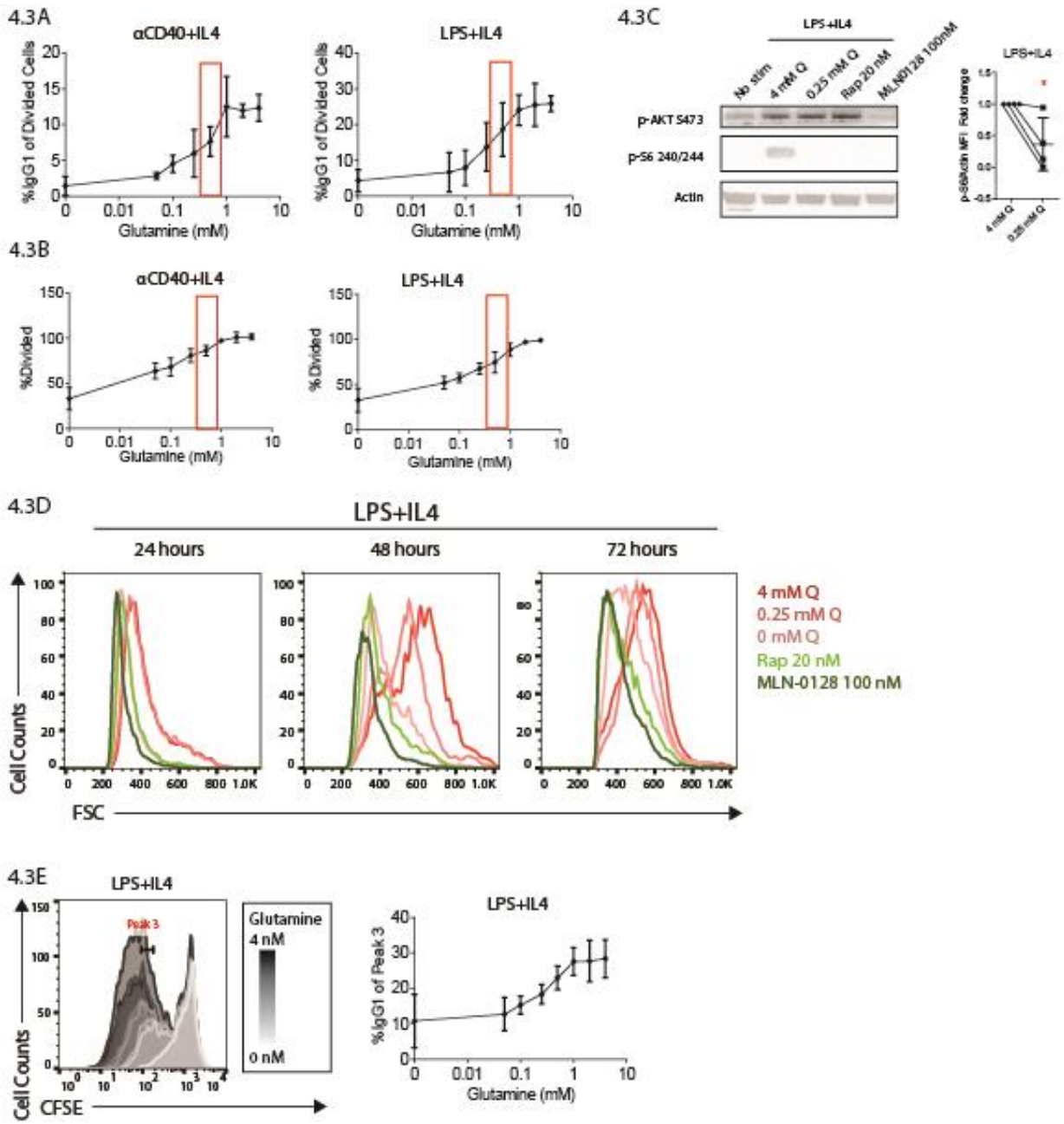

Figure 4.3 Glutamine deprivation reduces switching to IgG1. Cells were stimulated with αCD40+IL-4 or LPS+IL-4 in media with different glutamine concentrations as indicated. Percent IgG1 of the divided cells (4.3A) and percent divided (4.3B) is graphed. (4.3C) Cells were stimulated with LPS+IL-4 in media with indicated glutamine concentrations and inhibitors for 24 hours before harvesting for western. p-S6 signal was quantified over multiple experiments. (4.3D) Cell size was determined by flow cytometry at 24, 48 and 72 hours. (4.3E) %IgG1 gating on Peak 3 was determined by flow cytometry at 96h.

Since mTORC1 is a sensor of environmental inputs including nutrients and growth factors, we wanted to test the effect of physiological mTORC1 inhibition by nutrient restriction. Glutamine is used as an energy source by activated lymphocytes (20) and is also required for import of essential amino acids that activate mTORC1 (21). B cells require glutamine to proliferate and undergo Ig synthesis (22); however, the effect of glutamine restriction on antibody class switching has not been tested. Typical lymphocyte cell culture media contains 4 mM of glutamine. We found that 1 and 2 mM glutamine still preserved proliferation and class switching (%IgG1+) **(Fig. 4.3A, 4.3B)**. Complete glutamine withdrawal strongly reduced proliferation and %IgG1. As glutamine concentration increased to 0.4 mM, proliferation was mostly restored while switching to IgG1 was still reduced, similarly to low concentrations of rapamycin. B cells stimulated in 0.25mM glutamine had reduced mTORC1 activity as measured by pS6 and cell size (**Fig. 4.3C, 4.3D)**. Gating on cells in the third division confirmed that decreasing glutamine impairs switching to %IgG1 among cells that have divided similarly **(Fig. 4.3E)**. Overall, these results demonstrated that chemical (Rap) or physiological (glutamine deprivation) inhibition of mTORC1 suppresses class switching independently from proliferation.

Targeting eIF4E function reduces antibody class switching

Two major mTORC1 downstream effectors are known to regulate gene expression: S6Ks and the 4E-BP/eIF4E axis. We assessed the role of these pathways in Ig class switching. To test the effects of S6K inhibition, we treated B cells with an S6K1-selective inhibitor (S6K1i) and confirmed reduced phosphorylation of the direct S6K substrate, ribosomal protein S6 **(Fig. S4.3A).** S6K1 inhibition also caused increased p-AKT that frequently occurs due to loss of feedback (not shown). S6K1 inhibition significantly reduced switching to IgG1 following

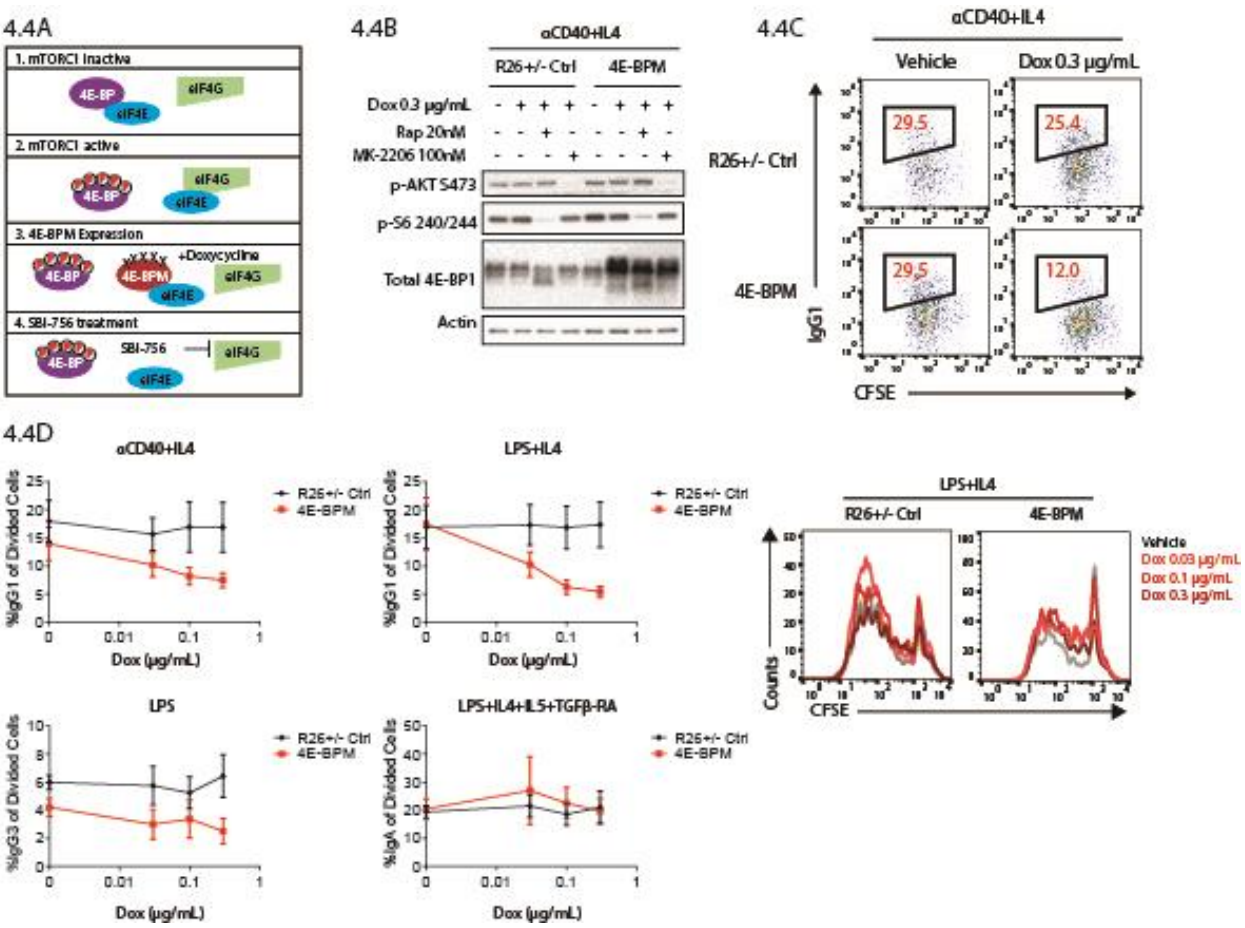

Figure 4.4 Genetic targeting of eIF4E activity reduces antibody class switching. (4.4A) (1-2) Model of 4E-BP and eIF4E signaling. (3) Genetic and (4) pharmacological approaches to inhibit eIF4E activity. (4.4B, 4.4C) Purified mouse splenic B cells from control mice or DOX-inducible 4E-BP mutant mice were stimulated with αCD40+IL-4 and tested for (4.4B) transgene expression by western and (4.4C) IgG1 switching among divided B cells. (4.4D) B cells stimulated under the conditions indicated for treated at 48hr with titrations of DOX. The percent of live B cells that have divided at least once (measured by CFSE or eFluor670) expressing IgG1, IgG3, or IgA was determined at 96hr. Data are representative of three or more experiments and shown as mean ±SD. The histograms on the right show cell division tracking by CFSE in cells treated with different concentrations of DOX. (4.4B) Cells were stimulated 48 hours then treated with inhibitors as indicated and harvested at 54 hours. Western blotting confirmed 4E-BP mutant expression.

αCD40+IL-4 or LPS+IL-4 stimulation but had no effect in LPS (IgG3) or IgA stimulating conditions **(Fig. S4.2B).** These results suggest that S6K1 activity contributes to mTORC1-driven switching under some conditions. Interestingly, S6K1 inhibition partially blocked proliferation with α-CD40+IL-4 but not in cells stimulated with LPS+IL-4 (**Fig. S4.2C**).

Next, we investigated the role of the 4E-BPs, a family of mTORC1 substrates that in non-phosphorylated forms compete with eIF4G for the same binding domain of eIF4E and inhibit eIF4F complex formation. We previously showed that Rap inhibits eIF4E function in lymphocytes more than other cell types, in part due to expression of the 4E-BP2 isoform that is more rapamycin sensitive than 4E-BP1 (9) and **(Fig. S4.1B)**. Thus, to test the role of eIF4E in class switching, we used transgenic mice in which a mutant form of 4E-BP1 (4E-BP1M) can be inducibly expressed by doxycycline (DOX) treatment. The 4E-BP1M protein has five S/T sites changed to alanine, such that the protein can no longer be phosphorylated by mTORC1. 4E-BP1M binds more avidly to eIF4E and inhibits initiation of cap-dependent translation regardless of mTORC1 activity **(Fig. 4.4A)**. When 4E-BP1M is induced prior to B cell activation, proliferation is strongly suppressed (9). Therefore we used a late addition of DOX (48hr) and confirmed 4E-BP1M protein expression by western blotting (**Fig. 4.4B**). In B cells stimulated with αCD40+IL-4 or LPS+IL-4 and treated at 48hr addition of increasing DOX concentrations, 4E-BP1M reduced %IgG1+ without reducing proliferation **(Fig. 4.4C, 4.4D)**. 4E-BP1M expression also reduced %IgG3+ but not %IgA+ **(Fig 4.4D, Table 4.1)**.

Table 4.1 Summary of results by antibody isotype

Isotype	Rap 48h	SBI 48h	4E-BPM 48h	AID-GFP MFI Rap	AID-GFP MFI SBI-756	Germline
IgG1 (αCD40+IL4)	↓*	↓*	↓**	↓ *	↓+	No change
IgG1 (LPS+IL4)	↓↓**	↓↓**	↓↓*	↓↓**	↓↓**	↓*
IgG3 (LPS)	↓*	↓*	↓*	↓*	↓	No change
IgA (LPS+IL4+IL5+TGFβ+RA)	No change	No change	No change	↓*	↓*	↓*

* Paired one-tailed t-test
+ N = 2

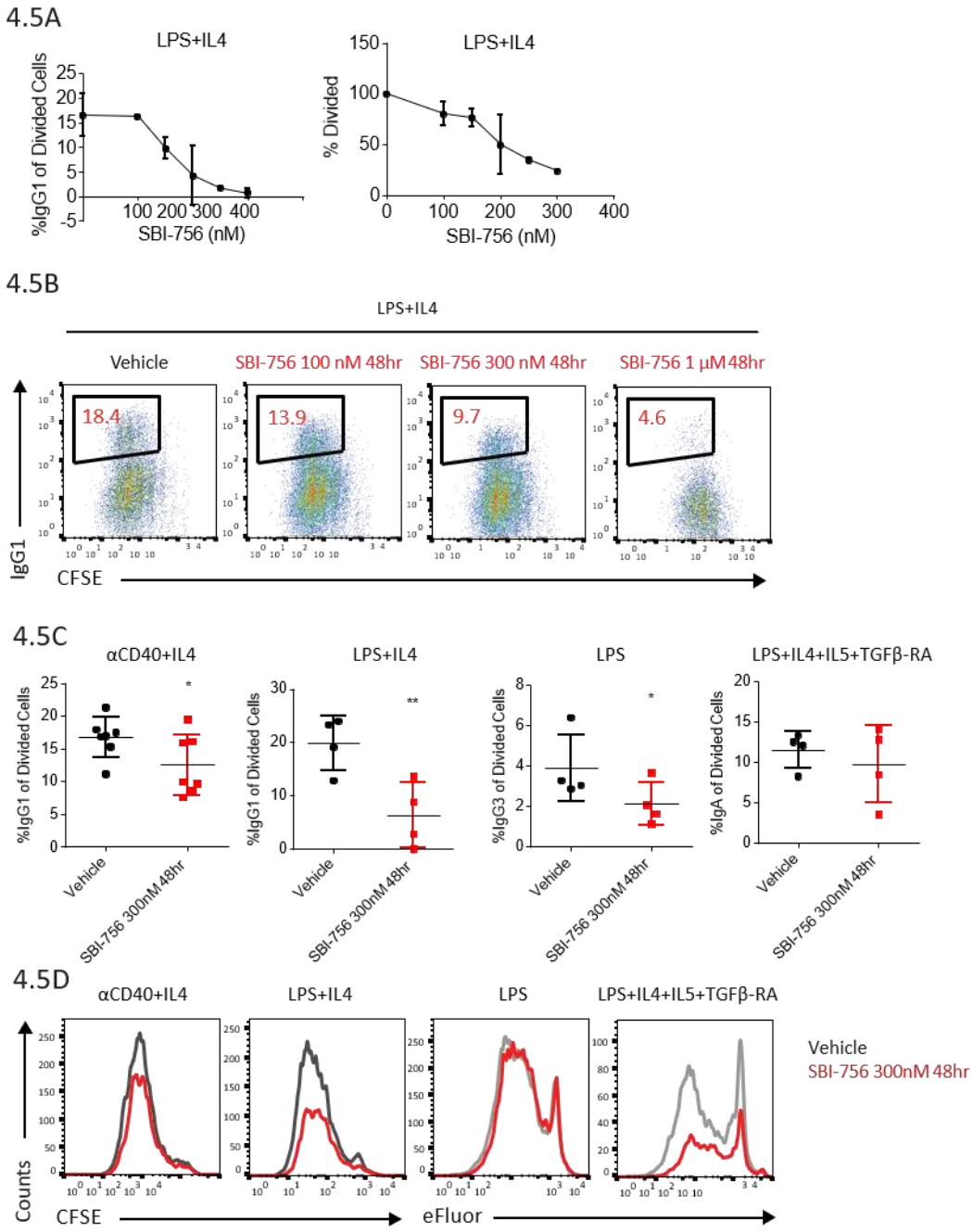

Figure 4.5 Pharmacological targeting of eIF4E activity with SBI-756 reduces antibody class switching. Cells were stimulated then treated with various concentrations of SBI-756 at 0 hrs (4.5A), or at 48 hrs after activation (4.5B). Percent of live B cells that have divided at least once expressing (4.5C) IgG1, IgG3, IgA and (4.5D) proliferation by CFSE or eFluor670 were measured at 96 hours by flow cytometry. Data are representative of three or more experiments and shown as mean ±SD. Significance was calculated using a paired one tailed student's t test. (*P<0.05; **P<0.01; ***P<0.001)

To complement this genetic model, we tested the compound SBI-756 which binds the scaffolding protein eIF4G and prevents its interaction with cap-binding protein eIF4E in melanoma cells (11). In B cells stimulated with LPS+IL-4, 150 nM SBI-756 partially reduced switching to IgG1 while proliferation was mainly preserved **(Fig. 4.5A)**. As SBI-756 concentration was increased, switching and proliferation were reduced further **(Fig. 4.5A)**. We also tested 48hr addition of SBI-756 **(Fig. 4.5B)**. Again, switching to IgG1 or IgG3 but not IgA was significantly reduced **(Fig. 4.5C, Table 4.1).** SBI-756 did slightly reduce cell accumulation under LPS+IL-4 and IgA stimulating conditions, however the number of cell divisions was similar under all conditions **(Fig. 4.5D)**. Hence, direct inhibition of eIF4F function does not affect ongoing B-cell proliferation, yet specifically inhibits Ig class switching. This selective effect is consistent with previous studies showing that 4E-BP/eIF4E axis affects the translation of subsets of specific mRNAs in a cell context-specific manner (23–25).

Rapamycin and SBI-756 disrupt cap-complex formation

To confirm that SBI-756 disrupts the cap-binding complex and to assess the effect of Rap, we used an *in situ* proximity ligation assay (PLA) (26). Analysis by confocal microscopy allows visualization and quantitation of the interactions between eIF4E and eIF4G **(Fig. 4.6A)** in activated B cells. We stimulated B cells with LPS+IL-4 and used the mTOR kinase inhibitor, MLN0128, as a control since this compound strongly disrupts eIF4E interaction with eIF4G (9). MLN0128 (100 nM), Rap (2 nM or 20 nM) and SBI-756 (300 nM) all significantly reduced eIF4E:eIF4G association compared to DMSO vehicle control **(Fig 4.6A)**. In activated B cells treated with Rap or SBI-756 at 48hr and tested 4hr later, we observed trends of reduced PLA signal that were not statistically significant (data not shown). To increase sensitivity, we

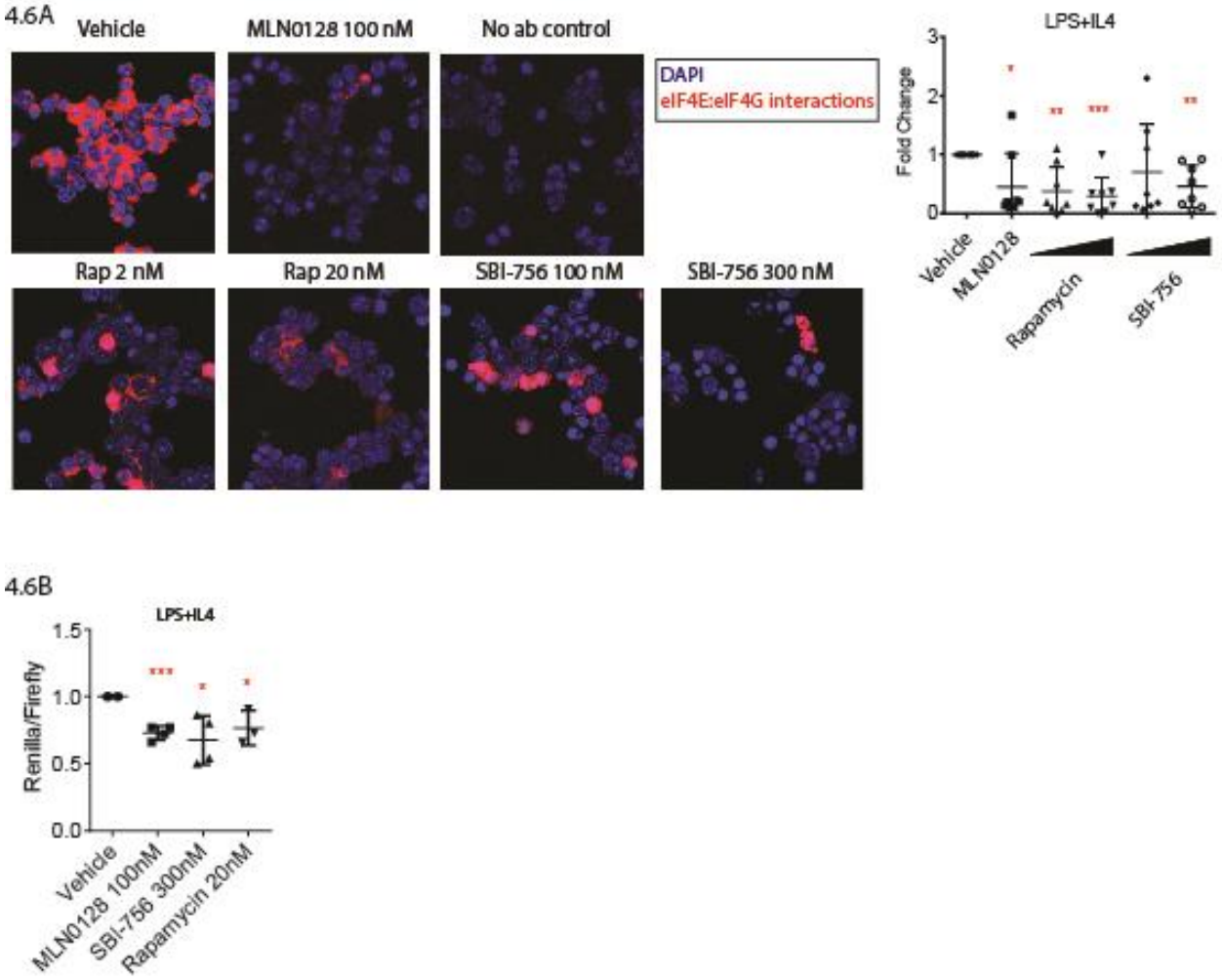

Figure 4.6 Inhibitors that reduce switching disrupt cap-complex formation. (4.6A) eIF4E-eIF4G interactions detected by proximity ligation assay (PLA) in purified mouse splenic B cells that were treated with inhibitors as indicated and stimulated with LPS+IL-4 for 48 hours before fixing and permeabilizing. Interactions are visualized as red signal. Nuclei are stained with DAPI (blue). 5 images in separate fields were taken for each condition. All data are shown as binary area analysis of PLA/DAPI ±SD. Fold change was calculated by normalizing to vehicle. Each point represents one independent experiment. Significance was calculated using a paired one tailed student's t test (*P<0.05; **P<0.01; ***P<0.001). (4.6B) We stimulated B cells for 48 hours with LPS+IL-4 and used a bicistronic dual Renilla-Firefly luciferase reporter construct to measure cap-dependent translation (Renilla luciferase) relative to cap-independent, polio IRES mediated translation (firefly luciferase) as an internal control. Each point represents one independent experiment. Fold change was calculated using vehicle condition. Significance was calculated using a paired one tailed student's t test. (*P<0.05; **P<0.01; ***P<0.001)

performed a dual luciferase reporter assay using a bicistronic dual Renilla-Firefly luciferase reporter construct. This construct measures cap-dependent translation by synthesis of the Renilla

luciferase as well as cap-independent, polio IRES mediated translation by synthesis of firefly luciferase as an internal control. In B cells activated with LPS+IL-4, 48hr addition of Rap or SBI-756 significantly reduced cap-dependent translation by 30-40% compared to vehicle **(Fig. 4.6B)**.

Rapamycin and SBI-756 reduce AID protein but not *Aicda* mRNA

Overall, these results suggest that cap-dependent translation is necessary for CSR. To identify at which step of the recombination event the mTORC1/eIF4E axis is involved, we first investigated the production of germline transcripts. When a B cell is activated, secondary signals such as IL-4, TGF-β and IFN-γ can direct the class of antibody to switch by promoting production of non-coding sterile RNAs (germline transcripts) encoded by the DNA of the accepter switch region. During transcription elongation of the region, the chromatin becomes more accessible for the CSR machinery to facilitate recombination to the targeted switch region (27). Using RT-PCR we measured germline transcripts Iγ-Cγ, Iγ3-Cγ3, and Iα-Cα, which are produced from IgG1, IgG3, and IgA switch regions respectively. As expected, Iγ-Cγ was detected under αCD40+IL-4 or LPS+IL-4 stimulating conditions but not under IgG3 (LPS only) or IgA conditions **(Fig. S4.4A)**. Similarly, Iγ3-Cγ3 and Iα-Cα were detected only under IgG3 or IgA switching conditions, respectively. In all conditions, 0hr addition of Rap strongly inhibited germline transcript production (**Fig. S4.4A**), consistent with a study of Raptor-deficient B cells (7). S6K1 inhibition reduced Iγ-Cγ transcripts in B cells stimulated with LPS+IL-4 **(Fig. S4.3D)**, suggesting a novel role for S6K1 in mTORC1-driven germline transcription under these conditions. However, the S6K1 inhibitor did not reduce germline transcripts under αCD40+IL-4, IgG3 or IgA switching conditions **(Fig. S4.4D)**. We also tested 48hr addition of Rap or SBI-756

which only reduced germline transcript production in LPS+IL-4 and IgA stimulating conditions but not with αCD40+IL-4 or LPS **(Fig. S4.4B)**. These results did not follow the same trends in our flow-based class switching experiments **(Table 4.1)**. This lack of correlation suggest that germline transcript production is not the mechanism by which mTORC1 activity and cap-dependent translation regulates class switching at the 48hr timepoint.

Class switching requires activation-induced cytidine deaminase (AID), a DNA mutator protein that initiates CSR by introducing mutations into the targeted switch regions of the Ig heavy chain locus (28, 29). Western blotting **(Fig. 4.7A)** showed that Rap added at 0hr or 48hr timepoints after LPS+IL-4 stimulation significantly reduced AID protein amounts. We used a GFP knock-in reporter of AID (AID-GFP mice) (30) to measure AID protein amounts using flow cytometry. Under all stimulating conditions, we found that 0 hr addition of a low concentration of Rap (0.2 nM) reduced AID expression per cell and that 48hr addition of Rap or SBI-756 also significantly reduced expression **(Fig. 4.7B-C, Table 4.1)**. The AKT inhibitor MK-2206 was used as a control to increase AID expression (5).

Reduced AID expression under IgA conditions was surprising given that 48hr addition of Rap or SBI-756 did not affect switching to IgA. We tested the effect of adding Rap at earlier timepoints (24, 40, and 44 hr) and found that switching to IgA was minimally affected even when Rap reduced proliferation **(Fig. S4.5A)**. However, Rap did reduce %IgG3+ in the same experiment, suggesting that the reduction in AID mainly affects switching to other isotypes under the IgA stimulating conditions **(Fig. S4.5B)**.

To determine if AID expression is regulated post-transcriptionally in activated B cells, we compared changes to *Aicda* mRNA and AID protein. Under LPS+IL-4 stimulating

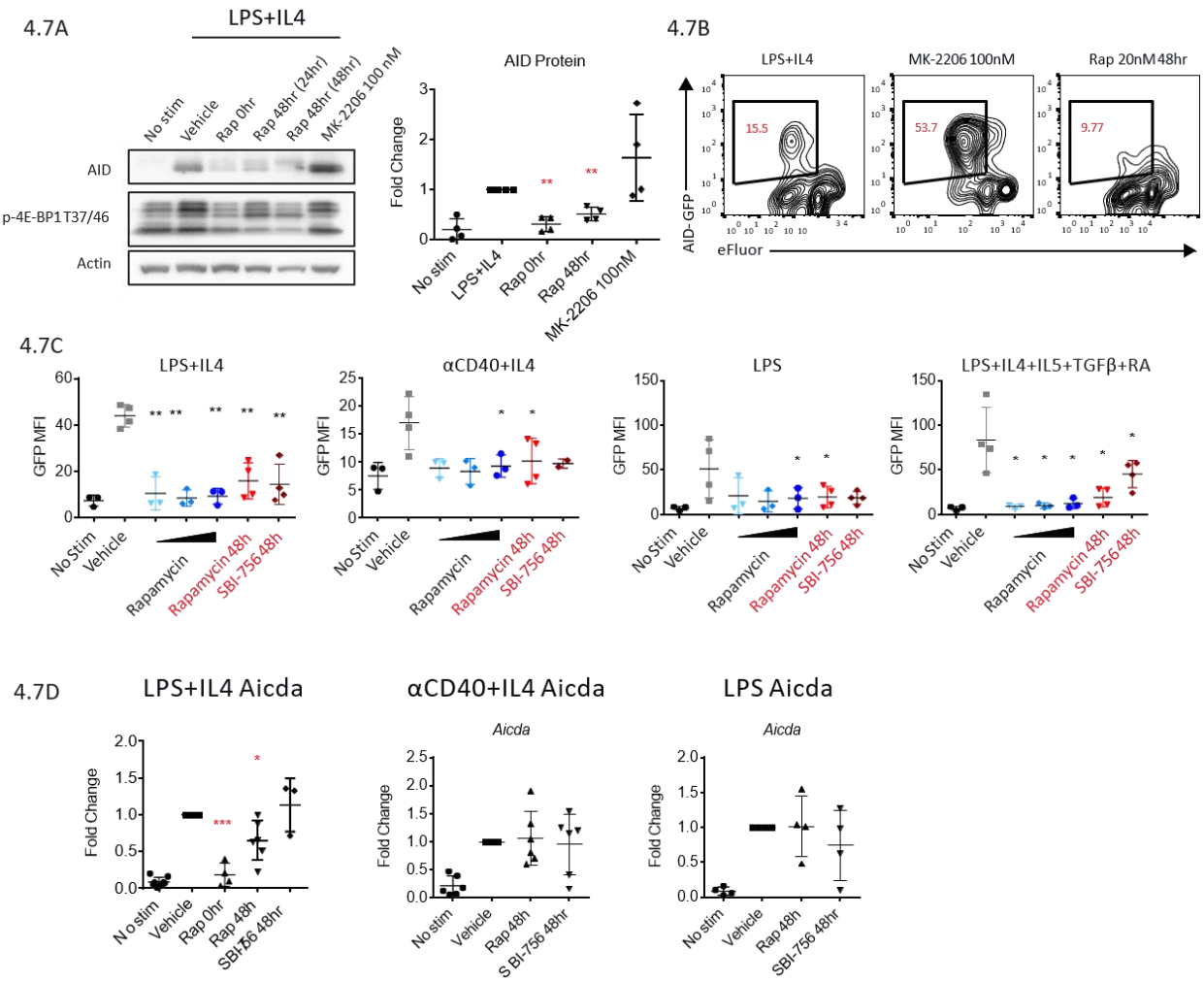

Figure 4.7 48 hour addition of Rap or SBI-756 reduces AID protein but not *Aicda* mRNA. (4.7A) B cells were purified and stimulated with LPS+IL-4 for 48 hours then treated with inhibitors as indicated. MK-2206 is an AKT inhibitor. In lanes 2-4 and 6, cells were harvested at 72 hours. Lane 5 cells were activated for 48 hours then treated with Rapamycin for an additional 48 hours before harvesting. AID amounts and 4E-BP phosphorylation were quantitated by western. (4.7B, 4.7C) B cells were purified from AID-GFP mice and stimulated with LPS+IL-4, αCD40+IL-4, LPS, or LPS+IL-4+IL-5+TGF-β+RA and treated with inhibitors as indicated. Divided cells were gated on eFluor670-lo cells and AID-GFP MFI among divided cells was analyzed at 96 hrs using flow cytometry. (4.7D) Purified B cells were stimulated with left to right: LPS+IL-4, αCD40+IL-4, or LPS and treated with inhibitors as indicated. Cells were harvested at 72 hours to measure *Aicda* mRNA by RT-qPCR. Each point represents one individual experiment. Fold change was calculated in comparison to vehicle treated. Significance was calculated using a paired one tailed student's t test. (*P<0.05; **P<0.01; ***P<0.001)

conditions, 0hr addition of Rap strongly reduced *Aicda* mRNA **(Fig. 4.7D)**, consistent with studies of B cells lacking Raptor (7). However, 48hr Rap addition had a lesser effect, and did not

reduce *Aicda* mRNA under αCD40+IL-4 or LPS stimulating conditions. Notably, 48hr addition of SBI-756 did not reduce *Aicda* mRNA under any switching conditions. Considering that Foxo proteins promote *Aicda* transcription (31) and Rap treatment can lead to increased AKT activity, we used ImageStream analysis to determine whether Rap reduced nuclear localization of Foxo1 in activated B cells (**Fig. S4.6A**). Instead we found that 48hr addition of either Rap or SBI-756 had the opposite effect, increasing the ratio of nuclear:cytoplasmic Foxo1 (**Fig. S4.6B**). Together these data suggest that the reduction in AID protein is not due to a decrease in *Aicda* transcription.

Discussion

Following the initial discovery of rapamycin as a potent immunosuppressant over 40 years ago (32), this natural product was found to inhibit proliferation and impair differentiation of both T and B lymphocytes (2, 33, 34). High doses of rapamycin profoundly impair antibody production (35), yet low doses have a selective effect on class switched antibody responses (6–8). mTORC1 is dynamically regulated in GCs (3) and responsive to environmental conditions such as hypoxia (4); furthermore, genetic deletion of Raptor has established that the mTORC1 complex has a B cell-intrinsic role in antibody class switching (7). However, the mechanisms by which mTORC1 regulates class switching remain unknown. Here, we show that Rap reduces eIF4E and eIF4G association to inhibit cap-dependent translation in activated B cells, and that directly inhibiting eIF4E activity can also reduce antibody class switching. We also show that the mechanism involves post-transcriptional inhibition of AID protein expression, which is a novel mechanism of regulating AID and B cell differentiation.

Our laboratory reported previously that the 4E-BP/eIF4E axis is rapamycin-sensitive in lymphocytes and required for both growth and proliferation following antigen receptor stimulation (9). Supporting the role of eIF4E in B cell proliferation, we found here that 0hr addition of SBI-756 suppresses B cell proliferation and eIF4E:eIF4G association. However, mTORC1/eIF4E activity is not necessary for proliferation 48 hours after activation. The finding that ongoing proliferation is mTORC1-independent is consistent with early studies showing lesser effects of Rap when added at late time points after B or T cell activation (2, 36). More recent work has confirmed this *in vivo* by showing that mTORC1 activity is not necessary to drive B cell proliferation during the dark zone stages of the germinal center (3). Since mTORC1 is active in light zone B cells (3) and required for IgG1 switching *in vivo* (7), it will be interesting to see how eIF4E signaling regulates GC differentiation. We tested SBI-756 in the SRBC immunization model and did not observe any differences in IgG1 secretion or GC B cell percentages (data not shown). This might be due to the pharmacokinetics of SBI-756 *in vivo*, which might not facilitate sustained inhibition of the eIF4E:eIF4G interaction. Further studies with genetic models in which mutations disrupt eIF4G and eIF4E binding will be useful to address this question and to study B-cell intrinsic effects.

We found that 48 hour addition of rapamycin or SBI-756 reduced switching to IgG3 and IgG1, but did not reduce IgA switching even though AID protein was reduced. One possible explanation is that the cells switching to IgA are enriched in marginal zone and B-1 cells (37) and that mTORC1 might not regulate AID and switching in these subsets. Marginal zone cells make up about 10% of B cells purified from the spleen and perhaps the overall AID being produced is outweighed by the reduction of AID in the follicular B cells.

B cell activation is accompanied by rapid and sustained activation of S6 kinases (38); however, little is known about the role of S6Ks in B cell function. Consistent with our previous work (9), we show here that S6K1 inhibition has minimal effect on proliferation of B cells stimulated with αIgM+IL-4. However, S6K1 inhibition did partially reduce proliferation induced by αCD40+IL-4 and diminished switching to IgG1. While S6K1 inhibition may be partially responsible for the effects of early Rap addition on antibody class switching, additional studies are required to better understand how S6K1 responds under the different stimuli to promote switching or proliferation.

Our findings demonstrate that the mTORC1/eIF4E axis plays a novel role in B cell differentiation. We and others have previously published that PI3K/AKT signals are involved in B cell differentiation and transcription of AID (5, 39, 40). The finding that AID expression can be regulated post-transcriptionally illustrates the need for better understanding and investigation of the translatome during B cell differentiation and how different signals control translation efficiency of different mRNAs. The 4E-BP/eIF4E axis downstream of mTORC1 has been studied extensively in cancer and shown to preferentially promote translation of mRNAs involved in metastasis and invasion, and growing evidence supports a key role for regulated translation in CD4 and CD8 T cell differentiation (41, 42). However, which mRNAs in activated B cells are regulated by translation efficiency remains an important question in the field. Cap-dependent translation is an attractive target for cancer therapy and efforts are underway to develop small molecule inhibitors of eIF4F components (eIF4E, eIF4G, eIF4A) for oncology (11, 26, 43–45). Further study of this pathway may provide mechanistic insight into how the immune system will be affected by eIF4F-targeted therapies. Indeed, the finding that the eIF4G antagonist SBI-756 reduces AID protein suggests that it may be useful as a combination therapy

with idelalisib, a PI3Kδ inhibitor, which increases AID expression and mutational activity in activated B cells and in human patients with chronic lymphocytic leukemia (46). Further studies are needed to determine whether eIF4F inhibitors suppress AID expression in human B leukemia and lymphoma cells.

Our findings emphasize that 4E-BP/eIF4E can regulate synthesis of important proteins necessary for B cell differentiation. Study of this pathway may provide mechanistic insight into antibody-mediated autoimmune diseases such as lupus and arthritis as well as the formation of protective antibody responses following vaccination.

Acknowledgements

We thank Jennifer Atwood for training on Amnis Imagestream, Egest Pone for helpful discussions, and Ivan Topisirovic for insightful comments on the manuscript.

References

1. Limon, J.J., and D.A. Fruman. 2012. Akt and mTOR in B Cell Activation and Differentiation. Front Immunol. 3: 228.

2. Aagaard-Tillery, K.M., and D.F. Jelinek. 1994. Inhibition of human B lymphocyte cell cycle progression and differentiation by rapamycin. Cell Immunol. 156: 493–507.

3. Ersching, J., A. Efeyan, L. Mesin, J.T. Jacobsen, G. Pasqual, B.C. Grabiner, D. Dominguez-Sola, D.M. Sabatini, and G.D. Victora. 2017. Germinal Center Selection and Affinity Maturation Require Dynamic Regulation of mTORC1 Kinase. Immunity. 46: 1045–1058.e6.

4. Cho, S.H., A.L. Raybuck, K. Stengel, M. Wei, T.C. Beck, E. Volanakis, J.W. Thomas, S. Hiebert, V.H. Haase, and M.R. Boothby. 2016. Germinal centre hypoxia and regulation of antibody qualities by a hypoxia response system. Nature. 537: 234–238.

5. Limon, J.J., L. So, S. Jellbauer, H. Chiu, J. Corado, S.M. Sykes, M. Raffatellu, and D.A. Fruman. 2014. mTOR kinase inhibitors promote antibody class switching via mTORC2 inhibition. Proc Natl Acad Sci U S A. 111: E5076–85.

6. Ye, L., J. Lee, L. Xu, A.-U.-R. Mohammed, W. Li, J.S. Hale, W.G. Tan, T. Wu, C.W. Davis, R. Ahmed, and K. Araki. 2017. mTOR Promotes Antiviral Humoral Immunity by Differentially Regulating CD4 Helper T Cell and B Cell Responses. J Virol. 91.

7. Raybuck, A.L., S.H. Cho, J. Li, M.C. Rogers, K. Lee, C.L. Williams, M. Shlomchik, J.W. Thomas, J. Chen, J.V. Williams, and M.R. Boothby. 2018. B Cell–Intrinsic mTORC1 Promotes Germinal Center–Defining Transcription Factor Gene Expression, Somatic Hypermutation, and Memory B Cell Generation in Humoral Immunity. The Journal of Immunology. .

8. Keating, R., T. Hertz, M. Wehenkel, T.L. Harris, B.A. Edwards, J.L. McClaren, S.A. Brown, S. Surman, Z.S. Wilson, P. Bradley, J. Hurwitz, H. Chi, P.C. Doherty, P.G. Thomas, and M.A. McGargill. 2013. The kinase mTOR modulates the antibody response to provide cross-protective immunity to lethal infection with influenza virus. Nat Immunol. 14: 1266–1276.

9. So, L., J. Lee, M. Palafox, S. Mallya, C.G. Woxland, M. Arguello, M.L. Truitt, N. Sonenberg, D. Ruggero, and D.A. Fruman. 2016. The 4E-BP-eIF4E axis promotes rapamycin-sensitive growth and proliferation in lymphocytes. Sci Signal. 9: ra57.

10. Hsieh, A.C., M. Costa, O. Zollo, C. Davis, M.E. Feldman, J.R. Testa, O. Meyuhas, K.M. Shokat, and D. Ruggero. 2010. Genetic dissection of the oncogenic mTOR pathway reveals druggable addiction to translational control via 4EBP-eIF4E. Cancer Cell. 17: 249–261.

11. Feng, Y., A.B. Pinkerton, L. Hulea, T. Zhang, M.A. Davies, S. Grotegut, Y. Cheli, H. Yin, E. Lau, H. Kim, S.K. De, E. Barile, M. Pellecchia, M. Bosenberg, J.-L. Li, B. James, C.A. Hassig, K.M. Brown, I. Topisirovic, and Z.A. Ronai. 2015. SBI-0640756 Attenuates the Growth of Clinically Unresponsive Melanomas by Disrupting the eIF4F Translation Initiation Complex. Cancer Res. 75: 5211–5218.

12. McAllister, E.J., J.R. Apgar, C.R. Leung, R.C. Rickert, and J. Jellusova. 2017. New Methods To Analyze B Cell Immune Responses to Thymus-Dependent Antigen Sheep Red Blood Cells. J Immunol. 199: 2998–3003.

13. Jang, G.M., L.E.-C. Leong, L.T. Hoang, P.H. Wang, G.A. Gutman, and B.L. Semler. 2004. Structurally distinct elements mediate internal ribosome entry within the 5'-noncoding region of a voltage-gated potassium channel mRNA. J Biol Chem. 279: 47419–47430.

14. Tangye, S.G., A. Ferguson, D.T. Avery, C.S. Ma, and P.D. Hodgkin. 2002. Isotype switching by human B cells is division-associated and regulated by cytokines. J Immunol. 169: 4298–4306.

15. Hodgkin, P.D., J.H. Lee, and A.B. Lyons. 1996. B cell differentiation and isotype switching is related to division cycle number. J Exp Med. 184: 277–281.

16. Hasbold, J., A.B. Lyons, M.R. Kehry, and P.D. Hodgkin. 1998. Cell division number regulates IgG1 and IgE switching of B cells following stimulation by CD40 ligand and IL-4. Eur J Immunol. 28: 1040–1051.

17. Rush, J.S., M. Liu, V.H. Odegard, S. Unniraman, and D.G. Schatz. 2005. Expression of activation-induced cytidine deaminase is regulated by cell division, providing a mechanistic basis for division-linked class switch recombination. Proc Natl Acad Sci U S A. 102: 13242–13247.

18. Bai, L., S. Deng, R. Reboulet, R. Mathew, L. Teyton, P.B. Savage, and A. Bendelac. 2013. Natural killer T (NKT)-B-cell interactions promote prolonged antibody responses and long-term memory to pneumococcal capsular polysaccharides. Proc Natl Acad Sci U S A. 110: 16097–16102.

19. Gaya, M., P. Barral, M. Burbage, S. Aggarwal, B. Montaner, A. Warren Navia, M. Aid, C. Tsui, P. Maldonado, U. Nair, K. Ghneim, P.G. Fallon, R.-P. Sekaly, D.H. Barouch, A.K. Shalek, A. Bruckbauer, J. Strid, and F.D. Batista. 2018. Initiation of Antiviral B Cell Immunity Relies on Innate Signals from Spatially Positioned NKT Cells. Cell. 172: 517–533.e20.

20. Brand, K., W. Fekl, J. von Hintzenstern, K. Langer, P. Luppa, and C. Schoerner. 1989. Metabolism of glutamine in lymphocytes. Metab Clin Exp. 38: 29–33.

21. Nicklin, P., P. Bergman, B. Zhang, E. Triantafellow, H. Wang, B. Nyfeler, H. Yang, M. Hild, C. Kung, C. Wilson, V.E. Myer, J.P. MacKeigan, J.A. Porter, Y.K. Wang, L.C.

Cantley, P.M. Finan, and L.O. Murphy. 2009. Bidirectional transport of amino acids regulates mTOR and autophagy. Cell. 136: 521–534.

22. Crawford, J., and H.J. Cohen. 1985. The essential role of L-glutamine in lymphocyte differentiation in vitro. J Cell Physiol. 124: 275–282.

23. Thoreen, C.C., L. Chantranupong, H.R. Keys, T. Wang, N.S. Gray, and D.M. Sabatini. 2012. A unifying model for mTORC1-mediated regulation of mRNA translation. Nature. 485: 109–113.

24. Gandin, V., L. Masvidal, L. Hulea, S.-P. Gravel, M. Cargnello, S. McLaughlan, Y. Cai, P. Balanathan, M. Morita, A. Rajakumar, L. Furic, M. Pollak, J.A. Porco, J. St-Pierre, J. Pelletier, O. Larsson, and I. Topisirovic. 2016. nanoCAGE reveals 5’ UTR features that define specific modes of translation of functionally related MTOR-sensitive mRNAs. Genome Res. 26: 636–648.

25. Hsieh, A.C., Y. Liu, M.P. Edlind, N.T. Ingolia, M.R. Janes, A. Sher, E.Y. Shi, C.R. Stumpf, C. Christensen, M.J. Bonham, S. Wang, P. Ren, M. Martin, K. Jessen, M.E. Feldman, J.S. Weissman, K.M. Shokat, C. Rommel, and D. Ruggero. 2012. The translational landscape of mTOR signalling steers cancer initiation and metastasis. Nature. 485: 55–61.

26. Boussemart, L., H. Malka-Mahieu, I. Girault, D. Allard, O. Hemmingsson, G. Tomasic, M. Thomas, C. Basmadjian, N. Ribeiro, F. Thuaud, C. Mateus, E. Routier, N. Kamsu-Kom, S. Agoussi, A.M. Eggermont, L. Désaubry, C. Robert, and S. Vagner. 2014. eIF4F is a nexus of resistance to anti-BRAF and anti-MEK cancer therapies. Nature. 513: 105–109.

27. Xu, Z., H. Zan, E.J. Pone, T. Mai, and P. Casali. 2012. Immunoglobulin class-switch DNA recombination: induction, targeting and beyond. Nat Rev Immunol. 12: 517–531.

28. Muramatsu, M., H. Nagaoka, R. Shinkura, N.A. Begum, and T. Honjo. 2007. Discovery of activation-induced cytidine deaminase, the engraver of antibody memory. Adv Immunol. 94: 1–36.

29. Neuberger, M.S. 2008. Antibody diversification by somatic mutation: from Burnet onwards. Immunol Cell Biol. 86: 124–132.

30. Crouch, E.E., Z. Li, M. Takizawa, S. Fichtner-Feigl, P. Gourzi, C. Montaño, L. Feigenbaum, P. Wilson, S. Janz, F.N. Papavasiliou, and R. Casellas. 2007. Regulation of AID expression in the immune response. J Exp Med. 204: 1145–1156.

31. Dengler, H.S., G.V. Baracho, S.A. Omori, S. Bruckner, K.C. Arden, D.H. Castrillon, R.A. DePinho, and R.C. Rickert. 2008. Distinct functions for the transcription factor Foxo1 at various stages of B cell differentiation. Nat Immunol. 9: 1388–1398.

32. Martel, R.R., J. Klicius, and S. Galet. 1977. Inhibition of the immune response by rapamycin, a new antifungal antibiotic. Can J Physiol Pharmacol. 55: 48–51.

33. Kay, J.E., L. Kromwel, S.E. Doe, and M. Denyer. 1991. Inhibition of T and B lymphocyte proliferation by rapamycin. Immunology. 72: 544–549.

34. Wicker, L.S., R.C. Boltz, V. Matt, E.A. Nichols, L.B. Peterson, and N.H. Sigal. 1990. Suppression of B cell activation by cyclosporin A, FK506 and rapamycin. Eur J Immunol. 20: 2277–2283.

35. Jones, D.D., B.T. Gaudette, J.R. Wilmore, I. Chernova, A. Bortnick, B.M. Weiss, and D. Allman. 2016. mTOR has distinct functions in generating versus sustaining humoral immunity. J Clin Invest. .

36. Terada, N., R.A. Franklin, J.J. Lucas, J. Blenis, and E.W. Gelfand. 1993. Failure of rapamycin to block proliferation once resting cells have entered the cell cycle despite inactivation of p70 S6 kinase. J Biol Chem. 268: 12062–12068.

37. Kaminski, D.A., and J. Stavnezer. 2006. Enhanced IgA class switching in marginal zone and B1 B cells relative to follicular/B2 B cells. J Immunol. 177: 6025–6029.

38. Donahue, A.C., and D.A. Fruman. 2003. Proliferation and survival of activated B cells requires sustained antigen receptor engagement and phosphoinositide 3-kinase activation. J Immunol. 170: 5851–5860.

39. Omori, S.A., M.H. Cato, A. Anzelon-Mills, K.D. Puri, M. Shapiro-Shelef, K. Calame, and R.C. Rickert. 2006. Regulation of class-switch recombination and plasma cell differentiation by phosphatidylinositol 3-kinase signaling. Immunity. 25: 545–557.

40. Wang, J., S. Liu, B. Hou, M. Yang, Z. Dong, H. Qi, and W. Liu. 2018. PTEN-Regulated AID Transcription in Germinal Center B Cells Is Essential for the Class-Switch Recombination and IgG Antibody Responses. Front Immunol. 9: 371.

41. Bjur, E., O. Larsson, E. Yurchenko, L. Zheng, V. Gandin, I. Topisirovic, S. Li, C.R. Wagner, N. Sonenberg, and C.A. Piccirillo. 2013. Distinct translational control in CD4+ T cell subsets. PLoS Genet. 9: e1003494.

42. Araki, K., M. Morita, A.G. Bederman, B.T. Konieczny, H.T. Kissick, N. Sonenberg, and R. Ahmed. 2017. Translation is actively regulated during the differentiation of CD8+effector T cells. Nat Immunol. 18: 1046–1057.

43. Moerke, N.J., H. Aktas, H. Chen, S. Cantel, M.Y. Reibarkh, A. Fahmy, J.D. Gross, A. Degterev, J. Yuan, M. Chorev, J.A. Halperin, and G. Wagner. 2007. Small-molecule inhibition of the interaction between the translation initiation factors eIF4E and eIF4G. Cell. 128: 257–267.

44. Pelletier, J., J. Graff, D. Ruggero, and N. Sonenberg. 2015. Targeting the eIF4F translation initiation complex: a critical nexus for cancer development. Cancer Res. 75: 250–263.

45. Malka-Mahieu, H., M. Newman, L. Désaubry, C. Robert, and S. Vagner. 2017. Molecular Pathways: The eIF4F Translation Initiation Complex-New Opportunities for Cancer Treatment. Clin Cancer Res. 23: 21–25.

46. Compagno, M., Q. Wang, C. Pighi, T.C. Cheong, F.L. Meng, T. Poggio, L.S. Yeap, E. Karaca, R.B. Blasco, F. Langellotto, C. Ambrogio, C. Voena, A. Wiestner, S.N. Kasar, J.R. Brown, J. Sun, C.J. Wu, M. Gostissa, F.W. Alt, and R. Chiarle. 2017. Phosphatidylinositol 3-kinase δ blockade increases genomic instability in B cells. Nature. 542: 489–493.

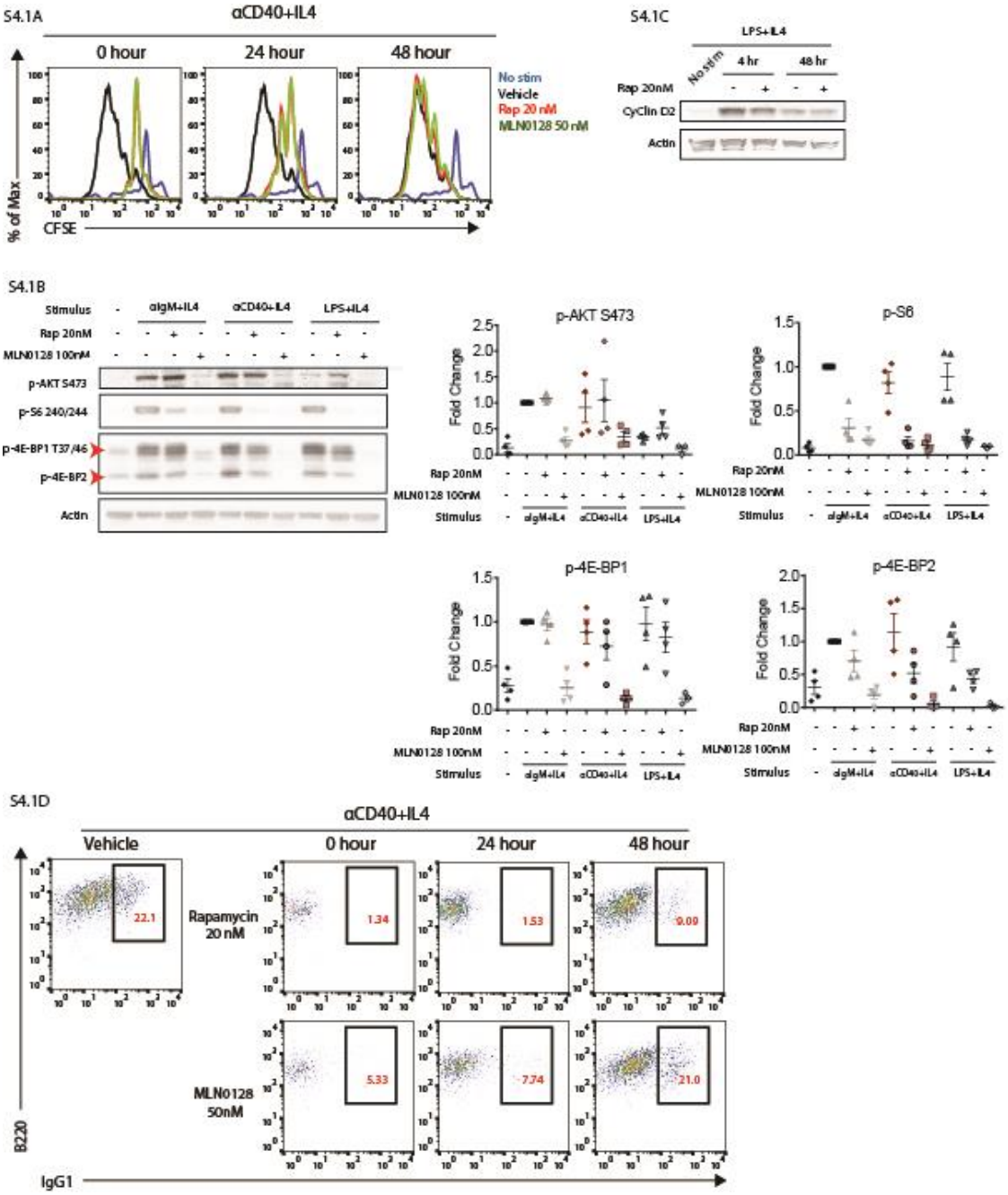

Supplementary Figure 4.1 48 hour addition of Rap but not MLN0128 reduces switching. Purified mouse splenic B cells were stimulated with αCD40+IL-4 and treated with vehicle, rapamycin or MLN0128 at 0 hour, 24 hour, or 48 hours after activation. (S4.1A) Proliferation by CFSE and (S4.1D) switching to IgG1 was measured by flow cytometry. Cells were stimulated with αIgM+IL-4, αCD40+IL-4, or LPS+IL-4 for 48 hours and treated with inhibitors for 1 hour before harvesting. (S4.1B) p-AKT, p-S6, p-4E-BP1, and p-4E-BP2 signal was quantitated by western. Note that the anti-phospho-4E-BP1 (T37/46) antibody also detects the equivalent sites on 4E-BP2 (9) (S4.1C) Cells were stimulated with LPS+IL-4 for 4 or 48 hours and treated with vehicle or rapamycin for 4 hours before harvesting for measurement of IgG1 switching. Data are representative of three or more experiments.

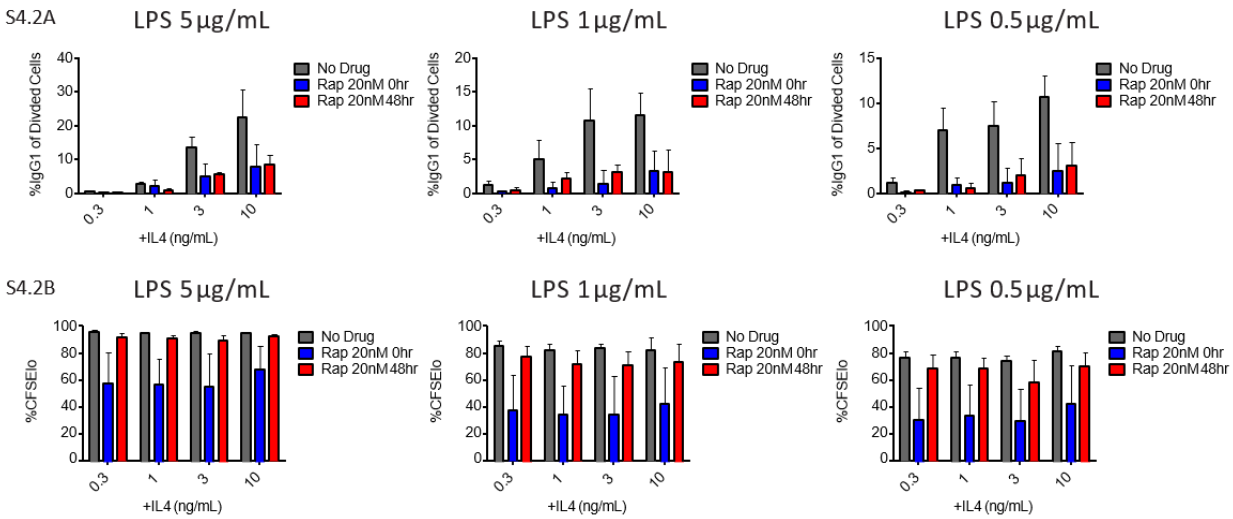

Supplementary Figure 4.2 IL-4 promotes switching to IgG1, and late addition of Rap reduces IgG1 switching but not cell division in B cells stimulated with a range of LPS and IL-4 concentrations Purified mouse splenic B cells were stimulated with indicated concentrations of LPS and IL-4 and treated with vehicle or rapamycin at 0 hour or 48 hour timepoints. Percent of live B cells that have divided at least once expressing IgG1 (S4.2A) and proliferation by CFSE (S4.2B) was determined by flow cytometry at 96h. Data are representative of three or more experiments and shown as mean ±SD.

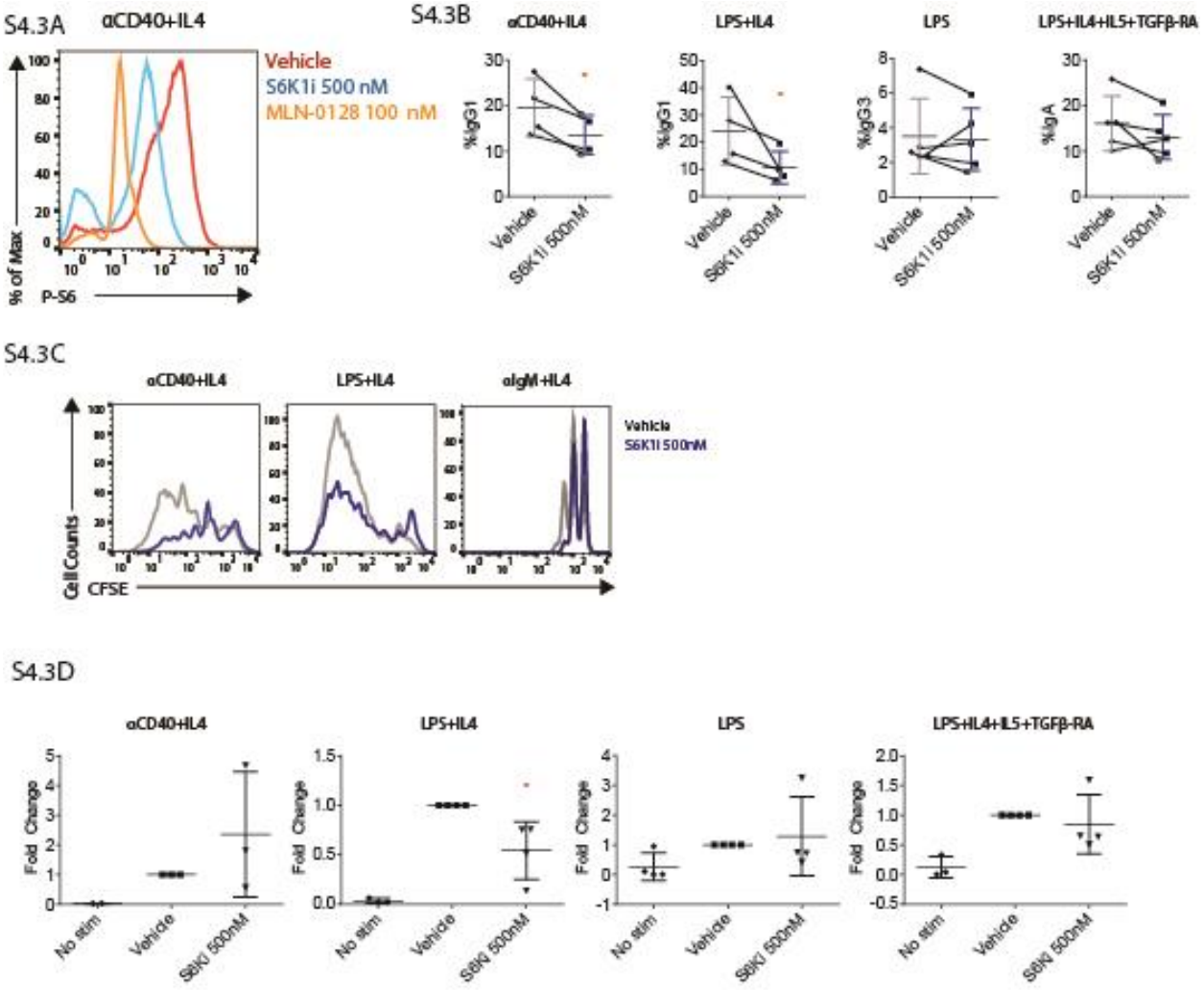

Supplementary Figure 4.3 S6K1 inhibitor reduces switching to IgG1. B cells were stimulated with αCD40+IL-4, LPS+IL-4, LPS or LPS+IL-4+IL-5+TGF-β+RA in the absence or presence of the S6K1 inhibitor LY 294002 500 nM. (S4.3A) p-S6 was measured by flow cytometry in cells stimulated with αCD40+IL-4. Percent of live B cells that have divided at least once expressing (S4.3B) IgG1, IgG3, IgA and (S4.3C) proliferation by CFSE and eFluor670 were measured at 96 hours by flow cytometry. In agreement with our previous findings (9), S6K1 inhibition had a minor effect on proliferation of cells stimulated with anti-IgM+IL-4 for 72 hours. (S4.3D) Cells were harvested at 48 hours and mRNA transcripts Iγ-Cγ, Iγ3-Cγ3, and Iα-Cα were measured by RT-qPCR. Fold change was calculated using vehicle treated. Significance was calculated using a paired one tailed student's t test. (*P<0.05; **P<0.01; ***P<0.001)

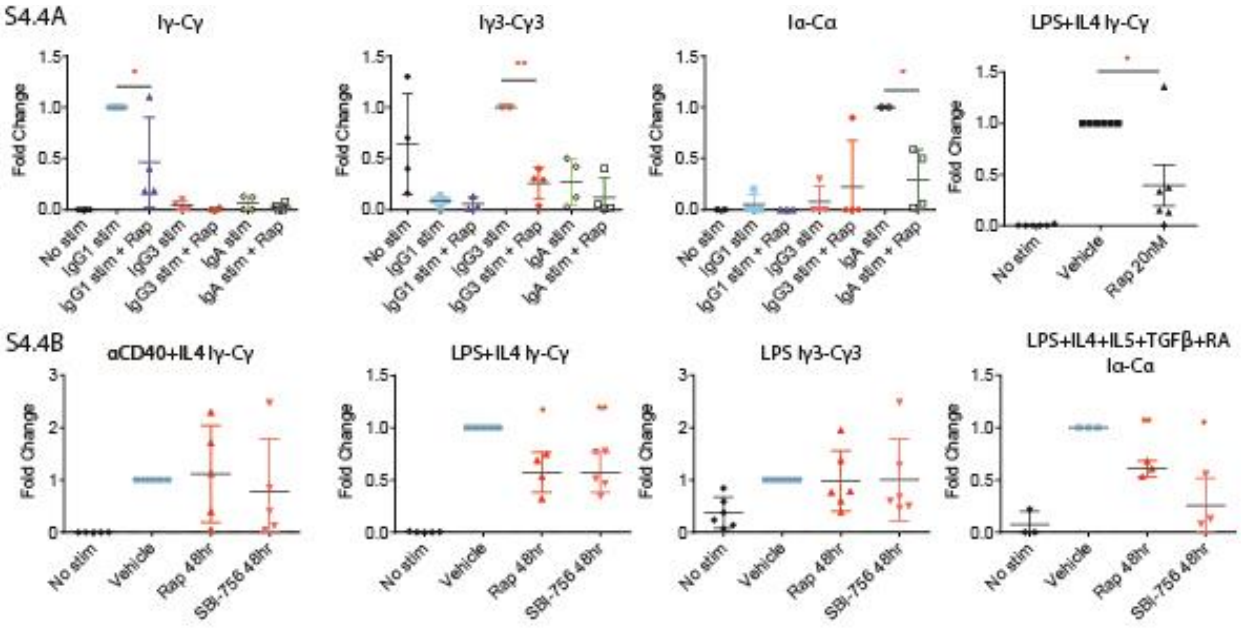

Supplementary Figure 4.4 Early addition of Rap reduces germline transcript production. Purified B cells were stimulated with αCD40+IL-4, LPS, LPS+IL-4+IL-5+TGF-β+RA or LPS+IL-4 and treated with Rap throughout the culture period. (S4.4A) Cells were harvested at 48 hours and mRNA transcripts Iγ-Cγ, Iγ3-Cγ3, and Iα-Cα were measured by RT-qPCR. For panel (S4.4B) cells were stimulated for 48 hours before treating with Rap and then harvested at 64 hours. Each point represents one independent experiment. Fold change in panel (S4.4A) was calculated using αCD40+IL-4 (IgG1 stim) for Iγ-Cγ, LPS (IgG3 stim) for Iγ3-Cγ3, and LPS+IL-4+IL-5+TGF-β+RA (IgA stim) for Iα-Cα. Fold change in panel (S4.4B) was calculated using vehicle treated. Significance was calculated using a paired one tailed student's t test. (*P<0.05; **P<0.01; ***P<0.001)

S4.5A

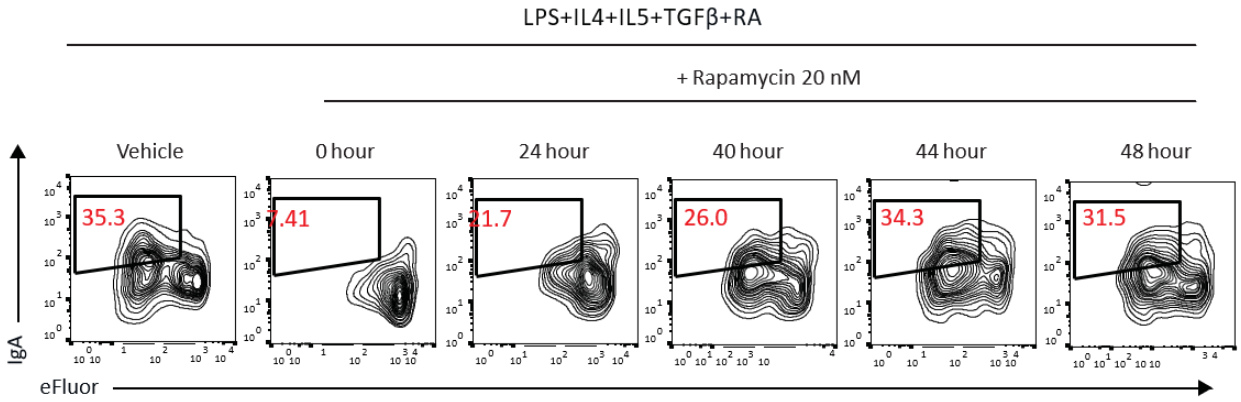

S4.5B

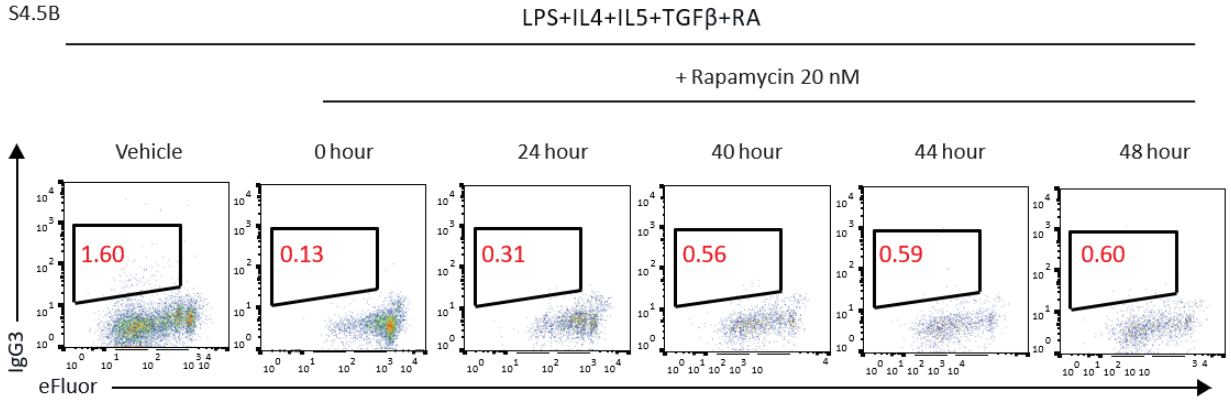

Supplementary Figure 4.5 Rap reduces switching to IgG3 but not IgA under IgA conditions. (S4.5A) B cells were stimulated with LPS+IL-4+IL-5+TGF-β+RA and treated with vehicle or rapamycin at the indicated timepoints. eFluor670 is a cell division tracking dye with a different emission spectrum than CFSE. Percent of live B cells that have divided at least once (based on eFluor670) expressing IgA or (S4.5B) IgG3 was determined by flow cytometry at 96h.

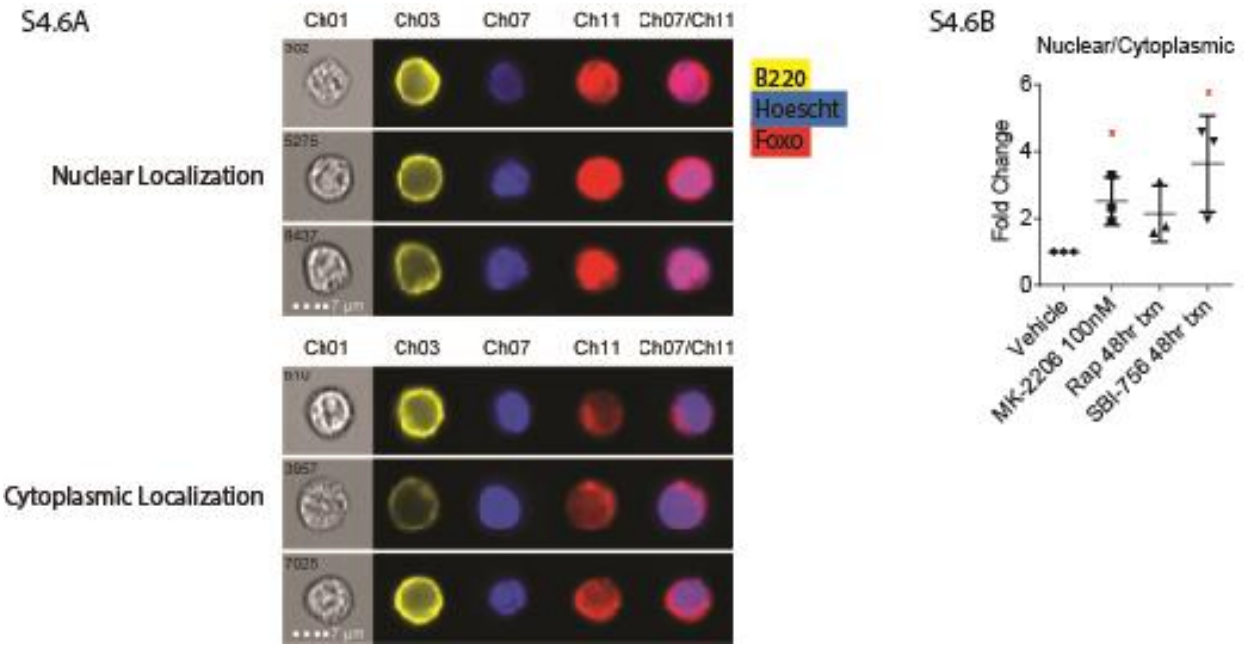

Supplementary Figure 4.6 48 hour treatment with Rap or SBI-756 does not decrease FOXO nuclear localization. B cells were purified and stimulated with LPS+IL-4 for 48 hours and treated with Rap, SBI-756 or MK-2206 for 4 hours before fixing and permeabilizing for staining of B220, Hoechst and intracellular FOXO. Cells were analyzed by ImageStream. One representative experiment is shown (S4.6A). Nuclear and cytoplasmic localization was analyzed in IDEAS software (S4.6B). Each point represents one individual experiment. Fold change was calculated using vehicle treated. Significance was calculated using a paired one tailed student's t test. (*P<0.05; **P<0.01; ***P<0.001)

CHAPTER 5

Differential Effects of *Eif4e* Gene Dosage in Murine Primary B cells and Leukemia Cells

Introduction

The eukaryotic translation initiation factor 4E (eIF4E) protein binds to the 7-methylguanosine cap present in most mRNAs, and recruits the scaffolding protein eIF4G and other proteins to form the translation initiation complex known as eIF4F. In cancer, eIF4F contributes to progression of the disease by preferentially translating mRNAs involved in sustained proliferative signaling, evasion of growth suppression, resistance to programmed cell death, replicative immortality, angiogenesis, invasion and metastasis (1). eIF4F activity and protein synthesis were found to be drivers in PI3K/AKT/mTOR driven lymphomagenesis (2) and in anti-BRAF and anti-MEK resistance in BRAF(V600)-mutant melanoma, colon, and thyroid cancer cell lines (3). This makes cap-dependent translation an attractive target for cancer therapy (4), and efforts are underway to develop small molecule inhibitors of eIF4E, eIF4G and eIF4A for oncology (5–7).

Several cancers have increased expression of eIF4E and initial studies using si-RNA knock-down inhibited cell growth in head and neck squamous cell carcinomas and in triple-negative breast cancer (8, 9). They also showed that eIF4E knock-down inhibited both rapamycin-insensitive and rapamycin-sensitive cell lines and did not activate the feedback loop to increase AKT phosphorylation (8). As further proof of concept, in a mouse model of Kras-driven lung disease, *Eif4e* haploinsufficiency significantly reduced cellular transformation due to differential translation requirements in cancer formation (10). While *Eif4e* homozygous knock-out is embryonic lethal, these *Eif4e* heterozygous mice had normal development and cellular protein synthesis. In a gain-of-function model, eIF4E-overexpressing transgenic (Tg) mice had

enhanced Myc tumorigenesis (11). These findings establish that altering eIF4E dosage has significant yet selective biological consequences during tumor progression.

While several studies have investigated the role of eIF4E in cap-dependent translation of mRNAs in cancer cells, only recently has translational regulation been gaining attention in lymphocyte activation and differentiation (12, 13). In lymphocytes, the 4E-binding protein (4E-BP)/eIF4E axis coordinates cell growth and proliferation during lymphocyte activation which is characterized by an increase in overall protein synthesis rates. Since mTORC1 only regulates a subset of mRNAs, this suggests that the axis is critical for the initial translation of specific mRNAs needed for global translation during lymphocyte activation (14). Our lab also found that mTORC1, whose activity controls 4E-BP binding to eIF4E, is important for B cell differentiation and antibody class switching **(Chapter 4)** and for pre-B cell leukemogenesis (15, 16). This pathway is important in both normal B cell function and tumorigenesis; thus, we wanted to test the effects of reduced eIF4E activity in these parallel systems. Our findings show that reduced eIF4E protein slows tumorigenesis in a mouse model of leukemia, while normal mouse primary B cells can maintain B cell proliferation and antibody class switching. This further supports the studies showing that cancer cells are more sensitive than non-transformed cells to reductions in eIF4E (10).

Materials and Methods

Mice and reagents

C57Bl/6J (B6) mice were bred at the University of California, Irvine, and used at between 6 and 12 weeks of age. *Eif4e*$^{+/-}$ mice with a heterozygous loss-of-function allele were obtained from the Ruggero lab (UC San Francisco) (10). All animals were studied in compliance with protocols

approved by the Institutional Animal Care and Use Committees of the University of California, Irvine. MLN0128 was purchased from Active Biochem. Rapamycin was purchased from Cell Signaling Technology. Inhibitors were included throughout the indicated cell treatment periods.

Generation of p190 BCR-ABL cell lines

Bone marrow (BM) cells were flushed from the tibias and femurs of 3-5 week old mice. Cells were incubated overnight with retroviral supernatants (p190 BCR-ABL-IRES-hCD4 or p190 BCR-ABL-IRES-GFP) in the presence of 5 µg/ml polybrene at 37°C, 5% CO2, with RPMI culture medium supplemented with 20% FCS, recombinant mouse IL-7 (10 ng/ml; Invitrogen) to promote cell cycle entry. Following overnight incubation, cells were spun down to remove virus and cultured with fresh RPMI+20% FCS medium supplemented with recombinant mouse (rm) IL-7 for 1 week. Cells were further cultured removing rmIL-7 for a second week and then further reducing to 10% FCS until a pure 100% human CD4+ of GFP+ cytokine- and stromal-independent culture was established. *In vitro* mixing experiments were initiated after removal of rm-IL7 and cells were mixed at a 1 to 1 ratio for CD4+ and GFP+ cells. Cells were cultured in RPMP+20% FCS medium during the outgrowth period.

In vivo transplant experiments with mouse p190 leukemia

Mouse p190 transformed BM cells were used to initiate leukemia in irradiated syngeneic B6 recipients. In all *in vivo* experiments, p190 transformed BM were prepared fresh (after the removal of rmIL-7 step) to initiate leukemia. Leukemic engraftment was determined in anesthetized animals by retro-orbital bleeds and analyzed by flow cytometry.

Mouse B cell culture

Splenic B cells were purified by negative selection (eBioscience Magnisort Mouse B cell enrichment kit). B cell purity measured by FACS analysis (FACSCalibur and CellQuest software; BD Biosciences) using anti-B220 antibody (Biolegend) yielded >95% B220+. Purified B cells were seeded at a final concentration of 1.5 x 10^6 cells per milliliter. For class switching experiments, B cells were stimulated 5 μg/mL anti-CD40 (HM40-3) agonistic antibody (eBioscience), or 5 μg/mL LPS (Sigma), together with 5 ng/mL mIL-4 (R&D Systems) for 96 h to induce switching to IgG1. All cells were cultured with RPMI 1640 supplemented with 10% (vol/vol) heat-inactivated FCS, 5 mM Hepes, 2 mM L-glutamine, 100 units/mL penicillin, 100 μg/mL streptomycin, 50 μM 2-mercaptoethanol.

Western Blotting Analysis

Antibodies specific for β-actin, eIF4E, total 4E-BP1, and total 4E-BP2 were purchased from Cell Signaling. Protein on western blots were analyzed using ImageJ to quantitate signal of each band. Signal was normalized with actin measurements and fold change was calculated using the stimulated/no drug control.

Flow cytometry, CFSE labeling, and antibodies

Cells were incubated with TruStain fcX in FACS buffer (0.5% BSA + 0.02% NaN3 in 1× HBSS) for 10 min on ice. Staining with antibodies was performed with FACS buffer and on ice for 20 min. Flow cytometry antibodies and other reagents used: B220 (eBioscience, RA3-6B2), IgG1 (BD, A85-1) and 7-Aminoactinomycin D (Invitrogen). CFSE labeling of B cells was performed

by resuspending cells to a concentration of 10 × 106 cells per mL with a concentration of 2.5 μM. Flow cytometric data were analyzed using FlowJo software (TreeStar).

Luciferase assay

Cap-dependent translation was measured using the luciferase reporter construct pRSTF-CVB3 containing the 5' non-coding region of the Coxsackie B3 virus cloned between the firefly and renilla luciferase (17). The construct was electroporated in serum-free media and cells recovered in complete RPMI media for 2 hours followed by inhibitor treatment for 8 hours. Following treatment, cells were lysed and renilla and firefly luciferase expression were measured using the Dual luciferase assay kit (Promega) using a luminometer. Renilla luciferase expression was normalized to Firefly luciferase expression and results were expressed relative to vehicle treated.

Results

eIF4E haploinsufficiency reduces p190 leukemia transformation

To study the role of eIF4E in tumorigenesis, we used the murine model of B precursor acute lymphoblastic leukemia (B-ALL). Ph+ B-ALL is initiated by the BCR-ABL oncogene that results from the Philadelphia chromosome (Ph) translocation. When human p190 BCR-ABL (p190 is the most common isoform of BCR-ABL found in Ph+ B-ALL) is retrovirally expressed in infected mouse bone marrow cells, the transformed progenitor B cell lines (termed p190 cells) will initiate B-ALL when transferred to recipient mice. To test the effects of reduced eIF4E gene dosage on p190 transformation, we co-cultured WT and *Eif4e*$^{+/-}$ cells after viral infection when cells were 10-20% marker positive expressing either GFP or human CD4 (hCD4) **(Fig. 5.1A).** Cells were mixed at 1:1 ratios of WT:WT, WT:Het, Het:WT, and Het:Het **(Fig. 5.1B)** and

their growth was monitored over a few days. We found that the WT p190 cells significantly outgrew the *Eif4e*$^{+/-}$ p190 cells both *in vitro* culture and *in vivo* in B6 mice while WT:WT and Het:Het mixes grew at a 1:1 ratio **(Fig. 5.1C-5.1D).** Measurement of eIF4E protein levels in the *Eif4e*$^{+/-}$ p190 cells showed that eIF4E was reduced but 4E-BP1 and 4E-BP2 remained the same as compared to WT **(Fig. 5.2).**

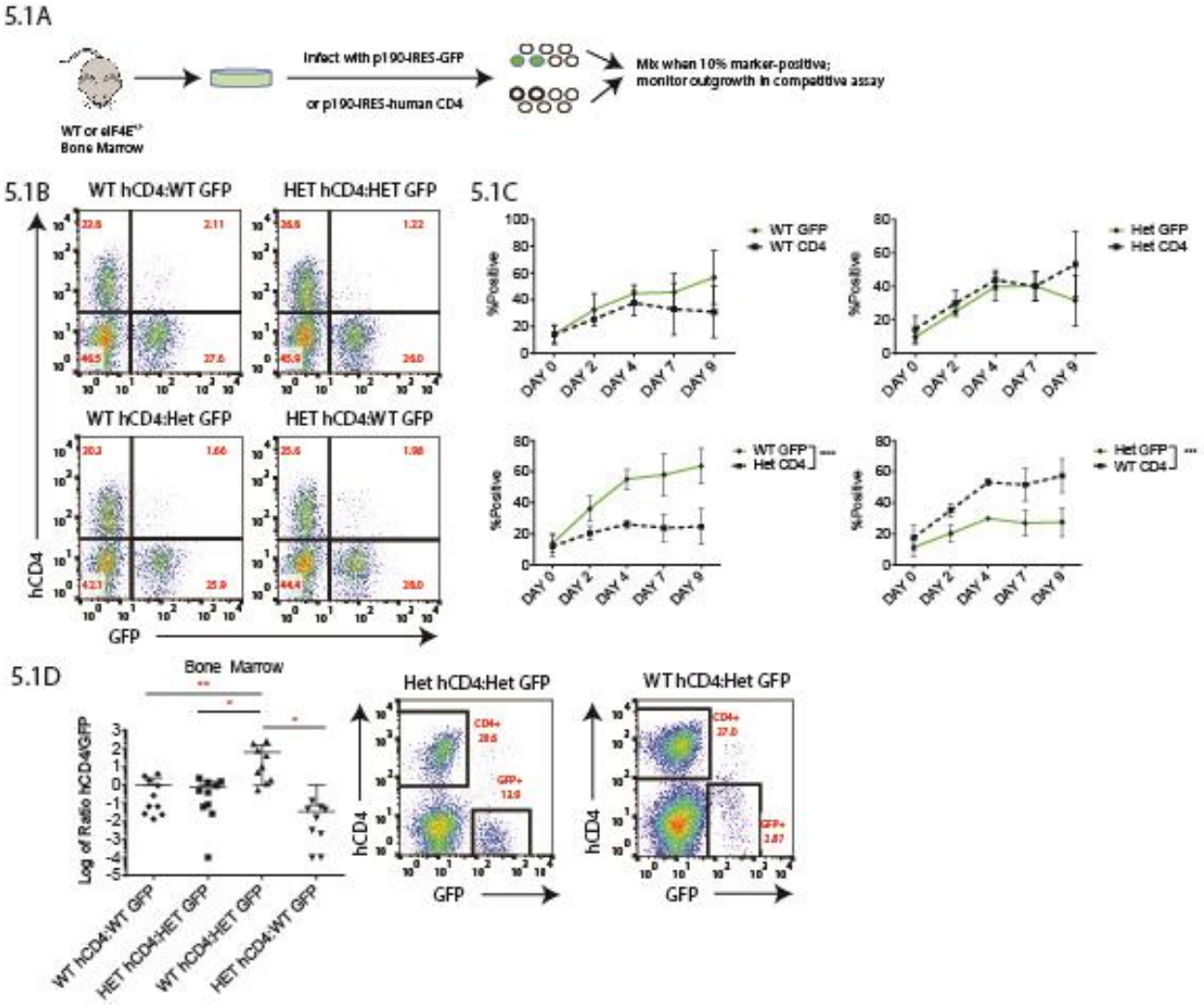

Figure 5.1 WT p190 cells outgrow *Eif4e+/-* p190 cells in a competitive growth assay. (5.1A) BM cells were infected with p190 BCR-ABL and cultured until 10% marker positive before mixing at a 1:1 ratio (5.1B) and their growth was monitored (5.1C) *in vitro* over 9 days or (5.1D) injected into B6 mice and measured after 18 days *in vivo*. For 5.1C %marker+ cells were measured by flow cytometry. Significance was calculated using two-way ANOVA with Sidak multiple comparison test. 5.1D shows log of ratio of hCD4+/GFP+ measured by flow cytometry. Significance was calculated using one-way ANOVA with Neuman Keuls multiple comparison test.

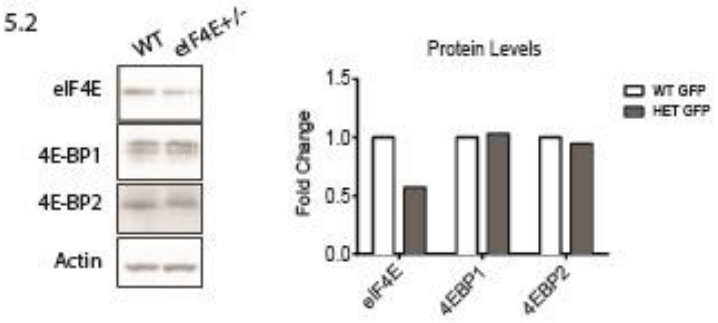

Figure 5.2 *Eif4e*$^{+/-}$ p190 cells have reduced eIF4E protein. p190 cells were harvested for western to measure eIF4E, 4E-BP1 and 4E-BP2. Signal was quantified over one experiment.

eIF4E haploinsufficiency reduces 4E-BP2 in normal B cells

We were also interested in the role of eIF4E in normal B cell function. In chapter 4 we showed that inducible expression of 4E-BP1M or SBI-756 treatment, both of which suppress association of eIF4E with eIF4G, reduces B cell proliferation and switching to IgG1. These findings provide evidence that eIF4F formation is important for B cell function and differentiation. We first analyzed B cell subsets in both WT and *Eif4e*$^{+/-}$ mice. We found that there were no differences in the percentages of transitional T1, T2, T3, marginal zone or follicular B cell subsets **(Fig. 5.3A).** There were also no differences in the overall cell counts of total splenocytes (data not shown).

We measured eIF4E, 4E-BP1 and 4E-BP2 protein levels in both unstimulated B cells and in B cells stimulated with LPS+IL-4 for 48 hours. There were no significant differences in the unstimulated B cells; however, both eIF4E and 4E-BP2 protein levels were reduced in the *Eif4e*$^{+/-}$ cells after stimulation (**Fig. 5.3B).** Interestingly, 4E-BP1 protein did not decrease **(Fig. 5.3B)** (14). Considering that activated *Eif4e*$^{+/-}$ cells had reduced amounts of the inhibitory 4E-BP2, we hypothesized that the efficiency of mRNA translation might be preserved. We measured cap-dependent translation using a bicistronic dual Renilla-Firefly luciferase reporter construct.

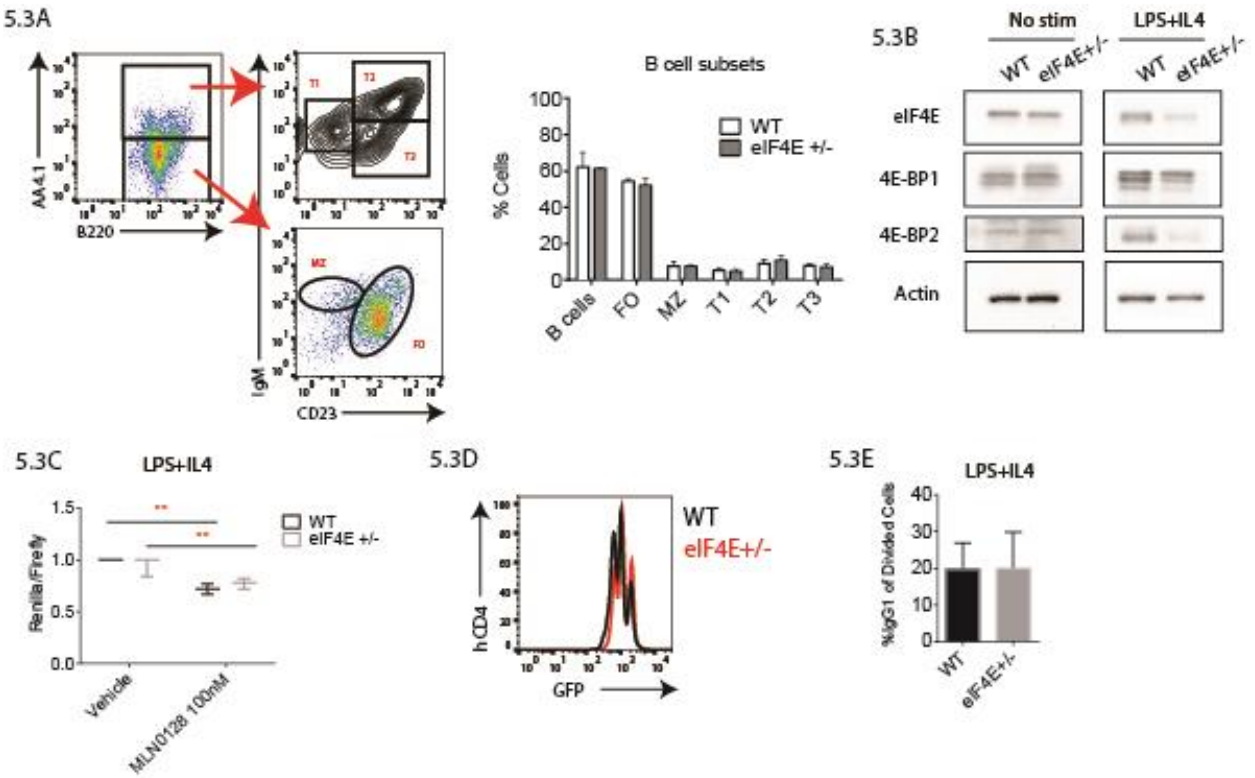

Figure 5.3 Stimulated *Eif4e*$^{+/-}$ mouse splenic B cells have reduced eIF4E and 4E-BP2. (5.3A) Splenocytes were stained for B cell subsets and analyzed by flow cytometry (5.3B) Purified mouse B cells were harvested without stimulation or after 16 hours of LPS+IL-4 stimulation for western blotting. (5.3C) Cells were stimulated for 48 hours before with LPS+IL-4 and transfected with a bicistronic dual Renilla-Firefly luciferase reporter construct to measure cap-dependent translation (Renilla luciferase) relative to cap-independent, polio IRES mediated translation (firefly luciferase) as an internal control. Each point represents one independent experiment. Fold change was calculated using vehicle condition. Significance was calculated using a paired one tailed student's t test. (**P<0.01) (5.3D) Cells were stimulated with anti-IgM+IL-4 and proliferation was measured by CFSE at 72 hours using flow cytometry. (5.3E) Cells were stimulated with LPS+IL-4 and percent of live B cells that have divided at least once expressing IgG1 were measured at 96 hours by flow cytometry.

This construct measures cap-dependent translation by synthesis of the Renilla luciferase as well as cap-independent, polio IRES mediated translation by synthesis of firefly luciferase as an internal control. Using this dual-luciferase assay, cap-dependent translation measured in *Eif4e*$^{+/-}$ cells was just as efficient as in the WT control cells **(Fig. 5.3C).**

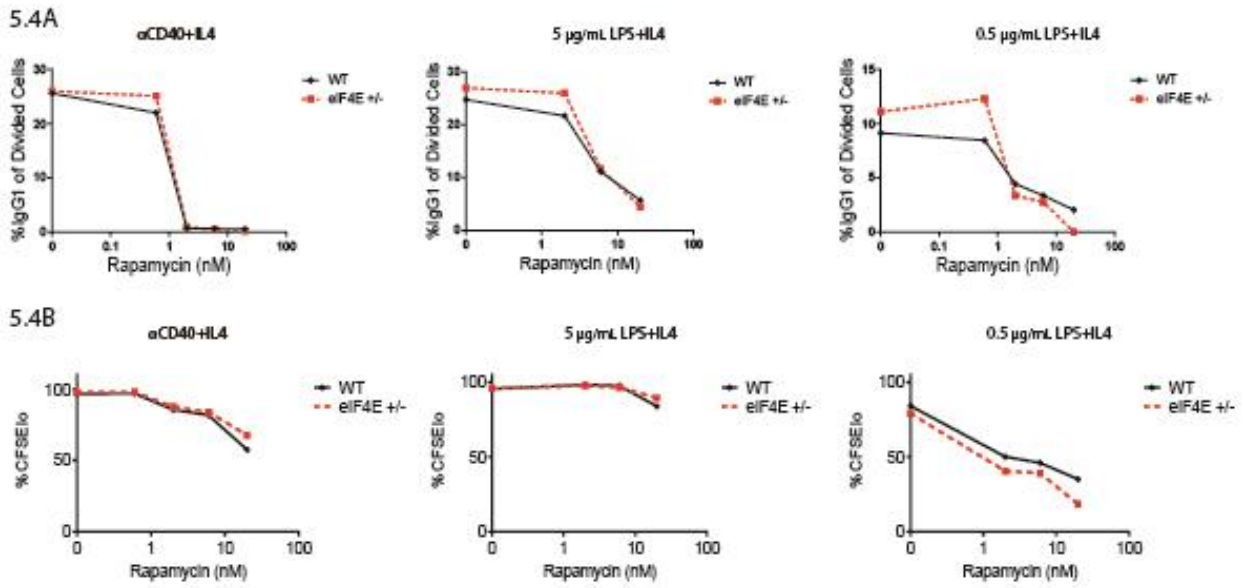

Figure 5.4 *Eif4e*$^{+/-}$ activated B cells have no defect in switching to IgG1. B cells were stimulated with αCD40+IL-4, 5 μg/mL LPS+IL-4, and 0.5 μg/mL LPS+IL-4 and treated with indicated concentrations of rapamycin. (5.4A) Percent of live B cells that have divided at least once expressing IgG1 and (5.4B) %CFSE lo were measured at 96 hours by flow cytometry.

eIF4E haploinsufficiency does not affect proliferation or switching to IgG1

We tested proliferation and switching to IgG1 and found no differences in *Eif4e*$^{+/-}$ compared to WT cells **(Fig. 5.3D-5.3E).** We also titrated concentrations of rapamycin to test if *Eif4e*$^{+/-}$ cells were more sensitive to the effects of rapamycin on switching to IgG1 or proliferation; again there were no differences **(Fig. 5.4).** Additionally, there were no differences in naturally occurring germinal center B cell populations isolated from Peyer's patches from the *Eif4e*$^{+/-}$ mice compared to WT (data not shown). Overall, this data suggests that normal cells can compensate for reduced eIF4E expression to sustain translation and B cell function. In contrast, transformed pre-B leukemia cells do not compensate for reduced eIF4E and show impaired fitness **(Fig. 5.5).**

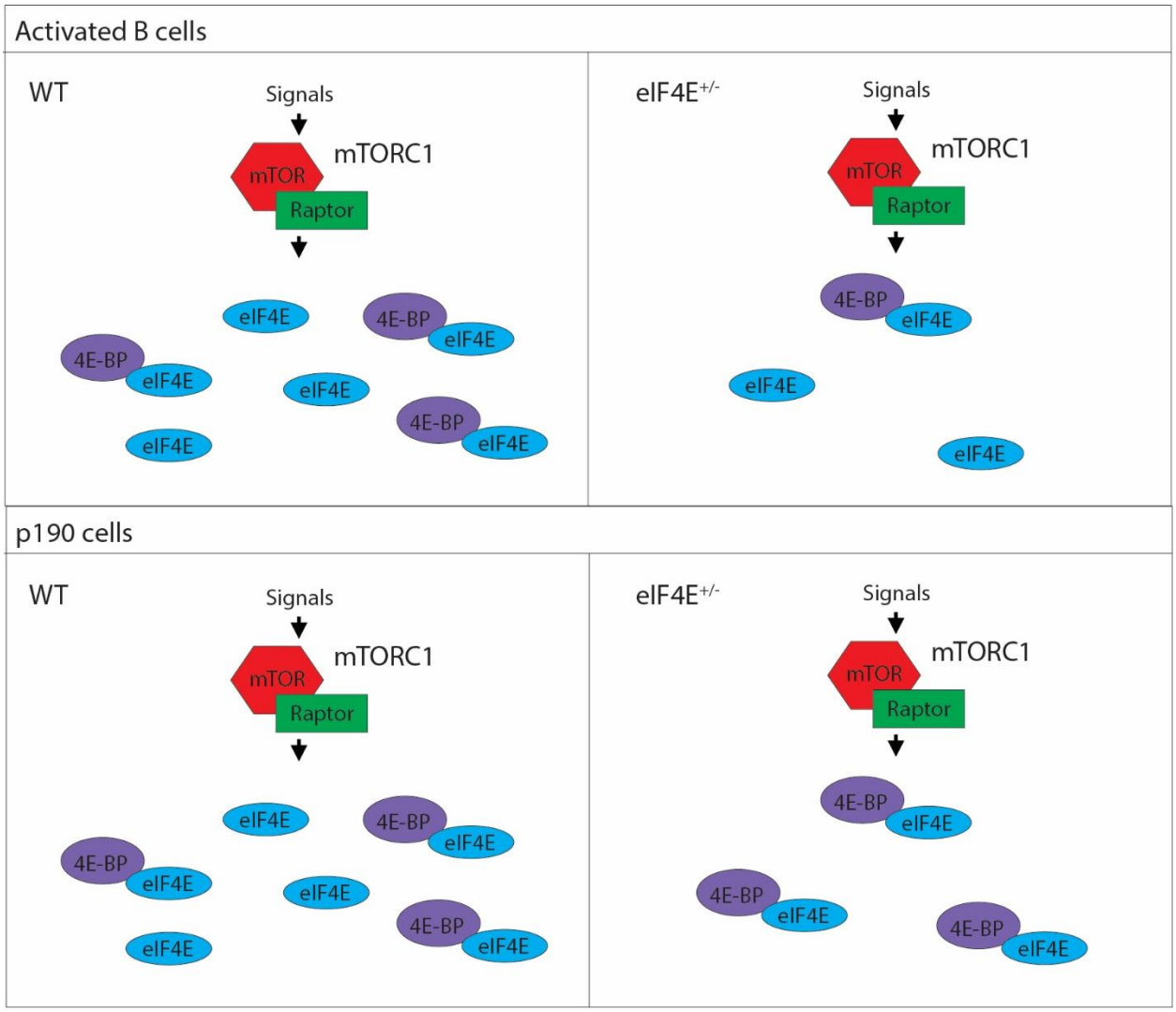

Figure 5.5 Model of eIF4E and 4E-BP ratios in normal B cells and transformed p190 cells.

Discussion

The eIF4F translation initiation complex is important in both tumorigenesis and normal B cell functions. Thus it is important to understand the effects that eIF4F targeting therapies for cancer will have on normal B cell differentiation. Here, we found that reducing eIF4E protein slows tumorigenesis of mouse p190 leukemia cell lines, while activated mouse splenic B cells are able to divide and undergo antibody class switching. Notably, primary mouse B cells

compensated for reduced eIF4E by reducing expression of the inhibitory 4E-BP2 and displayed normal rates of cap-dependent translation. In contrast, p190 cells derived from *Eif4e*$^{+/-}$ mice did not show altered expression of 4E-BPs. These data support the model that normal cells and cancer cells have differential requirements for eIF4E dosage.

In chapter 4 we showed that antibody class switching is reduced following genetic (4E-BPM) or chemical (SBI-756) disruption of the interaction of eIF4E with eIF4G; therefore, it was surprising to find that reduced eIF4E protein did not have an effect *in vitro*. However, the rates of cap-dependent translation in WT vs *Eif4e*$^{+/-}$ remained the same which suggests that the ratio of eIF4E to 4E-BP in non-transformed cells is an important mechanism of regulation. One important future experiment is to assess whether the *Eif4e*$^{+/-}$ p190 cells have reduced cap-dependent translation as well. It will also be interesting to test whether reduced eIF4E protein has an effect during *in vivo* immunization. It was also interesting to note that in activated B cells from *Eif4e*$^{+/-}$ mice there was reduced expression of 4E-BP2 but not the 4E-BP1 isoform. This was an interesting finding since we previously found that the 4E-BP2 isoform is more abundant in lymphocytes. Further investigation will be needed to determine if this regulation of 4E-BP2 protein is at the level of transcription or translation.

Our finding that the 4E-BPs are not reduced in the *Eif4e*$^{+/-}$ leukemia cells contrasts with other studies which did have reductions of 4E-BP expression, therefore, this mechanism of regulation may be dependent on cell type (8, 18). How the genetic model phenocopies chemical inhibition of eIF4E will be another area of investigation; however, our lab has found that chemical inhibition of eIF4E is able to reduce cap-dependent translation which suggests that this compensatory effect does not occur or is insufficient. In addition to chemical inhibitors, there are emerging technologies that can cause selective degradation of targeted proteins (19), potentially

such as eIF4E. Thus, this germline null allele system has its limitations as a preclinical model of drug treatment and we may need to develop other models. Examples include inserting mutations that disrupt eIF4G and eIF4E interactions to mimic chemical inhibitors or acute deletion of eIF4E or eIF4G using Cre-lox systems to mimic the degradation technology.

Another important question is by which mechanism do the WT p190 cells outgrow the *Eif4e*$^{+/-}$ cells. One possibility is that there is less BCR-ABL protein due to less mRNA translation in the *Eif4e*$^{+/-}$ p190 cells. This may cause more death or slower cell cycle in the *Eif4e*$^{+/-}$ p190 cells compared to the WT. Alternatively, if BCR-ABL protein is unaltered, *Eif4e*$^{+/-}$ p190 cells might have reduced translation of mRNAs encoding cell cycle or survival proteins such as cyclin D1 and MCL-1 or others which can be determined by polysome fractionation-RNA sequencing. Additionally, the *Eif4e*$^{+/-}$ cells may have a defect in their homing abilities *in vivo*. While we saw differences between the WT and Het p190s in the bone marrow, there were not many p190 cells found in the spleen. This may be tested by flow cytometry to measure the numbers of p190s cells that have migrated to the bone marrow and spleen 24 hours after injection.

Overall, these findings emphasize that normal cells and cancer cells have differential requirements for eIF4E protein amounts. This provides another proof-of-concept that cancer cells will be more sensitive than normal cells to therapies targeting eIF4E activity.

References

1. Malka-Mahieu, H., M. Newman, L. Désaubry, C. Robert, and S. Vagner. 2017. Molecular Pathways: The eIF4F Translation Initiation Complex-New Opportunities for Cancer Treatment. Clin Cancer Res. 23: 21–25.

2. Hsieh, A.C., M. Costa, O. Zollo, C. Davis, M.E. Feldman, J.R. Testa, O. Meyuhas, K.M. Shokat, and D. Ruggero. 2010. Genetic dissection of the oncogenic mTOR pathway reveals druggable addiction to translational control via 4EBP-eIF4E. Cancer Cell. 17: 249–261.

3. Boussemart, L., H. Malka-Mahieu, I. Girault, D. Allard, O. Hemmingsson, G. Tomasic, M. Thomas, C. Basmadjian, N. Ribeiro, F. Thuaud, C. Mateus, E. Routier, N. Kamsu-Kom, S. Agoussi, A.M. Eggermont, L. Désaubry, C. Robert, and S. Vagner. 2014. eIF4F is a nexus of resistance to anti-BRAF and anti-MEK cancer therapies. Nature. 513: 105–109.

4. Pelletier, J., J. Graff, D. Ruggero, and N. Sonenberg. 2015. Targeting the eIF4F translation initiation complex: a critical nexus for cancer development. Cancer Res. 75: 250–263.

5. Moerke, N.J., H. Aktas, H. Chen, S. Cantel, M.Y. Reibarkh, A. Fahmy, J.D. Gross, A. Degterev, J. Yuan, M. Chorev, J.A. Halperin, and G. Wagner. 2007. Small-molecule inhibition of the interaction between the translation initiation factors eIF4E and eIF4G. Cell. 128: 257–267.

6. Feng, Y., A.B. Pinkerton, L. Hulea, T. Zhang, M.A. Davies, S. Grotegut, Y. Cheli, H. Yin, E. Lau, H. Kim, S.K. De, E. Barile, M. Pellecchia, M. Bosenberg, J.-L. Li, B. James, C.A. Hassig, K.M. Brown, I. Topisirovic, and Z.A. Ronai. 2015. SBI-0640756 Attenuates the Growth of Clinically Unresponsive Melanomas by Disrupting the eIF4F Translation Initiation Complex. Cancer Res. 75: 5211–5218.

7. Rubio, C.A., B. Weisburd, M. Holderfield, C. Arias, E. Fang, J.L. DeRisi, and A. Fanidi. 2014. Transcriptome-wide characterization of the eIF4A' ' signature highlights plasticity in translation regulation. Genome Biol. 15: 476.

8. Soni, A., A. Akcakanat, G. Singh, D. Luyimbazi, Y. Zheng, D. Kim, A. Gonzalez-Angulo, and F. Meric-Bernstam. 2008. eIF4E knockdown decreases breast cancer cell growth without activating Akt signaling. Mol Cancer Ther. 7: 1782–1788.

9. Oridate, N., H.-J. Kim, X. Xu, and R. Lotan. 2005. Growth inhibition of head and neck squamous carcinoma cells by small interfering RNAs targeting eIF4E or cyclin D1 alone or combined with cisplatin. Cancer Biol Ther. 4: 318–323.

10. Truitt, M.L., C.S. Conn, Z. Shi, X. Pang, T. Tokuyasu, A.M. Coady, Y. Seo, M. Barna, and D. Ruggero. 2015. Differential Requirements for eIF4E Dose in Normal Development and Cancer. Cell. 162: 59–71.

11. Ruggero, D., L. Montanaro, L. Ma, W. Xu, P. Londei, C. Cordon-Cardo, and P.P. Pandolfi. 2004. The translation factor eIF-4E promotes tumor formation and cooperates with c-Myc in lymphomagenesis. Nat Med. 10: 484–486.

12. Araki, K., M. Morita, A.G. Bederman, B.T. Konieczny, H.T. Kissick, N. Sonenberg, and R. Ahmed. 2017. Translation is actively regulated during the differentiation of CD8+effector T cells. Nat Immunol. 18: 1046–1057.

13. Bjur, E., O. Larsson, E. Yurchenko, L. Zheng, V. Gandin, I. Topisirovic, S. Li, C.R. Wagner, N. Sonenberg, and C.A. Piccirillo. 2013. Distinct translational control in CD4+ T cell subsets. PLoS Genet. 9: e1003494.

14. So, L., J. Lee, M. Palafox, S. Mallya, C.G. Woxland, M. Arguello, M.L. Truitt, N. Sonenberg, D. Ruggero, and D.A. Fruman. 2016. The 4E-BP-eIF4E axis promotes rapamycin-sensitive growth and proliferation in lymphocytes. Sci Signal. 9: ra57.

15. Kharas, M.G., M.R. Janes, V.M. Scarfone, M.B. Lilly, Z.A. Knight, K.M. Shokat, and D.A. Fruman. 2008. Ablation of PI3K blocks BCR-ABL leukemogenesis in mice, and a dual PI3K/mTOR inhibitor prevents expansion of human BCR-ABL+ leukemia cells. J Clin Invest. 118: 3038–3050.

16. Janes, M.R., J.J. Limon, L. So, J. Chen, R.J. Lim, M.A. Chavez, C. Vu, M.B. Lilly, S. Mallya, S.T. Ong, M. Konopleva, M.B. Martin, P. Ren, Y. Liu, C. Rommel, and D.A. Fruman. 2010. Effective and selective targeting of leukemia cells using a TORC1/2 kinase inhibitor. Nat Med. 16: 205–213.

17. Jang, G.M., L.E.-C. Leong, L.T. Hoang, P.H. Wang, G.A. Gutman, and B.L. Semler. 2004. Structurally distinct elements mediate internal ribosome entry within the 5'-noncoding region of a voltage-gated potassium channel mRNA. J Biol Chem. 279: 47419–47430.

18. Yanagiya, A., E. Suyama, H. Adachi, Y.V. Svitkin, P. Aza-Blanc, H. Imataka, S. Mikami, Y. Martineau, Z.A. Ronai, and N. Sonenberg. 2012. Translational homeostasis via the mRNA cap-binding protein, eIF4E. Mol Cell. 46: 847–858.

19. Chu, T.-T., N. Gao, Q.-Q. Li, P.-G. Chen, X.-F. Yang, Y.-X. Chen, Y.-F. Zhao, and Y.-M. Li. 2016. Specific Knockdown of Endogenous Tau Protein by Peptide-Directed Ubiquitin-Proteasome Degradation. Cell Chem. Biol. 23: 453–461.

CHAPTER 6

Discussion and Future Directions

The activation of B cells and their differentiation into antibody secreting plasma cells is a critical component of the humoral immune response as a proper host-defense mechanism to invading pathogens (1). Central to their activation is the PI3K/AKT/mTOR signaling pathway which plays an important role in promoting B cell survival, proliferation and differentiation (2). Dysregulation of this pathway during B cell responses, however, can lead to B cell malignancies or autoimmunity as increased PI3K/AKT/mTOR signaling is frequently observed in these diseases (3). Targeting PI3Kδ with idelalisib has been approved for the treatment of patients with relapsed/refractory chronic lymphocytic leukemia (CLL; in combination with rituximab), relapsed follicular lymphoma, and relapsed small lymphocytic lymphoma (4). Interestingly, mutations leading to increased PI3Kδ signaling also cause immune deficiency in APDS patients and another PI3Kδ inhibitor, leniolisib, has shown disease improvement (5). PI3K inhibitors have also shown efficacy in preclinical autoimmune models (6, 7) and rapamycin recently showed encouraging results in a phase 1/2 trial in SLE patients (8). However, there has yet to be an inhibitor of this pathway clinically approved for B cell mediated autoimmune disease. While PI3Kδ and PI3Kδ/γ inhibitors showed efficacy in preclinical animal models, these results do not always predict clinical outcomes in patients. This highlights the need for better understanding of how the PI3K/mTOR signaling pathway is promoting disease. Thus the goal of this thesis is to investigate this integral signaling pathway and how it regulates B cell function and differentiation. This knowledge has the potential to improve therapeutic approaches for B cell immunodeficiencies and antibody-mediated autoimmune diseases.

A central mechanism by which PI3Kδ signaling directs B cell differentiation is through activation of AKT and inactivation of FOXO transcription factors (2). Loss of PTEN leads to increased PI3K signaling which strongly suppresses class switching recombination and increases IgM-plasmablast differentiation (9). Conversely, PI3Kδ inhibitors promote CSR through increased FOXO activity and transcription of the *Aicda* gene encoding AID (9). Interestingly, APDS patients frequently have decreased IgG and/or IgA with increased IgM, which fits the model of increased PI3Kδ signaling promoting IgM plasmablasts and suppressing class switching (10). In our 2017 study published in *Frontiers of Immunology*, we characterized a novel PI3Kδ inhibitor IPI-3063 which potently suppressed AKT phosphorylation and reduced proliferation of both mouse and human B cells *in vitro* at nanomolar concentrations. PI3Kδ inhibitors have shown efficacy for PI3Kδ-associated malignancies (4, 5); thus IPI-3063 with its potency at nanomolar concentrations has potential as a therapy, although additional studies will be required. We also investigated the effects of the dual PI3Kδ/γ inhibitor IPI-443 because we were initially interested to test if dual inhibition would have greater effects than inhibition of PI3Kδ only. We had first tested Infinity's clinical PI3Kδ/γ inhibitor compound IPI-145 rather than IPI-443 but found that it was no more effective in B cells than the PI3Kδ selective inhibitor IPI-3063. Thus, the second goal and main conclusion of Chapter 2 is that IPI-3063 has selective potency for PI3Kδ and inhibits B cell survival, proliferation, and plasmablast differentiation.

In Chapters 3 and 4 we focused downstream of PI3K to gain more knowledge of how mTOR signaling affects B cell differentiation. We first showed through both pharmacological and genetic manipulations that mTORC1 and mTORC2 have opposing roles in antibody class switching. By performing fine titrations of rapamycin and TOR-KIs, we noticed that at low

concentrations in which proliferation was preserved, rapamycin reduced switching whereas the TOR-KI compound INK128 enhanced switching. As we increased the concentrations of the inhibitors, there was a further reduction in proliferation but the compounds had opposite effects on class switching. Rapamycin further reduced CSR while cells were still able to switch during INK128 treatment. This experiment first established that the roles of mTORC1 and mTORC2 in cell division were independent of their roles in differentiation. We showed more evidence that Raptor-deficient B cells were able to undergo division were still reduced in the frequency of switching to IgG1. On the other hand, deletion of Rictor in B cells did not affect proliferation and increased switching. In Chapter 4, I further tested the role of proliferation in antibody class switching using the cell-cycle inhibitor, Palbociclib, and showed that slowing cell division alone was not enough to block switching to IgG1 as these cells switched to the same extent as in control (vehicle treated) cells.

We became interested in the phenomenon that mTOR regulation of antibody class switching was separate from division. mTOR is considered to be a central regulator of immune responses and elevated mTOR signaling may contribute to the development of autoimmune diseases (11–13). For example, mTOR is highly activated in lymphocytes of human patients with systemic lupus erythematosus (SLE) and in mouse models of lupus, suggesting that mTOR is involved in the production of self-reactive autoantibodies and disease pathogenesis (14–16). Current therapies for SLE include broad spectrum immunosuppression through the use of corticosteroids, which is usually associated with severe side effects, and biologicals to induce B cell depletion or target cytokines to limit B cell activation (17). These therapies, however, do not target the mechanism of production of pathogenic IgG antibodies and may also interfere with production of natural IgM, which has a protective role in autoimmunity (18). Better

understanding of how mTOR signaling regulates antibody class switching could lead to the development of therapies that can target the production of pathogenic IgG antibodies. The benefit to these therapies would also be that they have selective immunomodulatory action rather than broad non-specific immunosuppressive effects.

Another area of interest for immunomodulatory therapies is the field of immuno-oncology where there has been some success with checkpoint blockade and therapeutic antibodies. There has been interest in combining these therapies with small molecule agents to increase efficacy in a larger number of patients. Additionally, there has been a growing appreciation for new strategic therapies targeting the PI3K/AKT/mTOR pathway to promote tumor death via infiltrating immune cells in the tumor microenvironment (19–24). While the role of T cells and myeloid cells have been well established, there is also evidence that B cells are found in the tumor microenvironment and contribute to pro or anti-tumor responses as well (25). Investigation in how the PI3K/AKT/mTOR signaling pathway is involved in normal B cell responses potentially can lead to novel approaches to immune modulation in tumors.

In Chapter 3, we found that inhibition of mTORC2 increases antibody class switching and this is mediated through AKT and FOXO activity by regulating *Aidca* mRNA transcription **(Appendix 1)**. Chapter 4 further expands on the finding that Raptor deletion reduced switching in proliferating cells and addresses the question of which mTORC1 effectors are involved. While rapamycin showed promise during a phase 1/2 clinical trial with SLE patients (8), long-term rapamycin treatment can have serious side effects and targeting further downstream could potentially provide a better therapeutic window. We focused on the two main substrates involved in mTORC1-regulated gene expression, the S6Ks and 4E-BPs (26). Our characterization of the S6Ks and 4E-BPs uncovered novel and distinct roles in promoting antibody class switching. We

found that under LPS+IL-4 stimulation *in vitro*, S6K1 promotes Iγ-Cγ germline transcript production which is necessary for IgG1 switching. We also found that S6K1 was important for both switching to IgG1 and proliferation under αCD40+IL-4 activation. Our lab previously demonstrated that in B cells stimulated with anti-IgM+IL-4, the 4E-BP/eIF4E axis controlled both growth and proliferation while the S6Ks were dispensable (27); however, in that study we did not compare the function of S6Ks and eIF4E under antibody class switching conditions. Therefore, the findings in chapter 4 reveal that S6K1 does play a role in B cell differentiation. S6K1 regulates cap-dependent translation through phosphorylation of eIF4B (28) so we had also investigated whether S6K1i reduced AID protein and observed no change. However, more repeat experiments need to be done to confirm this. Future questions include whether high or low concentrations of S6K1i will have any effects on plasmablast differentiation and IgM secretion during *in vivo* SRBC immunization. It would be interesting to characterize S6K2 knock-out mice to test if this isoform plays a role as well. Lastly, I'd like to further investigate the role of S6Ks in different in vitro switching conditions and cytokine contributions to measure the levels of p-S6. If there are any differences in signaling activation this could account for how LPS+IL-4 may be promoting germline Iγ-Cγ transcription. I would also like to determine if S6K is involved in regulation of the transcription factors that promote germline transcription such as NF-κB or Stat6 for Iγ-Cγ transcripts (29).

Mechanistic and pharmacological investigation of the 4E-BP/eIF4E arm of mTORC1 signaling showed that inhibiting eIF4E activity decreased antibody class switching. We also found that inhibition of eIF4E reduced AID protein levels but not *Aidca* mRNA transcription. Whether this reduction in AID directly reduces germinal center B cells and antibody class switching can be tested by AID overexpression to rescue the effects of SBI-756 or Rap. An

alternative hypothesis is that eIF4E signaling is reducing antibody class switching through an AID independent mechanism, perhaps by affecting DNA repair. However, the finding that eIF4E and cap-dependent translation regulates AID protein is a novel and, importantly, a targetable mechanism. AID overexpression has been linked to both B-cell malignancies and autoimmune diseases (30), and idelalisib treatment increases AID expression and somatic mutations in leukemia cells from CLL patients (31). Thus, eIF4E targeted therapies can potentially be useful in reducing AID in these contexts. It is also likely that somatic hypermutation will be affected. When we tested the effects of SBI-756 on somatic hypermutation *in vitro* with αCD40+IL-4 stimulating conditions, however, we found no differences in overall mutational frequency of the CDR3 region (data not shown, in collaboration with Adoptive Biotechnologies, Seattle WA). Alternatively, a more physiologically relevant method would be to analyze sorted germinal center B cells from a genetic mouse model of eIF4E inhibition during an *in vivo* SRBC immunization. We also found that targeting eIF4E and S6K1 both reduced IgG1 *in vitro*. If these effects are maintained during *in vivo* models of autoimmune disease, then they potentially could be useful in treating antibody-mediated diseases. Interestingly, inhibition of eIF4E reduced switching to IgG1 and IgG3 but not IgA even though AID protein was reduced. Further investigation is needed to better understand the role of mTORC1 and 4E-BP/eIF4E in IgA switching mechanisms; however the result that IgA is unaffected by inhibition of these signaling nodes is promising since IgA is important in maintaining gut homeostasis (32).

The finding that cap-dependent translation regulates B cell differentiation demonstrates the importance of studying changes in gene expression at the levels of both translation and transcription. B cell differentiation in the germinal center is a highly energetic process with increased glucose uptake and massive cell growth. Thus, it makes sense that as a nutrient sensor,

mTORC1 has a checkpoint function to regulate translation and ensure there are sufficient nutrients to meet cellular energy demands. This idea is consistent with our glutamine studies in which cells are receiving activation signals but still do not divide. It would also be informative to identify the mRNAs that are being translationally regulated by mTORC1 during B cell differentiation, using polysome fractionation-RNA sequencing. Study of mRNAs at different time-points of B cell activation from early to later stages may lead to insights in B cell differentiation such as changes in metabolism and plasma or memory B cell formation.

It will also be interesting to determine the mechanism in which the mRNAs are regulated by mTORC1 activity in lymphocytes and whether it is through consensus sequences in the 5'UTRs (33–36). This can be determined by polysome fractionation and sequencing the 5'UTRs of the purified mRNAs using nanoCAGE technology. Considering that mTORC1 signaling is dynamic and regulates the dark zone/light zone formations of the germinal center (37), it will be interesting to investigate how eIF4E activity is involved in translation of the mRNAs important for the light zone stage, where mTORC1 activity was shown to be necessary (37). This could be tested using chemical or genetic inhibition of eIF4E during an *in vivo* immunization and measuring or sorting light zone and dark zone B cell populations to perform polysome fractionation RNA-sequencing.

To investigate these questions, we will have to develop or refine the tools we currently have, including SBI-756. When we tested the effects of SBI-756 on antibody production *in vivo,* we found no differences in IgG1 and IgM production during a sheep red blood cell (SRBC) immunization (data not shown). In a cancer model, our laboratory found SBI-756 to be effective at reducing growth of OCI-LY1 lymphoma xenografts and could cause tumor regression when given in combination with venetoclax (ABT-199), a BCL-2 inhibitor (data not shown). The same

concentration of SBI-756 was used in both models. Potential hypotheses for why SBI-756 dosing did not reduce switching to IgG1 *in vivo* include (A) SBI-756 accumulates more in cancer cells; (B) cancer cells have increased sensitivity to eIF4E inhibition, consistent with the data in Chapter 5 showing that eIF4E gene dosage was a rate-limiting factor for tumorigenesis in a mouse model of B-ALL but not for antibody class switching; or (C) SBI-756 at the dose used does not sufficiently inhibit cap-dependent translation in activated B cells *in vivo*. Future directions include determining the pharmacodynamics of SBI-756 and establishing an assay for measuring cap-dependent translation *ex vivo.*

SBI-756 is a small molecule with anti-cancer properties reported in cellular and *in vivo* models of melanoma (38). Mass spectrometry experiments suggested that SBI-756 binds to the eIF4G scaffolding protein, and functional experiments show that the compound disrupts the eIF4E:eIF4G interaction (38). Therefore, to genetically model the effects of SBI-756 on primary cells, a relevant model would be to introduce mutations in the *Eif4g1* gene encoding eIF4G that reduce binding to eIF4E (39). By maintaining eIF4E protein levels, hopefully this would overcome the compensatory mechanism of 4E-BP2 reduction that we observed in activated B cells from $Eif4e^{+/-}$ mice in chapter 5. Another model would be to use *Eif4e*-flox or *Eif4g1*-flox mice to delete at different stages of B cell activation, although whether B cells would be able to compensate after acute deletion of eIF4E or eIF4G would have to be determined. Additionally, it will be important to determine if the reduction of 4E-BP is due to decreased translation or through other mechanisms such as increased degradation.

While the PI3K/AKT/mTOR signaling network has been known to be important for B cell differentiation there is still much to learn about its contributions to immune-related diseases

as well as the progression of B-cell malignances. As emphasized in this dissertation, better understanding will give us new insight to develop novel therapies and treat these diseases.

References

1. Charles A Janeway, J., P. Travers, M. Walport, and M.J. Shlomchik. 2001. The Humoral Immune Response - Immunobiology - NCBI Bookshelf. .

2. Limon, J.J., and D.A. Fruman. 2012. Akt and mTOR in B Cell Activation and Differentiation. Front Immunol. 3: 228.

3. Pauls, S.D., S.T. Lafarge, I. Landego, T. Zhang, and A.J. Marshall. 2012. The phosphoinositide 3-kinase signaling pathway in normal and malignant B cells: activation mechanisms, regulation and impact on cellular functions. Front Immunol. 3: 224.

4. Yang, Q., P. Modi, T. Newcomb, C. Quéva, and V. Gandhi. 2015. Idelalisib: First-in-Class PI3K Delta Inhibitor for the Treatment of Chronic Lymphocytic Leukemia, Small Lymphocytic Leukemia, and Follicular Lymphoma. Clin Cancer Res. 21: 1537–1542.

5. Rao, V.K., S. Webster, V.A.S.H. Dalm, A. Šedivá, P.M. van Hagen, S. Holland, S.D. Rosenzweig, A.D. Christ, B. Sloth, M. Cabanski, A.D. Joshi, S. de Buck, J. Doucet, D. Guerini, C. Kalis, I. Pylvaenaeinen, N. Soldermann, A. Kashyap, G. Uzel, M.J. Lenardo, D.D. Patel, C.L. Lucas, and C. Burkhart. 2017. Effective “activated PI3Kδ syndrome”-targeted therapy with the PI3Kδ inhibitor leniolisib. Blood. 130: 2307–2316.

6. Winkler, D.G., K.L. Faia, J.P. DiNitto, J.A. Ali, K.F. White, E.E. Brophy, M.M. Pink, J.L. Proctor, J. Lussier, C.M. Martin, J.G. Hoyt, B. Tillotson, E.L. Murphy, A.R. Lim, B.D. Thomas, J.R. Macdougall, P. Ren, Y. Liu, L.-S. Li, K.A. Jessen, C.C. Fritz, J.L. Dunbar, J.R. Porter, C. Rommel, V.J. Palombella, P.S. Changelian, and J.L. Kutok. 2013. PI3K-δ and PI3K-γ inhibition by IPI-145 abrogates immune responses and suppresses activity in autoimmune and inflammatory disease models. Chem Biol. 20: 1364–1374.

7. Stark, A.-K., S. Sriskantharajah, E.M. Hessel, and K. Okkenhaug. 2015. PI3K inhibitors in inflammation, autoimmunity and cancer. Curr Opin Pharmacol. 23: 82–91.

8. Lai, Z.-W., R. Kelly, T. Winans, I. Marchena, A. Shadakshari, J. Yu, M. Dawood, R. Garcia, H. Tily, L. Francis, S.V. Faraone, P.E. Phillips, and A. Perl. 2018. Sirolimus in patients with clinically active systemic lupus erythematosus resistant to, or intolerant of, conventional medications: a single-arm, open-label, phase 1/2 trial. The Lancet. 391: 1186–1196.

9. Omori, S.A., M.H. Cato, A. Anzelon-Mills, K.D. Puri, M. Shapiro-Shelef, K. Calame, and R.C. Rickert. 2006. Regulation of class-switch recombination and plasma cell differentiation by phosphatidylinositol 3-kinase signaling. Immunity. 25: 545–557.

10. Wentink, M., V. Dalm, A.C. Lankester, P.A. van Schouwenburg, L. Schölvinck, T. Kalina, R. Zachova, A. Sediva, A. Lambeck, I. Pico-Knijnenburg, J.J.M. van Dongen, M. Pac, E. Bernatowska, M. van Hagen, G. Driessen, and M. van der Burg. 2017. Genetic defects in PI3Kδ affect B-cell differentiation and maturation leading to hypogammaglobulineamia and recurrent infections. Clin Immunol. 176: 77–86.

11. Thomson, A.W., H.R. Turnquist, and G. Raimondi. 2009. Immunoregulatory functions of mTOR inhibition. Nat Rev Immunol. 9: 324–337.

12. Powell, J.D., K.N. Pollizzi, E.B. Heikamp, and M.R. Horton. 2012. Regulation of immune responses by mTOR. Annu Rev Immunol. 30: 39–68.

13. Weichhart, T., and M.D. Säemann. 2009. The multiple facets of mTOR in immunity. Trends Immunol. 30: 218–226.

14. Wu, T., X. Qin, Z. Kurepa, K.R. Kumar, K. Liu, H. Kanta, X.J. Zhou, A.B. Satterthwaite, L.S. Davis, and C. Mohan. 2007. Shared signaling networks active in B cells isolated from genetically distinct mouse models of lupus. J Clin Invest. 117: 2186–2196.

15. Kato, H., and A. Perl. 2014. Mechanistic target of rapamycin complex 1 expands Th17 and IL-4+ CD4-CD8- double-negative T cells and contracts regulatory T cells in systemic lupus erythematosus. J Immunol. 192: 4134–4144.

16. Lai, Z.-W., R. Borsuk, A. Shadakshari, J. Yu, M. Dawood, R. Garcia, L. Francis, H. Tily, A. Bartos, S.V. Faraone, P. Phillips, and A. Perl. 2013. Mechanistic target of rapamycin activation triggers IL-4 production and necrotic death of double-negative T cells in patients with systemic lupus erythematosus. J Immunol. 191: 2236–2246.

17. Yanaba, K., J.-D. Bouaziz, T. Matsushita, C.M. Magro, E.W. St Clair, and T.F. Tedder. 2008. B-lymphocyte contributions to human autoimmune disease. Immunol Rev. 223: 284–299.

18. Manson, J.J., C. Mauri, and M.R. Ehrenstein. 2005. Natural serum IgM maintains immunological homeostasis and prevents autoimmunity. Springer Semin Immunopathol. 26: 425–432.

19. Ali, K., D.R. Soond, R. Pineiro, T. Hagemann, W. Pearce, E.L. Lim, H. Bouabe, C.L. Scudamore, T. Hancox, H. Maecker, L. Friedman, M. Turner, K. Okkenhaug, and B. Vanhaesebroeck. 2014. Inactivation of PI(3)K p110δ breaks regulatory T-cell-mediated immune tolerance to cancer. Nature. 510: 407–411.

20. Eil, R., S.K. Vodnala, D. Clever, C.A. Klebanoff, M. Sukumar, J.H. Pan, D.C. Palmer, A. Gros, T.N. Yamamoto, S.J. Patel, G.C. Guittard, Z. Yu, V. Carbonaro, K. Okkenhaug, D.S. Schrump, W.M. Linehan, R. Roychoudhuri, and N.P. Restifo. 2016. Ionic immune suppression within the tumour microenvironment limits T cell effector function. Nature. 537: 539–543.

21. Liu, Y., S. Pandeswara, V. Dao, Á. Padrón, J.M. Drerup, S. Lao, A. Liu, V. Hurez, and T.J. Curiel. 2017. Biphasic rapamycin effects in lymphoma and carcinoma treatment. Cancer Res. 77: 520–531.

22. Dao, V., Y. Liu, S. Pandeswara, R.S. Svatek, J.A. Gelfond, A. Liu, V. Hurez, and T.J. Curiel. 2016. Immune-Stimulatory Effects of Rapamycin Are Mediated by Stimulation of Antitumor γδ T Cells. Cancer Res. 76: 5970–5982.

23. De Henau, O., M. Rausch, D. Winkler, L.F. Campesato, C. Liu, D.H. Cymerman, S. Budhu, A. Ghosh, M. Pink, J. Tchaicha, M. Douglas, T. Tibbitts, S. Sharma, J. Proctor, N. Kosmider, K. White, H. Stern, J. Soglia, J. Adams, V.J. Palombella, K. McGovern, J.L. Kutok, J.D. Wolchok, and T. Merghoub. 2016. Overcoming resistance to checkpoint blockade therapy by targeting PI3Kγ in myeloid cells. Nature. 539: 443–447.

24. Kaneda, M.M., K.S. Messer, N. Ralainirina, H. Li, C.J. Leem, S. Gorjestani, G. Woo, A.V. Nguyen, C.C. Figueiredo, P. Foubert, M.C. Schmid, M. Pink, D.G. Winkler, M. Rausch, V.J. Palombella, J. Kutok, K. McGovern, K.A. Frazer, X. Wu, M. Karin, R. Sasik, E.E.W. Cohen, and J.A. Varner. 2016. PI3Kγ is a molecular switch that controls immune suppression. Nature. 539: 437–442.

25. Tsou, P., H. Katayama, E.J. Ostrin, and S.M. Hanash. 2016. The emerging role of B cells in tumor immunity. Cancer Res. 76: 5597–5601.

26. Choo, A.Y., S.-O. Yoon, S.G. Kim, P.P. Roux, and J. Blenis. 2008. Rapamycin differentially inhibits S6Ks and 4E-BP1 to mediate cell-type-specific repression of mRNA translation. Proc Natl Acad Sci U S A. 105: 17414–17419.

27. So, L., J. Lee, M. Palafox, S. Mallya, C.G. Woxland, M. Arguello, M.L. Truitt, N. Sonenberg, D. Ruggero, and D.A. Fruman. 2016. The 4E-BP-eIF4E axis promotes rapamycin-sensitive growth and proliferation in lymphocytes. Sci Signal. 9: ra57.

28. Raught, B., F. Peiretti, A.-C. Gingras, M. Livingstone, D. Shahbazian, G.L. Mayeur, R.D. Polakiewicz, N. Sonenberg, and J.W.B. Hershey. 2004. Phosphorylation of eucaryotic translation initiation factor 4B Ser422 is modulated by S6 kinases. EMBO J. 23: 1761–1769.

29. Dunnick, W.A., J. Shi, V. Holden, C. Fontaine, and J.T. Collins. 2011. The role of germline promoters and I exons in cytokine-induced gene-specific class switch recombination. J Immunol. 186: 350–358.

30. Okazaki, I., H. Hiai, N. Kakazu, S. Yamada, M. Muramatsu, K. Kinoshita, and T. Honjo. 2003. Constitutive expression of AID leads to tumorigenesis. J Exp Med. 197: 1173–1181.

31. Compagno, M., Q. Wang, C. Pighi, T.C. Cheong, F.L. Meng, T. Poggio, L.S. Yeap, E. Karaca, R.B. Blasco, F. Langellotto, C. Ambrogio, C. Voena, A. Wiestner, S.N. Kasar, J.R.

Brown, J. Sun, C.J. Wu, M. Gostissa, F.W. Alt, and R. Chiarle. 2017. Phosphatidylinositol 3-kinase δ blockade increases genomic instability in B cells. Nature. 542: 489–493.

32. Lycke, N.Y., and M. Bemark. 2017. The regulation of gut mucosal IgA B-cell responses: recent developments. Mucosal Immunol. 10: 1361–1374.

33. Gandin, V., L. Masvidal, L. Hulea, S.-P. Gravel, M. Cargnello, S. McLaughlan, Y. Cai, P. Balanathan, M. Morita, A. Rajakumar, L. Furic, M. Pollak, J.A. Porco, J. St-Pierre, J. Pelletier, O. Larsson, and I. Topisirovic. 2016. nanoCAGE reveals 5' UTR features that define specific modes of translation of functionally related MTOR-sensitive mRNAs. Genome Res. 26: 636–648.

34. Thoreen, C.C., L. Chantranupong, H.R. Keys, T. Wang, N.S. Gray, and D.M. Sabatini. 2012. A unifying model for mTORC1-mediated regulation of mRNA translation. Nature. 485: 109–113.

35. Hsieh, A.C., Y. Liu, M.P. Edlind, N.T. Ingolia, M.R. Janes, A. Sher, E.Y. Shi, C.R. Stumpf, C. Christensen, M.J. Bonham, S. Wang, P. Ren, M. Martin, K. Jessen, M.E. Feldman, J.S. Weissman, K.M. Shokat, C. Rommel, and D. Ruggero. 2012. The translational landscape of mTOR signalling steers cancer initiation and metastasis. Nature. 485: 55–61.

36. Truitt, M.L., C.S. Conn, Z. Shi, X. Pang, T. Tokuyasu, A.M. Coady, Y. Seo, M. Barna, and D. Ruggero. 2015. Differential Requirements for eIF4E Dose in Normal Development and Cancer. Cell. 162: 59–71.

37. Ersching, J., A. Efeyan, L. Mesin, J.T. Jacobsen, G. Pasqual, B.C. Grabiner, D. Dominguez-Sola, D.M. Sabatini, and G.D. Victora. 2017. Germinal Center Selection and Affinity Maturation Require Dynamic Regulation of mTORC1 Kinase. Immunity. 46: 1045–1058.e6.

38. Feng, Y., A.B. Pinkerton, L. Hulea, T. Zhang, M.A. Davies, S. Grotegut, Y. Cheli, H. Yin, E. Lau, H. Kim, S.K. De, E. Barile, M. Pellecchia, M. Bosenberg, J.-L. Li, B. James, C.A. Hassig, K.M. Brown, I. Topisirovic, and Z.A. Ronai. 2015. SBI-0640756 Attenuates the Growth of Clinically Unresponsive Melanomas by Disrupting the eIF4F Translation Initiation Complex. Cancer Res. 75: 5211–5218.

39. Grüner, S., D. Peter, R. Weber, L. Wohlbold, M.-Y. Chung, O. Weichenrieder, E. Valkov, C. Igreja, and E. Izaurralde. 2016. The Structures of eIF4E-eIF4G Complexes Reveal an Extended Interface to Regulate Translation Initiation. Mol Cell. 64: 467–479.

APPENDIX 1

mTOR kinase inhibitors promote antibody class switching via mTORC2 inhibition

Jose J. Limon[a,b], Lomon So[a,b], Stefan Jellbauer[b,c], Honyin Chiu[a,b], Juana Corado[a], Stephen M. Sykes[d], Manuela Raffatellu[b,c], and David A. Fruman[a,b,1]

[a]Department of Molecular Biology & Biochemistry, [b]Institute for Immunology, and [c]Department of Microbiology & Molecular Genetics, University of California, Irvine, CA 92697; and [d]Fox Chase Cancer Center, Philadelphia, PA 19111

Edited by Kevan M. Shokat, University of California, San Francisco, CA, and approved October 22, 2014 (received for review April 18, 2014)

The mammalian target of rapamycin (mTOR) is a kinase that functions in two distinct complexes, mTORC1 and mTORC2. In peripheral B cells, complete deletion of mTOR suppresses germinal center B-cell responses, including class switching and somatic hypermutation. The allosteric mTORC1 inhibitor rapamycin blocks proliferation and differentiation, but lower doses can promote protective IgM responses. To elucidate the complexity of mTOR signaling in B cells further, we used ATP-competitive mTOR kinase inhibitors (TOR-KIs), which inhibit both mTORC1 and mTORC2. Although TOR-KIs are in clinical development for cancer, their effects on mature lymphocytes are largely unknown. We show that high concentrations of TOR-KIs suppress B-cell proliferation and differentiation, yet lower concentrations that preserve proliferation increase the fraction of B cells undergoing class switching in vitro. Transient treatment of mice with the TOR-KI compound AZD8055 increased titers of class-switched high-affinity antibodies to a hapten–protein conjugate. Mechanistic investigation identified opposing roles for mTORC1 and mTORC2 in B-cell differentiation and showed that TOR-KIs enhance class switching in a manner dependent on forkhead box, subgroup O (FoxO) transcription factors. These observations emphasize the distinct actions of TOR-KIs compared with rapamycin and suggest that TOR-KIs might be useful to enhance production of class-switched antibodies following vaccination.

kinase | B lymphocyte | rapamycin | class switching | differentiation

B-cell activation by antigen leads to clonal expansion, followed by differentiation into plasma cells secreting antigen-specific antibodies. Early in an immune response, some B cells differentiate rapidly into plasmablasts that secrete antibodies that are mostly of the IgM isotype and of low affinity. Other B cells adopt a germinal center (GC) fate and undergo class switch recombination (CSR) and somatic hypermutation. Ultimately, GC B cells that survive selection become plasma cells secreting high-affinity antibodies of various isotypes or become long-lived memory B cells.

Extracellular inputs including B-cell receptor engagement, Toll-like receptor ligation, and cytokines, all activate the signaling enzyme phosphoinositide 3-kinase (PI3K) and its downstream target AKT (also known as protein kinase B) in B cells (1). PI3K/AKT signaling and other inputs activate the mammalian target of rapamycin (mTOR), a multifunctional kinase that promotes cell growth, division, and metabolic reprogramming (1, 2). The mTOR kinase is present in two cellular complexes, mTOR-complex 1 (mTORC1) defined by the raptor subunit and mTOR-complex 2 (mTORC2) defined by rictor (3). The classical mTOR inhibitor rapamycin forms a complex with FKBP12 that partially inhibits mTORC1 and can disrupt mTORC2 assembly upon prolonged cellular exposure. mTORC1 acts downstream of AKT and other signals to promote biosynthetic processes essential for cell growth and division. mTORC2 acts upstream of AKT by phosphorylating Ser-473 in the AKT hydrophobic motif. mTORC2 and AKT function are required for subsequent phosphorylation of forkhead box, subgroup O (FoxO) transcription factors (4, 5). When phosphorylated, FoxO factors exit the nucleus and transcription of FoxO target genes is reduced.

Recent studies illustrate the complexity of mTOR function in B cells. Conditional deletion of the mTOR gene in mouse B cells strongly impairs proliferation and GC differentiation (6). Inactivation of mTORC2 in B cells, via rictor deletion, reduces mature B-cell survival and impairs antibody responses and GC formation (7). At concentrations above 1 nM, rapamycin markedly impairs proliferation of both mouse and human B cells and suppresses antibody responses (8, 9). However, at lower concentrations that preserve B-cell proliferation, rapamycin still suppresses class switching but unexpectedly promotes IgM responses that provide heterosubtypic protection from influenza (6, 10). These studies suggest that overall mTOR signaling, as well as the relative activity of mTORC1 and mTORC2, controls the ability of B cells to divide and to differentiate.

ATP-competitive mTOR kinase inhibitors (TOR-KIs) block activity of both mTORC1 and mTORC2, and were developed to overcome limitations of rapamycin as anticancer agents (11, 12). We reported that TOR-KIs do not block proliferation of normal mature B cells at concentrations that cause cell cycle arrest in pre-B leukemia cells (9). However, the impact of TOR-KIs on immune function is still poorly characterized. In this study, we tested whether TOR-KIs can skew the differentiation of activated B cells. We found that partial mTORC1/mTORC2 inhibition or mTORC2 deletion increases CSR, whereas selective inhibition of mTORC1 suppresses CSR.

Significance

Rapamycin is an immunosuppressive drug that partially inhibits the cellular kinase mammalian target of rapamycin (mTOR). This study uncovers previously unidentified mechanisms of mTOR signaling in B cells. Antigen recognition and other signals activate mTOR, a central driver of lymphocyte proliferation and differentiation. However, mTOR forms two protein complexes (mTORC1 and mTORC2) whose roles in B-cell differentiation are poorly defined. We found that a new class of ATP-competitive mTOR kinase inhibitors (TOR-KIs) can augment antibody class switching at concentrations that partially inhibit mTOR activity. Mechanistic studies indicate that mTORC1 loss suppresses, whereas mTORC2 loss promotes, class switching. The dominant effect of TOR-KIs is to promote switching through mTORC2 inhibition. These findings establish distinct immunomodulatory activity of TOR-KIs compared with the canonical mTOR inhibitor rapamycin.

Author contributions: J.J.L., L.S., S.J., H.C., S.M.S., M.R., and D.A.F. designed research; J.J.L., L.S., S.J., H.C., J.C., and S.M.S. performed research; S.M.S. contributed new reagents/analytic tools; J.J.L., L.S., S.J., H.C., J.C., M.R., and D.A.F. analyzed data; and J.J.L., L.S., S.J., H.C., S.M.S., M.R., and D.A.F. wrote the paper.

The authors declare no conflict of interest.

This article is a PNAS Direct Submission.

[1]To whom correspondence should be addressed. Email: dfruman@uci.edu.

This article contains supporting information online at www.pnas.org/lookup/suppl/doi:10.1073/pnas.1407104111/-/DCSupplemental.

Results

High Concentrations of TOR-KIs Block B-Cell Proliferation. We reported previously that the TOR-KI compound PP242, when added at a concentration of 100 nM, fully suppresses mTOR signaling in B cells without blocking proliferation (9). This result was surprising because the allosteric mTOR inhibitor rapamycin had only partial effects on signaling yet fully blocked B-cell proliferation (9). Our initial signaling measurements were taken 15 min after B-cell stimulation (9), so we speculated that the effects of PP242 might be transient and wear off before the cell commits to division. To test this idea, we conducted a time course measuring phosphorylation of the ribosomal S6 protein at the Ser-240/244 site (p-S6), which is a sensitive readout of mTORC1 activity. Consistent with our prediction, 100 nM PP242 blocked p-S6 to near completion at 3 h after B-cell stimulation but much less at 24 and 48 h (Fig. 1 *A* and *B*). By 48 h, the cells had proliferated nearly to the same extent as control vehicle-treated B cells, as assessed by carboxyfluorescein succinimidyl ester (CFSE) dilution (Fig. 1*B*). In contrast, increasing the concentration of PP242 to 400 nM caused sustained inhibition of p-S6 and blocked proliferation similar to cells treated with 10 nM rapamycin. Based on these results, in subsequent B-cell differentiation experiments, we used PP242 and other TOR-KIs at concentrations that have a minimal impact on proliferation (Fig. 2 *A* and *D* and Fig. S1*A*) and partially reduce phosphorylation of mTORC1 and mTORC2 substrates at 24 h (Fig. S1*B*).

TOR-KIs Increase B-Cell Isotype Switching in Vitro. In a previous study, we administered PP242 to mice and assessed the effect on antibody responses to the T cell-dependent (TD) antigen nitrophenyl-ovalbumin (NP-OVA) (9). We found that PP242 did not strongly suppress NP-specific IgM or IgG1 and caused a significant increase in the percentage of B cells with a GC phenotype in some experiments (9). To define the B cell-intrinsic effects of TOR-KIs further, we assessed the differentiation of purified splenic B cells. We used four different TOR-KIs with distinct chemical structures (INK128, PP242, Ku-0063794, and AZD8055) to minimize the potential for off-target effects. Each compound increased the percentage of IgG1-switched B220^{+} B cells induced by anti-CD40 plus IL-4, a condition that mimics signals during a TD response and favors isotype switching to IgG1 (Fig. 2 *A* and *B*). Direct inhibition of AKT isoforms AKT1 and AKT2 also increased the frequency of switching to IgG1 (Fig. 2 *A* and *B*). Similar results were observed when B cells activated by LPS plus IL-4 were treated with INK128, PP242, Ku-0063794, or AZD8055 (Fig. 2*C*). Consistent with increased switching to the IgG1 isotype, postrecombination Iμ-Cγ1 transcripts were increased in B cells treated with TOR-KIs (Fig. S2). In addition, TOR-KI–treated B cells displayed an elevation in *Aicda* transcripts encoding activation-induced cytidine deaminase (Fig. 2*G*), the mutator protein required for initiation of CSR (13).

As reported previously (14, 15), inhibiting PI3K strongly induced switching to IgE with lesser effects of AKT inhibition (Fig. S3). Under these conditions, TOR-KIs had minimal effects on switching to IgE, an isotype important for allergic responses (Fig. S3). Hence, the enhanced switching to IgG1 caused by TOR-KIs is distinct from the IgE increases caused by PI3K inhibition.

We next assessed the effect of TOR-KIs on differentiation into plasmablasts and antibody-secreting cells (ASCs) following stimulation with LPS. Plasmablast differentiation, as measured by cells with a B220^{low}CD138^{+} phenotype, was decreased in a concentration-dependent manner by TOR-KIs, whereas AKT inhibition had no significant effect (Fig. 2 *D* and *E*). TOR-KIs also reduced IgM production, as measured by ELISA from cell culture supernatants of LPS-stimulated B cells (Fig. 2*F*). Thus, our results demonstrate that TOR-KIs can directly alter B-cell differentiation fate, causing increased CSR and a reciprocal decrease in plasmablast and ASC differentiation.

In contrast to the effects of TOR-KIs, rapamycin reduced both CSR and ASC differentiation (Fig. 2). The suppression of both differentiation pathways is consistent with early studies of rapamycin action in B cells (8).

TOR-KIs Promote High-Affinity IgG1 Production in Vivo. To extend these observations to an in vivo system, we assessed the effect of TOR-KIs on B-cell responses in mice. Chronic treatment of mice with TOR-KIs did not increase antigen-specific IgG or IgM production consistently (9) (Fig. S4). We reasoned that continuous

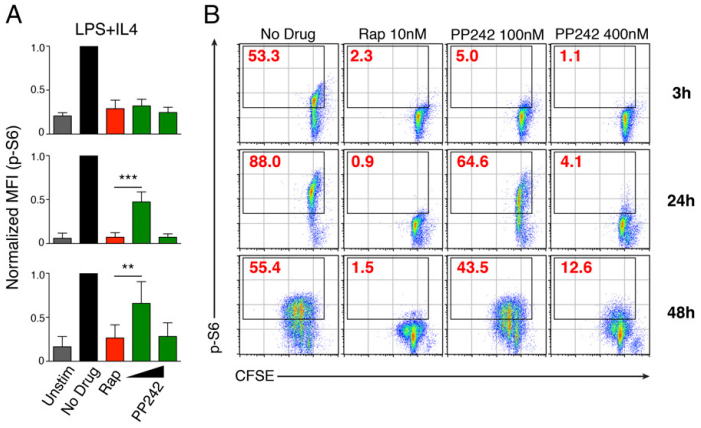

Fig. 1. High concentrations of TOR-KIs reduce mTORC1 activity and block B-cell proliferation. (*A* and *B*) Purified splenic B cells were labeled with CFSE to track cellular proliferation and cultured with media only or stimulated with LPS + IL-4 or LPS + IL-4 and inhibitors at the indicated concentrations. (*A*) mTORC1 activity was assessed at the indicated time points (*B*, *Far Right*) by intracellular staining (ICS) for p-S6 (S240/244 site) on proliferated cells. The graphs depict mean ± SEM of the p-S6 [median fluorescence intensity (MFI)] ($n = 3$). Data were normalized to the stimulated, no-drug treatment condition. (**$P < 0.01$, one-way ANOVA with Tukey's multiple comparison test). Unstim, unstimulated. (*B*) CFSE-labeled B cells were stimulated with LPS + IL-4 without or with inhibitors at the indicated concentrations for 48 h. Data are representative of three independent experiments. Rap, rapamycin.

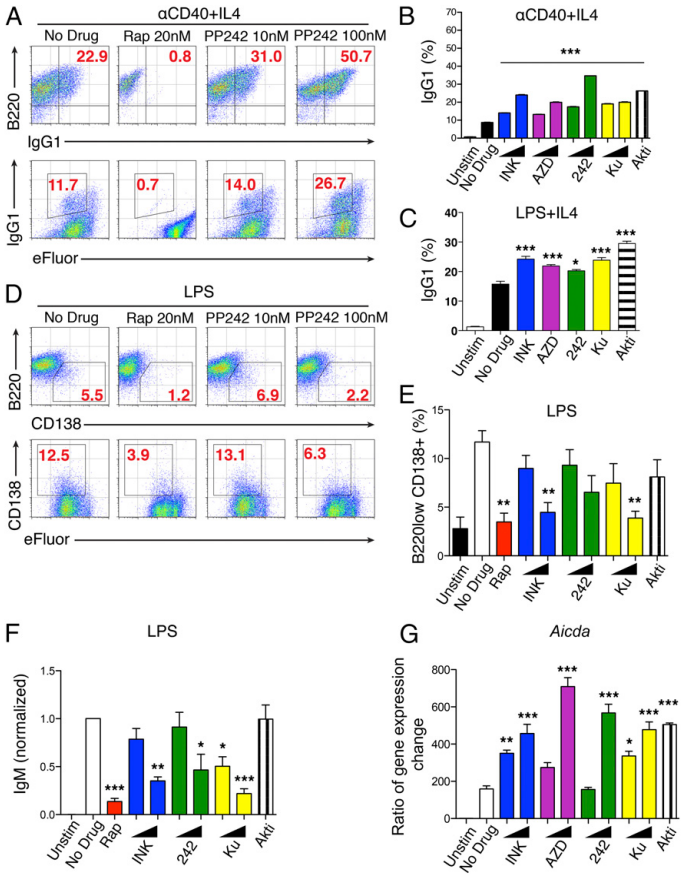

Fig. 2. TOR-KIs increase in vitro B-cell CSR and decrease plasmablast differentiation. (*A* and *B*) Purified B cells were cultured with media only or stimulated with αCD40 + IL-4 in the absence or presence of the inhibitors indicated. (*A*) Dot plots show IgG1$^+$ B cells (*Top*) and the cell division history of eFluor670-labeled B cells (*Bottom*; eFluor670 is a cell division tracking dye with a different emission spectrum than CFSE), as determined by FACS after 4 d. Other TOR-KIs in this study had similar effects on cell division at the concentrations used for differentiation experiments. (*B*) Percentage of live B cells that have divided at least once (based on eFluor670 division history) expressing surface IgG1 was determined by FACS after 4 d. (*C*) Switching to IgG1 was assessed as in *B*, except cells were stimulated with LPS + IL-4. (*D*) Representative FACS plots of plasmablast differentiation in purified B cells stimulated with LPS or LPS and indicated inhibitors for 3 d. (*Bottom*) B cells were labeled with eFluor670 to track division history. (*E*) Graph of the percentage of live B cells with a plasmablast phenotype determined by FACS after 3 d of stimulation as indicated in *D*. (*F*) Purified B cells were stimulated with LPS in the absence or presence of the inhibitors indicated. The amount of IgM in cell supernatants was quantitated by ELISA after 4 d, and data were normalized to the stimulated, no-drug treatment condition. (*G*) *Aicda* mRNA transcripts were quantitated by qPCR in B cells stimulated with αCD40 + IL-4. For *A* and *D*, data are representative of three or more independent experiments. For *B*, *C*, *E*, *F*, and *G*, graphs depict the mean and SEM of $n \geq 3$ samples per condition. (*$P < 0.05$; **$P < 0.01$; ***$P < 0.001$ by one-way ANOVA with Tukey's multiple comparison test, measured vs. the no-drug sample). Akti, Akt inhibitor VIII; AZD, AZD8055; INK, INK128; Ku, Ku-0063794; 242, PP242.

treatment might suppress terminal differentiation of GC cells into plasma cells. Therefore, we tested whether transient TOR-KI administration can enhance antibody responses in vivo.

Of the inhibitors tested in vitro (Fig. 2 *B* and *C*), we chose AZD8055 for most in vivo experiments because it is well tolerated at a dose with anticancer activity in mice (20 mg·kg^{-1}·d^{-1}) (16, 17). Mice were treated daily for a total of 4 d with AZD8055 or vehicle alone, beginning the day before immunization and stopping 2 d postimmunization (PID 2). Immunization with NP-OVA was performed on PID 0, and mice were boosted on PID 21, thus allowing for the interrogation of both primary and secondary humoral immune responses. Transient AZD8055 treatment significantly increased primary NP-specific IgG1 antibody titers at PID 21 ($P < 0.05$) (Fig. 3*A*). Secondary responses measured 7 d after antigen boosting (PID 28) were also augmented in AZD8055-treated mice (Fig. 3*A*). Transient AZD8055 treatment also significantly increased the production of high-affinity anti-NP antibody in the primary and secondary responses (Fig. 3*B*). Similar results were observed in a separate cohort of mice treated transiently with INK128 before and after NP-OVA immunization (Fig. S5).

Augmented B-cell class switching could be driven, in part, by drug effects on non-B cells in vivo. For example, the differentiation of follicular helper T (T_{FH}) cells is known to be influenced by PI3K activity (18). Interestingly, mice in the AZD8055 treatment group showed an increase in T_{FH}-cell percentages, as measured

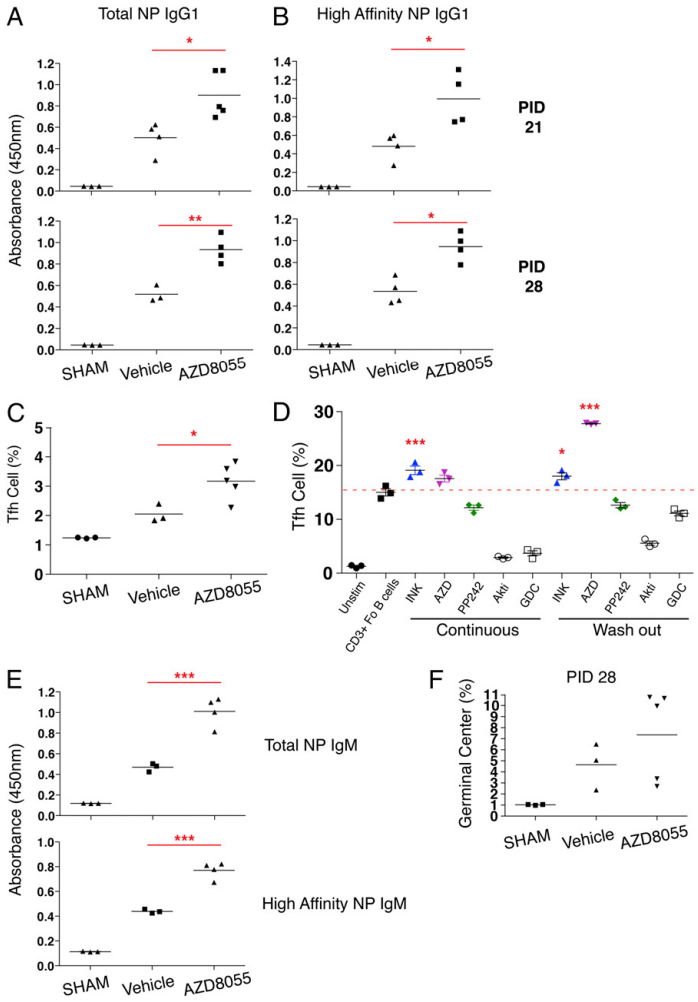

Fig. 3. Transient treatment with AZD8055 increases class-switched antibody responses in vivo. Mice were immunized with NP-OVA and treated daily for 4 d with AZD8055 at 20 mg/kg (PID −1 to PID 2). (*A* and *B*) Total and high-affinity NP-specific IgG1 production was measured by ELISA in sera collected during both the primary (PID 21) and secondary (PID 28) immune responses. (*C*) Percentage of spleen cells with a T_{FH} phenotype ($CD4^+CXCR5^{high}PD\text{-}1^+$) was determined by FACS at PID 28. (*D*) Purified $CD4^+$ T cells were cultured under skewing conditions and restimulated to determine the percentage of cells producing cytokines characteristic of T_{FH} cells ($IL\text{-}21^+IL\text{-}17A^-$). Cells were cultured in the continuous presence of inhibitors (*Left*) or for 24 h with inhibitors, followed by washout of drug from the cultures (*Right*). (*E*) Total and high-affinity NP-specific IgM was measured at PID 28. (*F*) Percentage of spleen cells with a GC phenotype ($B220^+$, IgD^{low}, $CD38^-$, and Fas^+) was determined by FACS at PID 28. (*$P < 0.05$; **$P < 0.01$; ***$P < 0.001$ by one-way ANOVA with Tukey's multiple comparison test, measured vs. the vehicle group).

by a $CD4^+$ C-X-C chemokine receptor type 5-high ($CXCR5^{high}$) programmed cell death protein 1-positive ($PD1^+$) immunophenotype (Fig. 3*C*). Treatment of CD4 T cells with the TOR-KIs AZD8055 and INK128 in vitro potentiated T_{FH} cell differentiation, whereas PI3K or AKT inhibitors suppressed T_{FH}-cell percentages (Fig. 3*D*). The effect of AZD8055 was significantly stronger when the drug was removed from the culture after 24 h (Fig. 3*D*). Thus, the ability of TOR-KIs to promote class switching may involve increased T_{FH}-cell differentiation.

Next, we evaluated other parameters of B-cell differentiation at PID 28. Transient AZD8055 treatment increased production of NP-specific IgM in the secondary response, including high-affinity IgM (Fig. 3*E*). This result suggests that transient pharmacological inhibition of mTOR does not block terminal differentiation of IgM-secreting plasma cells, and might instead lead to increased output of post-GC cells secreting high-affinity IgM. At PID 28, the percentage of GC B cells was not significantly increased in AZD8055-treated animals compared with the vehicle control group (Fig. 3*F*). To gain a preliminary assessment of memory B-cell formation, we enumerated the percentage of $B220^+$, IgD^-, surface $IgG1^+$ NP-binding cells at PID 28. As expected, vehicle-treated immunized animals showed a trend

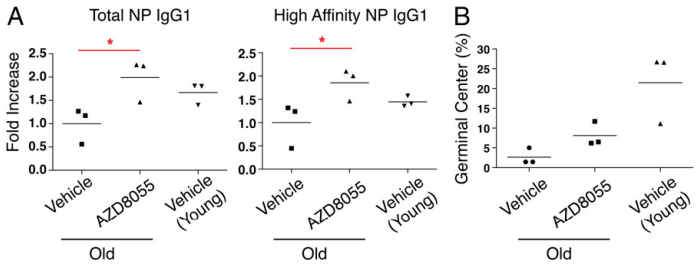

Fig. 4. Transient treatment with AZD8055 improves the humoral response in aged mice in vivo. Aged mice (~1.5 y old) were transiently treated with AZD8055 as described above and immunized with NP-OVA. (*A*) Production of total and high-affinity NP-specific IgG1 was measured by ELISA, with vehicle-treated young immunized mice as a comparison. (*B*) Percentage of spleen cells with a GC phenotype was determined by FACS at PID 28. (*$P < 0.05$, one-way ANOVA with Tukey's multiple comparison test, measured vs. the vehicle group.)

toward increased NP-binding IgG1$^+$ cells compared with sham-immunized controls at this time point (mean = 0.35 ± 0.07% vs. 0.19 ± 0.09%; $P = 0.06$). The percentage of NP-binding IgG1$^+$ cells was significantly increased in the AZD8055-treated group (mean = 0.54 ± 0.07%; $P < 0.05$ vs. vehicle). Together, these data show that transient TOR-KI treatment, starting 1 d before and ending 2 d after immunization with a TD antigen, improves the outcome of the humoral immune response. Specifically, TOR-KI–treated mice show higher titers and affinity of antigen-specific class-switched antibody and generate an increased percentage of B cells with a memory phenotype.

Next, we assessed the antibody response to a live-attenuated strain of *Salmonella* Typhimurium. The early humoral response to *Salmonella* in C57BL/6 mice is dominated by IgM antibodies and an extrafollicular IgG2c response, with GCs delayed until several weeks after infection (19, 20). In C57BL/6 mice infected with a vaccine strain of *Salmonella*, transient treatment with AZD8055 starting the day before immunization was poorly tolerated. We then switched to a protocol in which mice were treated during days 3–6 after immunization. Under these conditions, AZD8055 did not alter the early IgM response or induce IgG3 production at day 14 postinfection (Fig. S6*A*), whereas it decreased early IgG2c production. However, by day 29 post-infection, there was a significant increase in *Salmonella*-specific antibodies of IgM isotype, increased IgG3 in three of four mice, and no difference in IgG2c isotype (Fig. S6*B*). At day 29 post-infection, the percentage of T_{FH} cells was also increased in AZD8055-treated mice, and two mice in this group had elevated GC B-cell percentages (Fig. S6*C*). Further work is needed to identify conditions in which TOR-KIs strongly improve antibody production to pathogens and vaccines; nevertheless, the in vivo data largely recapitulate our in vitro findings.

TOR-KIs Improve Antibody Responses in Aged Mice. Age-related decreases in immune function can be attributed to defects in the innate and adaptive immune compartments, including humoral immunity (21). Therefore, we assessed the impact of AZD8055 on in vivo humoral responses to NP-OVA in aged mice, using the transient dosing protocol as described above. We observed a reduction in NP-specific IgG1 in aged mice compared with young mice, which was largely reversed by AZD8055 treatment (Fig. 4*A*). Total and high-affinity NP-specific IgG1 antibody titers from AZD8055-treated mice 7 d after boosting were statistically significant ($P < 0.05$) vs. the vehicle-treated group (Fig. 4*A*). These data provide evidence that TOR-KI treatment in the vaccine setting may help correct age-related defects in CSR and help improve humoral immune responses in the elderly. Similar to young AZD8055-treated mice, the percentage of GC B cells was not significantly increased at PID 28 in AZD8055-treated aged mice (Fig. 4*B*).

Rapamycin Reduces CSR by a Mechanism Partly Independent of Proliferation. To gain further insight into the mechanism of mTOR inhibitor action, we measured B-cell proliferation and IgG1 class switching over an extended dose–response of rapamycin or INK128 (Fig. 5). The partial mTORC1 inhibitor rapamycin reduced CSR at concentrations as low as 0.02 nM, with complete inhibition achieved by 0.4 nM. INK128 enhanced CSR at 10 nM, but higher concentrations caused increasing inhibition. Notably, rapamycin ablated CSR even at a concentration (0.4 nM) that partially preserved proliferation, whereas some B cells treated with a high concentration of INK128 (100 nM) still switched to IgG1 even without proliferation. Thus, the roles of mTORC1 and mTORC2 in cell division are partly independent of their roles in differentiation.

Inactivation of mTORC1 vs. mTORC2 Has Opposing Effects on CSR. As a genetic approach to assess the roles of mTORC1 and mTORC2, we isolated B cells from mice possessing conditional (floxed) alleles of rictor or raptor. Deletion of rictor using CD19Cre (rictor-flox/CD19Cre; termed rictor$^{\Delta B}$) did not significantly alter B-cell subset frequencies (Fig. S7*A*). In resting mature B cells, rictor expression was not completely reduced, suggesting incomplete and/or ongoing deletion (Fig. 6*A*). Consistent with reduced mTORC2 function, AKT phosphorylation at S473 was lower in B cells from rictor$^{\Delta B}$ mice (Fig. 6*A*). Importantly, this effect was specific to mTORC2, because S6 phosphorylation, a sensitive readout of mTORC1, was unaffected in rictor$^{\Delta B}$ B cells (Fig. 6*A*). To address the role of mTORC1, we analyzed B cells from raptor$^{\Delta B}$ mice in which the raptor-flox allele is deleted at the transitional B-cell stage using CD21Cre. As with rictor$^{\Delta B}$, B-cell development was largely normal in raptor$^{\Delta B}$ (Fig. S7*B*). Raptor expression was also not completely reduced in resting mature B cells (Fig. 6*D*), and this partial deletion corresponded to a reduced but not complete reduction in S6 phosphorylation in raptor$^{\Delta B}$ B cells (Fig. 6*D*).

Next, we tested functional responses in B cells with partial loss of rictor or raptor. In response to anti-CD40 plus IL-4, rictor-deficient B cells proliferated to a similar degree as WT, whereas raptor-deficient cells proliferated less (Fig. 6 *B* and *E*). To compare the capacity of cells to undergo class switching, we gated on divided cells and calculated the percentage of IgG1$^+$ cells. The results showed consistently less switching in divided raptor$^{\Delta B}$ B cells compared with control (Fig. 6*F*). These findings are consistent with the effects of rapamycin on B-cell division and differentiation (Fig. 5). In contrast, rictor$^{\Delta B}$ B cells showed significantly more switching to IgG1 than control (Fig. 6*C*). Importantly,

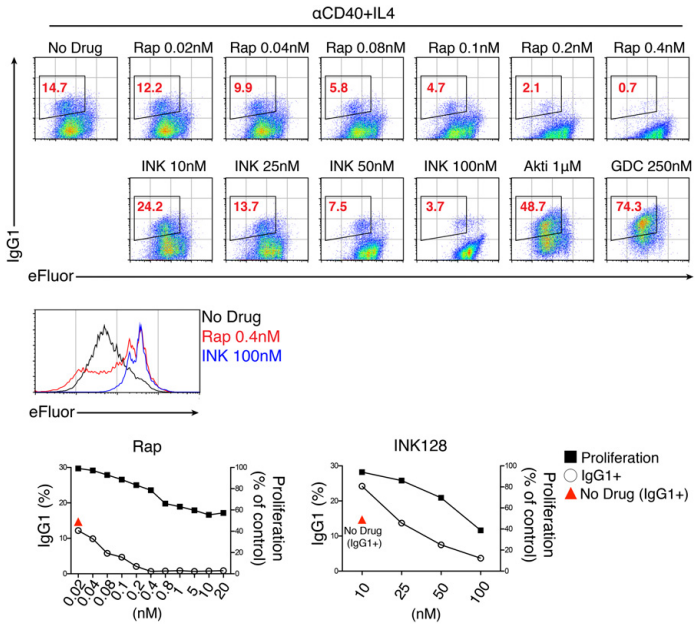

Fig. 5. Rapamycin has a more profound effect on B-cell proliferation and CSR than TOR-KIs. Purified B cells were labeled with eFluor670 to measure cell division and were stimulated with αCD40 + IL-4 in the presence or absence of indicated inhibitors. Representative FACS plots are shown for the different treatment conditions (*Upper*), and a FACS proliferation histogram is shown for high-dose rapamycin and INK128 (*Middle*). (*Lower*) Effects of inhibitor concentration on cellular proliferation and CSR are represented on line graphs. Data are representative of two independent experiments.

adding low-dose TOR-KI (1–5 nM INK128) to rictor$^{\Delta B}$ B cells did not further increase CSR (Fig. 6*C*).

We also measured plasmablast generation in B cells stimulated with LPS alone. The raptor$^{\Delta B}$ B cells showed reduced ASC generation, whereas the rictor$^{\Delta B}$ B cells were similar to control (Fig. 6 *C* and *F*). Together, these genetic interventions support the conclusion that mTORC1 inhibition suppresses both CSR and plasmablast generation, whereas mTORC2 inhibition increases CSR with little effect on plasmablast generation.

FoxO Is Required for TOR-KI–Mediated Increases in CSR. FoxO transcription factors are phosphorylated and inactivated by AKT and by serum- and glucocorticoid-regulated kinases (SGKs) in a manner dependent on mTORC2 (4, 5). Considering that FoxO factors are required for class switching (22), it is possible that TOR-KIs increase CSR through a FoxO-dependent mechanism. To test this possibility, we measured differentiation in B cells lacking FoxO1, FoxO3a, and FoxO4. Mice bearing floxed alleles of *Foxo1*, *Foxo3a*, and *Foxo4* and the inducible Mx1-Cre transgene (23, 24) were injected two times with polyinosinic:polycytidylic acid (polyI:C) before purification of splenic B cells. As a control, we confirmed that TOR-KIs increased IgG1 switching in B cells from polyI:C-treated FoxO triple-floxed mice lacking Mx1-Cre (Fig. S8). In cells from Mx1-Cre^{+} mice, intracellular staining for FoxO1 protein expression revealed incomplete deletion, with ~50% of B220^{+} cells showing low FoxO1 expression (Fig. 7*A*). The presence of a mixed population allowed us to compare differentiation in *Foxo1*-deficient (FoxO1-low) and *Foxo1*-sufficient (FoxO1-high) cells within the same culture (Fig. 7*A*). Fig. 7*B* shows that TOR-KI treatment caused a concentration-dependent increase in IgG1-switched cells among the FoxO1-high population, consistent with the effects in WT B cells and Mx1-Cre^{-} cells. Strikingly, FoxO depletion caused a nearly complete block in IgG1 switching in vehicle-treated cells and prevented the CSR increase in TOR-KI–treated cells (Fig. 7*B*). FoxO1-low cells also did not increase CSR when treated with the AKT1/2 inhibitor or with a pan-PI3K inhibitor, GDC-0941. The latter observation is consistent with the finding that the PI3K p110δ inhibitor IC87114 does not increase CSR in *Foxo1*-deficient B cells under IgG1 switching conditions (22). These data reconfirm the role of FoxO transcription factors in basal CSR and provide further evidence that TOR-KI–mediated CSR enhancement is through the AKT-FoxO signaling axis.

Discussion

TOR-KIs are a powerful new class of compounds that inhibit both rapamycin-sensitive and rapamycin-resistant mTOR functions. These agents not only have great promise for clinical management of cancer but also represent new chemical tools for probing the function of mTOR kinase activity in various cell types. Here, we have used a panel of chemically distinct TOR-KIs to demonstrate that mTOR kinase inhibition increases the fraction of activated B cells undergoing antibody class switching. These results were seen at TOR-KI concentrations that cause transient mTORC1/2 inhibition and only partially reduced signaling after 24 h in B cells. The effect of AKT inhibition or partial mTORC1/2 inhibition to increase CSR requires FoxO transcription factors. In addition, the expression of *Aicda* in activated B cells is known to be FoxO1-dependent (22), and *Aicda* mRNA was increased in cells treated with TOR-KIs or AKT inhibitor. These data support the model that mTORC2 inhibition by TOR-KIs reduces AKT activity, increasing FoxO activity to drive the enhanced class-switching response in TOR-KI–treated B cells (Fig. 8). This model is consistent with previous

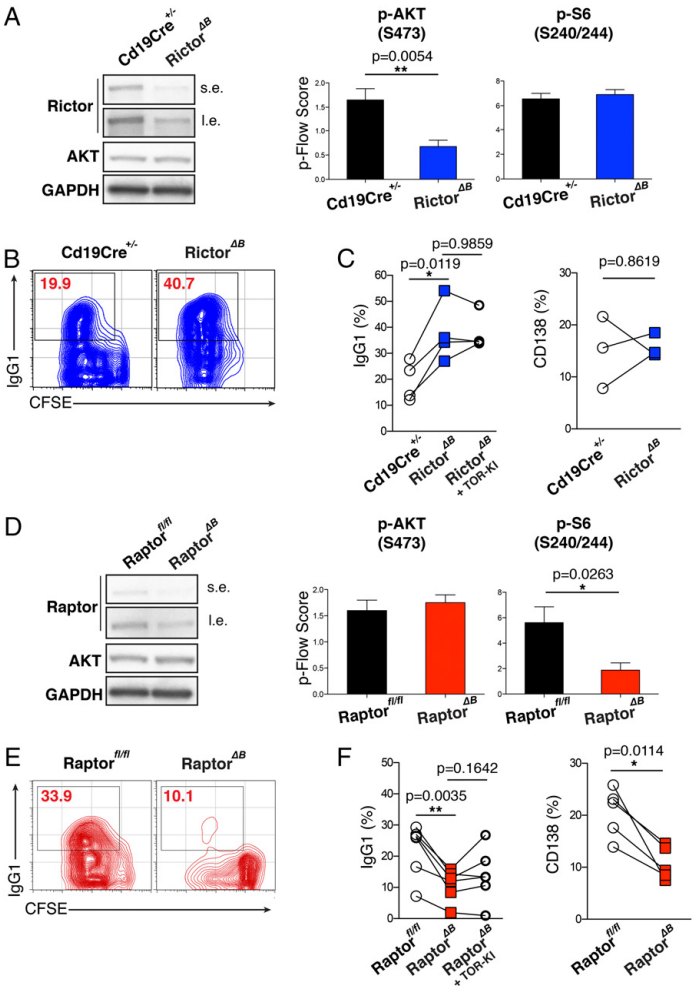

Fig. 6. Inactivation of mTORC1 vs. mTORC2 has opposing effects on CSR. (*A*) Purified resting B cells from either control (CD19Cre$^{+/-}$) or rictor-flox/CD19Cre (rictor$^{\Delta B}$) were subjected to Western blotting to check rictor protein levels (*Left*). RBC-lysed total splenocytes from the indicated genotypes were activated with αCD40 + IL-4 for 24 h, and intracellular phosphoflow (p-Flow) analysis was performed to measure mTORC1 (pS6-S240/244) and mTORC2 (pAKT-S473) activity. The fold change in median fluorescence intensity was calculated and subjected to $\log_2$ conversion to obtain p-Flow score values as previously described (9). Data are reported as mean ± SD [$n = 3$ (pAKT) or $n = 2$ (pS6)]. An unpaired Student *t* test was used for statistical analysis of the pAKT data. l.e., long exposure; s.e., short exposure. (*B*) Purified B cells were labeled with CFSE and activated with αCD40 + IL-4 for 4 d. The percentage of live B cells that had divided at least once (based on CFSE division history) expressing surface IgG1 was determined by FACS after 4 d. (*C*, *Left*) Percentage of B cells expressing surface IgG1 after 4 d of activation with αCD40 + IL-4 is plotted for several experiments. In the +TOR-KI condition, INK128 was added at a concentration of 1–5 nM. (*C*, *Right*) Percentage of B cells expressing surface CD138 after 4 d of activation with LPS is plotted. (*D*, *Left*) Western blotting was performed the same way as in *A* but with resting B cells from control (raptor$^{fl/fl}$) or raptor-flox/CD21Cre (raptor$^{\Delta B}$). (*D*, *Right*) Intracellular p-Flow analysis to measure mTORC1 and mTORC2 activity after 24 h of αCD40 + IL-4 activation. Data are reported as mean ± SD ($n = 3$) for both pAKT and pS6. An unpaired Student *t* test was used for statistical analysis. (*E*) Representative FACS plots as in *B*. (*F*) Same analysis as in *C*. A paired Student *t* test was used for statistical analysis of both *C* and *F*.

studies showing that PI3K activity suppresses CSR through AKT-dependent inactivation of FoxO1, whereas PI3K inhibition or FoxO activation promotes CSR (22, 25).

The enhanced production of class-switched antibodies by mTORC1/mTORC2 inhibition is surprising, considering the well-known immunosuppressive activity of rapamycin and the impaired survival and differentiation of mouse B cells lacking mTOR (6). Our in vitro studies establish the importance of using intermediate doses of competitive mTOR inhibitors that transiently inhibit both mTORC1 and mTORC2. At higher concentrations, TOR-KIs sustain mTOR inhibition and block B-cell proliferation to a similar degree as rapamycin, probably through strong mTORC1 inhibition (Fig. 8). Supporting the model that TOR-KIs increase CSR via mTORC2 inhibition, genetic loss of mTORC2 (via partial rictor deletion) causes increased CSR that is not elevated further by TOR-KI treatment. Our findings contrast with a

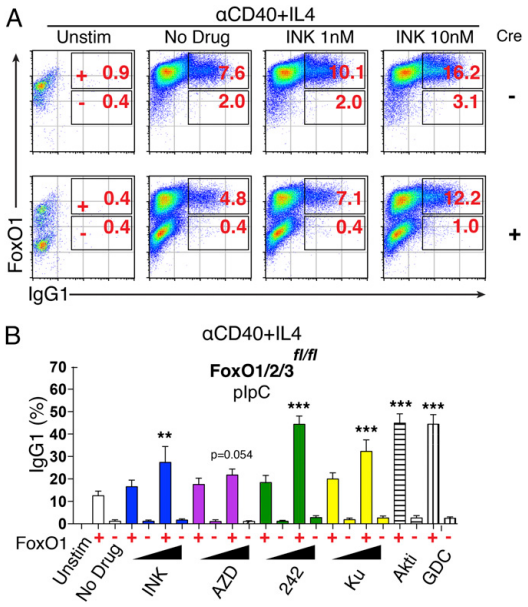

Fig. 7. Increases in B-cell CSR are mediated by FoxO transcription factors. (*A*) Purified B cells from polyI:C-treated FoxO triple-floxed mice lacking Mx1-Cre were treated with the indicated inhibitors, followed by stimulation with αCD40 + IL-4. The percentage of IgG1-switched cells was determined as in Fig. 2. (*A* and *B*) PolyI:C-treated FoxO triple-floxed mice (FoxO1/2/3$^{fl/fl}$) expressing Mx1-Cre were treated with polyI:C and stimulated with αCD40 + IL-4. Intracellular staining was used to distinguish FoxO-deleted cells (indicated by red – signs) from nondeleted cells (indicated by red + signs) in the same population. (*B*) Percentage of IgG1-switched B cells was reported as mean ± SEM (**$P < 0.01$; ***$P < 0.001$ by one-way ANOVA with Tukey's multiple comparison test, measured on FoxO-sufficient cells vs. the no-drug sample). GDC, GDC-0941.

recent report that deletion of rictor in B cells reduces survival and proliferation, and impairs class switching (7). It appears that these systems achieve differential efficiency of rictor deletion. Boothby and coworkers (7) obtained efficient deletion using Vav-Cre, where rictor is deleted in all hematopoietic cells, or using an inducible Cre (fused to the estrogen receptor hormone binding domain) by which chronic in vivo tamoxifen treatment directs rictor deletion in all cell types. We used CD19Cre, which mediated partial deletion of rictor in B cells and partial but not complete loss of mTORC2 signaling. Partial rictor deletion allowed B cells to survive and proliferate, and led to enhanced class switching. The results we obtained with rapamycin titrations are consistent with recent evidence that mTORC1 inhibition can suppress CSR independent of proliferation (10) (Fig. 8). An interesting finding is that when both complexes are partially inhibited by intermediate concentrations of TOR-KIs, the effect of mTORC2 inhibition is dominant for CSR (enhancement), whereas mTORC1 inhibition is dominant for ASC generation (inhibition).

Our findings also demonstrate that TOR-KIs can improve humoral immune responses in vivo. Daily dosing with AZD8055 for a limited time (4 d) increased antigen-specific IgG1 production in young and aged mice immunized with a model antigen. Extended treatment with INK128 did not enhance IgG1 production, possibly resulting from impaired plasma cell differentiation. The in vitro data suggest that TOR-KIs promote CSR, in part, through B cell-intrinsic effects. However, AZD8055 was reported to enhance innate immune activation to promote anticancer immune responses (26); therefore, mTOR inhibition might augment immune responses, in part, through stimulating inflammatory cytokine production (27, 28). In addition, our data show that TOR-KIs can promote T_{FH}-cell differentiation both in vitro and in vivo. Further experiments will be needed to determine the mechanism of enhanced T_{FH} differentiation and how this effect is modulated by different drug doses and schedules.

Overall, our findings emphasize that targeted inhibitors of the PI3K/AKT/mTOR pathway have important immunomodulatory effects at concentrations that do not strongly suppress lymphocyte clonal expansion. Additional studies will be required to determine whether TOR-KIs stimulate faster or more potent antibody responses to different immunogens and with distinct adjuvants and routes of administration. Eventually, TOR-KI treatment could be used to improve vaccine efficacy or to boost the production of class-switched antibodies in animals for biomedical applications.

Materials and Methods

Mice and Reagents. C57BL6 mice were bred at the University of California, Irvine, and used at between 6 and 12 wk of age. Aged mice, 16–18 mo old, on a C56Bl6/SJL mixed background with a transgenic GFP expressed under CD88 promoter were kindly donated by Andrea Tenner (University of California, Irvine). *Raptor*$^{fl/fl}$ mice on a C57BL6 background were obtained from the Jackson Laboratories (stock no. 013138) and have been described previously (29). *Rictor*$^{fl/fl}$ mice on a C57BL6 background were a generous gift from Mark Magnuson (Vanderbilt University, Nashville, TN) and have been

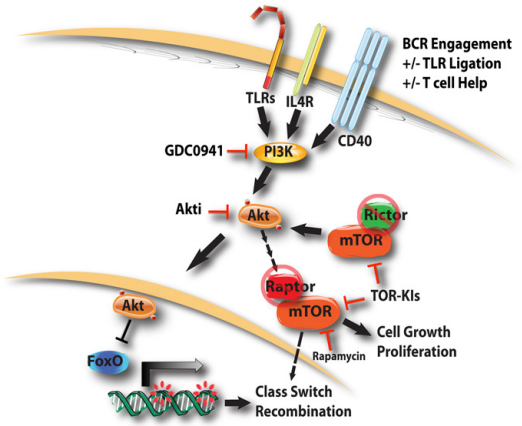

Fig. 8. Roles of mTOR complexes in CSR and the effects of distinct classes of mTOR inhibitors. Activated B cells initiate CSR in response to T cell-derived signals (CD40, IL-4) and/or innate pattern recognition [Toll-like receptor (TLR) engagement]. These signals converge on the lipid kinase PI3K, leading to activation of the Ser/Thr kinase AKT. The predominant action of AKT is to suppress CSR by inactivating FoxO transcription factors that are required for this process (22, 25). Thus, inhibitors of PI3K or AKT tend to increase CSR. mTOR exists in two complexes with complex roles in CSR. mTORC1 (defined by the raptor subunit) promotes CSR through an unknown mechanism (multiple arrows) that is partially independent of the role of mTORC1 in B-cell proliferation. Consequently, deletion of raptor or treatment with the selective mTORC1 inhibitor rapamycin suppresses CSR. mTORC2 (defined by the rictor subunit) suppresses CSR by promoting AKT phosphorylation, leading to FoxO inactivation. Thus, partial deletion of rictor increases CSR. When B cells are treated with TOR-KIs at submaximal concentrations that preserve proliferation, the mTORC2 effect dominates and CSR increases. At higher concentrations, full inhibition of both mTORC1 and mTORC2 suppresses proliferation and CSR. Although AKT can promote mTORC1 activity (multiple arrows), inhibition of PI3K/AKT does not completely suppress mTORC1 signaling in activated B cells (36).

described previously (30). CD21-Cre mice were obtained from the Jackson Laboratories (stock no. 006368). *FoxO1/3/4*$^{fl/fl}$*; Mx1-Cre*$^{+}$ and *FoxO1/3/4*$^{fl/fl}$*; Mx1-Cre*$^{-}$ mice were bred at Harvard Medical School (Boston, MA). All animals were studied in compliance with protocols approved by the Institutional Animal Care and Use Committees of the University of California, Irvine, and Harvard Medical School. The active site mTORC1/2 inhibitors PP242, AZD8055, WYE-354, and Ku-0063794 were purchased from Chemdea, and INK128 was obtained from Intellikine. The p110δ-selective PI3K inhibitor IC87114 and pan-PI3K class I inhibitor GDC-0941 were obtained from Intellikine. The inhibitor of AKT1 and AKT2, Akt inhibitor VIII, was purchased from Chemdea. The mTOR allosteric inhibitor, rapamycin, was purchased from LC Labs.

Primary Cell Culture. Mouse splenic B cells were purified by negative selection using anti-CD43 biotinylated antibody, followed by incubation with anti-biotin magnetic microbeads and separation on MACS columns (Miltenyi Biotec). B-cell purity was >98% as measured by FACS analysis (FACSCalibur and CellQuest software; BD Biosciences) using anti-B220 antibody (BioLegend). Purified B cells were seeded at a final concentration of $0.2 \times 10^{\wedge 6}$ cells per milliliter. For ASC differentiation, B cells were stimulated with 5 μg/mL LPS (Sigma) for 72 h, and for IgG1 CSR, B cells were stimulated with 3 units of CD40L (a gift from Paolo Casali, University of California, Irvine), 1 μg/mL anti-CD40 (HM40-3) agonistic antibody (BioLegend), or 5 μg/mL LPS (Sigma), together with 2.5 ng/mL mIL-4 (R&D Systems) for 96 h. All B cells were cultured in RPMI 1640 supplemented with 10% (vol/vol) heat-inactivated FCS, 5 mM Hepes, 2 mM L-glutamine, 100 units/mL penicillin, 100 μg/mL streptomycin, 50 μM 2-mercaptoethanol, 1× MEM nonessential amino acids (Mediatech), and 1× sodium pyruvate (Mediatech). To assess mTORC1 activity after stimulation, cells were fixed and permeabilized using BD Cytofix/Cytoperm buffer (BD Biosciences) for 15 min at room temperature. Cells were subsequently washed with 0.5% Tween-20 in PBS and stained with a p-S6 (S240/244) antibody conjugated to Alexa Fluor 647 (Cell Signaling Technologies).

In Vitro B-Cell Inhibitor Treatment. Where the use of pharmacological inhibitors was indicated, a 1× concentration of inhibitor was added to corresponding wells containing purified B cells and allowed to incubate for 15 min at 37 °C in a tissue culture incubator. Following the incubation time, another 1× concentration of inhibitor was added to each corresponding well, followed by a 2× concentration of stimuli. Well contents were mixed by pipetting following both inhibitor additions. Pharmacological inhibitors were used at the following concentrations: PP242 (10 nM, 100 nM, and 400 nM), AZD8055 (1 nM and 10 nM), INK128 (1 nM, 5 nM, 10 nM, and 50 nM), Ku-0063794 (100 nM and 300 nM), rapamycin (0.02 nM, 0.04 nM, 0.08 nM, 0.1 nM, 0.2 nM, 0.4 nM, 0.8 nM, 1 nM, 5 nM, 10 nM, and 20 nM), Akti (500 nM and 1 μM), GDC-0941 (100 nM and 250 nM), and IC87114 (500 nM and 1 μM).

RNA Extraction, RT, and Quantitative RT-PCR. B-cell RNA was extracted using TRIzol reagent (Invitrogen), followed by organic phase purification with Quick-RNA MiniPrep according to the manufacturer's protocol (Zymo Research). For *Aicda*, purified B cells were stimulated with CD40L plus IL-4 or anti-CD40 plus IL-4 for 66 h. For postrecombination Iμ-Cγ1, B cells were stimulated as stated above. cDNA synthesis was carried out on 500 ng to 1 μg of total RNA using iScript Reverse Transcription Supermix (BioRad) for RT-quantitative PCR (qPCR). Gene expression of postrecombination Iμ-Cγ1 and *Aicda* was performed using iTaq Universal SYBR Green Supermix (BioRad), appropriate primers, and Eppendorf Mastercycler ep realplex2 and realplex 2.2 software. Mouse L32 was used as the housekeeping gene. The ratio of gene expression change was determined by the delta-(delta-Ct) method. The following primers were used for qPCR: Iμ-Cμ forward primer 5′-ACCTGGGAATGTATGGTTGTGGCTT-3′ and reverse primer 5′-TCTGAACCTTCAAGGATGCTCTTG-3′, Iμ-Cγ1 forward primer 5′-ACCTGGGAATGTATGGTTGTGGCTT-3′ and reverse primer 5′-ATGGAGTTAGTTTGGGCAGCA-3′, *Aicda* forward primer 5′-TGCTACGTGGTGAAGAGGAG-3′ and reverse primer 5′-TCCCAGTCTGAGATGTAGCG-3′, and mL32 forward primer 5′-AAGCGAAACTGGCGGAAAC-3′ and reverse primer 5′-TAACCGATGTTGGGCATCAG-3′.

FoxO1/2/3 Deletion and FoxO1 Intracellular Staining. For in vivo deletion, *FoxO1/3/4*$^{fl/fl}$*; Mx1-Cre*$^{+}$ and *FoxO1/3/4*$^{fl/fl}$*; Mx1-Cre*$^{-}$ mice were treated i.p. twice, 4 d apart, with 12.5 mg/kg of polyI:C (Amersham), and mice were killed 48 h after the last polyI:C injection. Spleens were harvested, and B cells were purified as described above. FoxO1-deleted B cells were identified by intracellular staining with a rabbit monoclonal antibody against FoxO1 (C29H4; Cell Signaling Technologies). Briefly, B cells were fixed with 2% (vol/vol) paraformaldehyde for 20 min at room temperature, washed, and then permeabilized for 30 min at room temperature with a solution containing 0.2% saponin, 0.05% Nonidet P-40, and 2% (wt/vol) BSA in PBS (permeabilization buffer). Staining for FoxO1 involved a three-layer staining procedure. First, B cells were stained with anti-FoxO1 antibody, followed by a biotinylated donkey anti-rabbit IgG (Southern Biotech), and, lastly, streptavidin-APC (BioLegend). Fc receptors were blocked with TruStain fcX (BioLegend), and all stains and washes were performed with permeabilization buffer.

NP-Ova Immunization and Transient AZD8055 Treatment. Mice were immunized with NP(18)-OVA (Biosearch Technologies) via i.p. injection. NP(18)-OVA was precipitated with Imject alum (Pierce) at a 1:1 ratio to yield a final concentration of 0.05 mg/mL, and mice were each injected with 100 μL (5 μg of antigen). A boost was given at PID 21. For AZD8055 treatment, mice were dosed p.o. once per day with 100 μL of formulated drug at a concentration of 20 mg/kg for a total of 4 d commencing 1 d before NP(18)-OVA immunization and ending on PID 2. Formulation of AZD8055 has been described previously (31). Mice were bled on PID 14 and PID 21 by lancinating the facial vein with a sterile Goldenrod animal lancet (Medipoint). PID 28 blood was collected by cardiac puncture after mice were euthanized with CO_2 gas. Collected blood was allowed to coagulate at room temperature for 10 min and then spun down, and the clear serum fraction was collected and stored for future use at −80 °C.

B-Cell Culture Supernatant and Serum ELISA. For cell culture ELISA to measure total IgM, supernatants from purified B cells stimulated with LPS were collected after 4 d and diluted 1:20 in 2% (wt/vol) BSA in PBS. Nunc Maxisorp plates (Thermo Fisher) were coated with anti-mouse IgM (RMM-1; BioLegend) at 10 μg/mL in 50 μL of total sample in PBS and allowed to incubate overnight at 4 °C. Diluted supernatant samples were incubated on coated plates for 1 h at 37 °C. HRP-conjugated rabbit anti-mouse IgM secondary antibody (Zymed) was used. For NP-specific antibody titers, dilution series were performed using sera from vehicle-treated mice to find the EC_{50} for the different time points and antibody isotypes. The corresponding dilutions that rendered the EC_{50}s were then used for the antibody ELISAs for all samples. Nunc Maxisorp plates were coated at a concentration of 10 μg/mL in a 50-μL total volume with NP(26)-BSA or NP(5)-BSA (Biosearch Technologies) for high-affinity antibody discrimination. HRP-conjugated rabbit anti-mouse IgM secondary antibody and HRP-conjugated goat anti-mouse IgG1 secondary antibody (Southern Biotech) were used for IgM and IgG1 measurements, respectively.

Flow Cytometry, CFSE Labeling, and Antibodies. Before cell surface staining, cells were incubated with TruStain fcX in FACS buffer (0.5% BSA + 0.02% NaN_3 in 1× HBSS) to block Fc receptors for 10 min on ice. Immunophenotyping of mice was performed on splenocytes after RBC lysis. Staining with antibodies was subsequently performed, also with FACS buffer and on ice for 20 min. Flow cytometry antibodies and other reagents used were as follows: CD4 (OKT4), B220 (RA3-6B2), IgG1 (RMG1-1), PD-1 (29F.1A12), IL-21 (FFA21), and IL-17A (TC11-18H10.1) (all from BioLegend); IgD (11-26c), CD38 (90), IgM (eB121-15F9), CD21 (4E3), and CD93 (AA4.1) (all from eBioscience); NP-phycoerythrin (Biosearch Technologies); and Fas (CD95; clone Jo2), CD138 (281-2), and CXCR5 (2G8) (all from BD Biosciences). CFSE labeling of B cells to track proliferation was performed as described elsewhere (32). Flow cytometric data were analyzed using FlowJo software (TreeStar).

Bacterial Strain and Growth Conditions. Attenuated *Salmonella enterica* serovar Typhimurium strain SB824 (*sptP*::Kan Δ*aroA*) is a derivative of strain SL3261, and it was previously described (33–34). Serovar Typhimurium was routinely incubated aerobically at 37 °C in LB broth (10 g of tryptone, 5 g of yeast extract, and 10 g of NaCl per liter).

Immunization of Mice with Recombinant *Salmonella* and AZD8055 Dosing. Specific pathogen-free female C57BL/6 mice, 6–8 wk old, were purchased from Taconic. For the experiments, animals were housed in groups of five mice under barrier conditions. Mice were immunized via i.p. injection with $5 \times 10\wedge 3$ cfu of the indicated *Salmonella* vaccine strain. Where indicated, mice were dosed with AZD8055 at 10 mg/kg p.o. for a total of 4 d beginning on PID 3.

***Salmonella* FACS.** Attenuated *Salmonella enterica* serovar Typhimurium strain SB824 was grown overnight under static conditions. A total of $1 \times 10\wedge 9$ bacteria were aliquoted out into 1.7-mL microcentrifuge tubes and

Supporting Information

Limon et al. 10.1073/pnas.1407104111

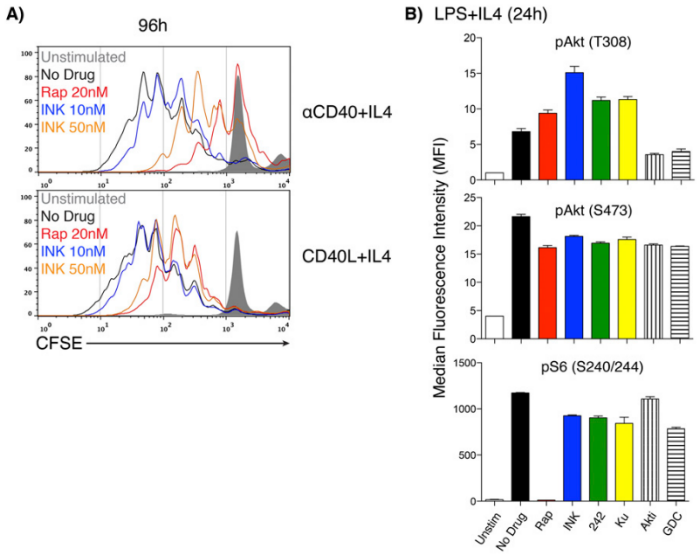

Fig. S1. (*A*) Purified B cells were labeled with CFSE and cultured in media alone or with the stimulants αCD40 + IL-4 or CD40L + IL-4 in the presence or absence of indicated inhibitors. (*B*) Intracellular phosphoflow detection of AKT phosphorylation in B cells stimulated for 24 h with LPS + IL-4 and the indicated inhibitors. Median fluorescence intensity (MFI) is shown as the mean ± SEM of three samples from different mice. The p-S6 was also measured as readout of mTORC1 activity. Akti, Akt inhibitor VIII; GDC, GDC-0941; INK, INK128; Ku, Ku-0063794; Rap, rapamycin; 242, PP242; Unstim, unstimulated.

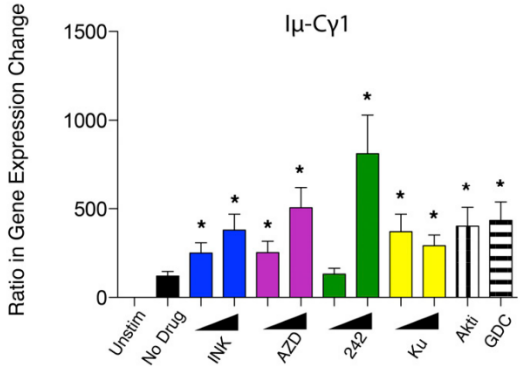

Fig. S2. qPCR measurement of postrecombination Iμ-Cγ1 transcripts. RNA was purified from B cells from four separate mice stimulated with αCD40 + IL-4 for 66 h and then reverse-transcribed. The ratio of gene expression change was determined by the delta-(delta-Ct) method. *$P < 0.05$ by a paired, two-tailed Student *t* test, measured vs. no-drug sample.

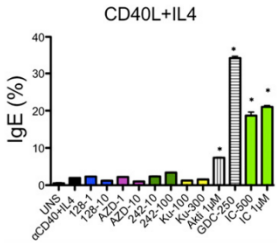

Fig. S3. Percentage of B cells that have switched to IgE was measured 4 d after stimulation with αCD40 + IL-4 and the indicated inhibitors. In this experiment, the data for three different mice were processed separately and the graph depicts mean ± SEM (n = 3). *P < 0.001 vs. αCD40 + IL-4 alone; ^P < 0.001 vs. Akti condition. IC = IC87114.

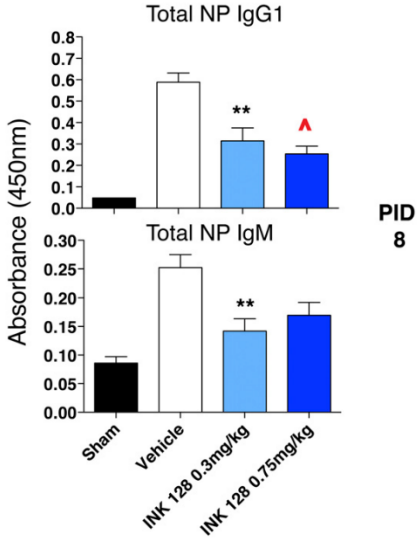

Fig. S4. Continuous treatment with INK128 decreases antigen-specific antibody production in vivo. Mice were immunized with NP-OVA and treated daily with INK128 at the indicated concentrations beginning on PID −1 and ending on PID 7. NP-specific IgM and IgG1 antibody production was measured by ELISA in sera collected at PID 8. ELISA data are depicted as A_{450} values. (**P < 0.01; ^P < 0.001 by one-way ANOVA with Tukey's multiple comparison test, measured vs. the vehicle group).

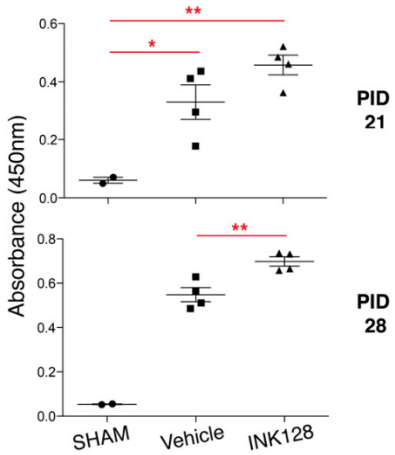

Fig. S5. Transient treatment of mice with INK128 increases NP-specific IgG1. Mice were immunized with NP-OVA and treated daily for 4 d with INK128 at 0.75 mg/kg (PID −1 to PID 2). ELISA data, from sera collected during the primary (PID 21) and secondary (PID 28) immune responses, are depicted as A_{450} values. (*$P < 0.05$; **$P < 0.01$ by one-way ANOVA with Tukey's multiple comparison test, measured vs. the vehicle group).

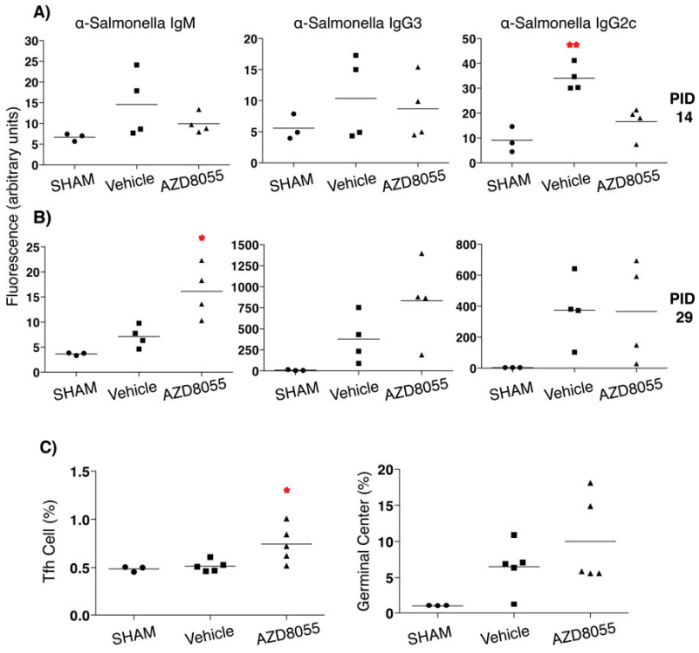

Fig. S6. TOR-KIs augment the late antibody response to *Salmonella* Typhimurium. (*A* and *B*) Mice were transiently treated with AZD8055 and immunized with a vaccine strain of *Salmonella* Typhimurium. Early (*A*, PID 14) and later (*B*, PID 29) anti-*Salmonella* IgM, IgG3, and IgG2c antibodies were measured by a FACS-based assay. Data are reported as mean fluorescence intensity. (*C*) Percentages of T_{FH} and GC B cells at PID 29 were measured by FACS. (*$P < 0.05$; **$P < 0.01$ by one-way ANOVA with Tukey's multiple comparison test, measured vs. the vehicle group).

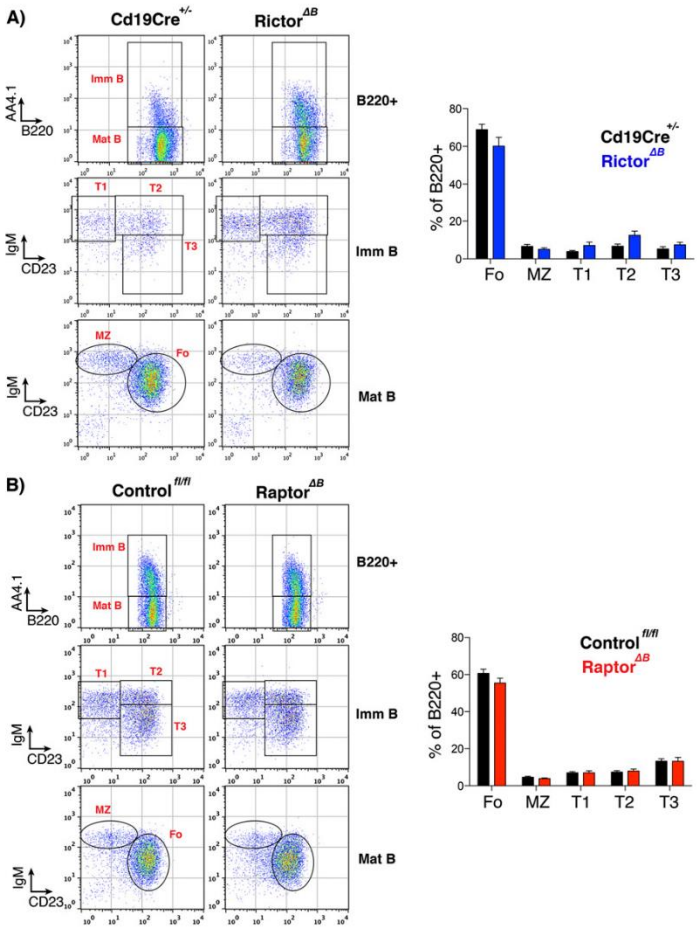

Fig. S7. B-cell subset analysis by FACS in rictor$^{\Delta B}$ and raptor$^{\Delta B}$. Splenic cells after RBC lysis were stained with appropriate antibodies to identify the major B-cell subsets present in indicated mice. (*A*, *Left*) B-cell subset analysis in rictor$^{\Delta B}$ mice. A representative gating scheme to identify different B-cell subsets is shown, with the red font indicating the different subsets. (*A*, *Right*) Data are averaged from at least six different mice. Fo, follicular B cells; Imm B: B220^{+}AA4.1^{+} immature B cells; Mat B, B220^{+}AA4.1^{-} mature B cells; MZ, marginal zone B cells; T1, T2, and T3, transitional B cells. (*B*) B-cell subset analysis in raptor$^{\Delta B}$ mice as in *A*.

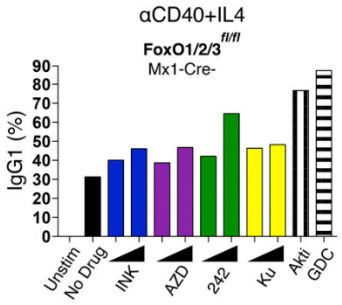

Fig. S8. TOR-KIs increase in vitro B-cell CSR in polyI:C-treated FoxO triple-floxed (FoxO1/2/3$^{fl/fl}$)/Mx1-Cre mice. Purified B cells from polyI:C-treated (FoxO1/2/3$^{fl/fl}$) mice lacking Mx1-Cre were treated with the indicated inhibitors, followed by stimulation with αCD40 + IL-4. The percentage of IgG1-switched cells was determined as in Fig. 2. Similar results were obtained in a second experiment.